

RECEIVED: August 5, 2014

REVISED: August 12, 2015

ACCEPTED: August 27, 2015

PUBLISHED: September 24, 2015

The rare semi-leptonic B_c decays involving orbitally excited final mesons

Wan-Li Ju,^a Guo-Li Wang,^a Hui-Feng Fu,^b Zhi-Hui Wang^c and Ying Li^d

^aDepartment of Physics, Harbin Institute of Technology,
Harbin, 150001, China

^bDepartment of Physics, Tsinghua University,
Beijing, 100084, China

^cDepartment of Physics, Beifang University of Nationalities,
Yinchuan, 750021, China

^dDepartment of Physics, Yantai University,
Yantai 264-005, China

E-mail: w1-ju.hit@163.com, gl_wang@hit.edu.cn,
huifengfu@tsinghua.edu.cn, wzh19830606@163.com, liying@ytu.edu.cn

ABSTRACT: The rare processes $B_c \rightarrow D_{(s)J}^{(*)} \mu \bar{\mu}$, where $D_{(s)J}^{(*)}$ stands for the final meson $D_{s_0}^*(2317)$, $D_{s_1}(2460, 2536)$, $D_{s_2}^*(2573)$, $D_0^*(2400)$, $D_1(2420, 2430)$ or $D_2^*(2460)$, are studied within the Standard Model. The hadronic matrix elements are evaluated in the Bethe-Salpeter approach and furthermore a discussion on the gauge-invariant condition of the annihilation hadronic currents is presented. Considering the penguin, box, annihilation, color-favored cascade and color-suppressed cascade contributions, the observables dBr/dQ^2 , A_{LP_L} , A_{FB} and P_L are calculated.

KEYWORDS: Rare Decays, B-Physics, Standard Model

ARXIV EPRINT: [1407.7968](https://arxiv.org/abs/1407.7968)

Contents

1	Introduction	2
2	Transition amplitudes of BP, Ann, CS and CF contributions	4
3	Hadronic transition matrix elements in the BS method	5
3.1	General arguments on hadronic currents	5
3.2	Wave functions in BS method	7
3.3	Calculations of hadronic matrix elements	9
3.3.1	Hadronic matrix elements of $P \rightarrow S$ processes	9
3.3.2	Hadronic matrix elements of $P \rightarrow T$ processes	10
3.3.3	Hadronic matrix elements of $P \rightarrow A$ processes	10
3.4	The definitions of form factors	12
3.5	Numerical results of form factors	13
3.5.1	Parameters in the calculations	13
3.5.2	Results and discussions on form factors	14
4	The observables	15
4.1	The calculations of observables	15
4.2	Numerical results of the observables	16
4.2.1	The observables of $B_c \rightarrow D_{s0}^*(2317)\mu\bar{\mu}$ decays	16
4.2.2	The observables of $B_c \rightarrow D_{s2}^*(2573)\mu\bar{\mu}$ decays	17
4.2.3	The observables of $B_c \rightarrow D_{s1}(2460)\mu\bar{\mu}$ decays	18
4.2.4	The observables of $B_c \rightarrow D_{s1}(2536)\mu\bar{\mu}$ decays	18
4.2.5	The observables of $B_c \rightarrow D_J^{(*)}\mu\bar{\mu}$ decays	19
4.3	The experimentally excluded regions and integrated branching fractions	19
5	Discussions	20
5.1	Estimations of the theoretical uncertainties	20
5.2	Testing the hadronic matrix elements	21
6	Conclusion	23
A	Definitions of $\mathcal{F}_{V1-7}^\alpha$ and $\mathcal{F}_{A1-3}^\alpha$	24
B	Definitions of P_i, P_f, ϵ_A, ϵ_T and ϵ_H^μ	25

1 Introduction

The rare decays $b \rightarrow s(d)\bar{l}l$ have particular features. These transitions are of the single-quark flavor-changing neutral current (FCNC) processes, which are forbidden at tree level in the Standard Model (SM) but mediated by loop processes. Hence, within the SM, the $b \rightarrow s(d)\bar{l}l$ amplitudes are greatly suppressed. The situation is different for the standard model extensions, where many new particles beyond the SM are predicted. These new particles can virtually enter the loops relevant to FCNC processes or induce the transitions at tree level, which makes that the observables predicted in the standard model extensions may significantly deviate from the ones in the SM. This sensitive nature to the effects beyond the SM can be exploited as a tool for stringently testing the SM and indirectly hunting the New Physics (NP).

In literatures, the $b \rightarrow s\bar{l}l$ processes were extensively analyzed in the decays $B \rightarrow K^{(*)}\bar{l}l$. In recent years, the decays $B \rightarrow K_1(1270, 1400)\bar{l}l$ [1], $B \rightarrow K_0^*(1430)\bar{l}l$ [2–9] and $B \rightarrow K_2^*(1430)\bar{l}l$ [8, 10–21] have also been emphasized. However, according to ref. [22], the mass differences among the $K_J^{(*)}$ s, where $K_J^{(*)}$ s denote the mesons $K_1(1270)$, $K_1(1400)$, $K_0^*(1430)$ and $K_2^*(1430)$, are small and their widths are rather wide. This leads to the problem that the observables in a certain kinematic region may receive contributions from several different channels and it is not easy to separate them confidently. For instance, as estimated in ref. [8], at $m_{K\pi} \sim 1.4$ GeV, the longitudinal differential branching fraction $dBr_L(B \rightarrow K\pi\bar{l}l)/dm_{K\pi}^2$ is affected by the channels $B \rightarrow K_0^*(1430)\bar{l}l$, $B \rightarrow K_2^*(1430)\bar{l}l$, $B \rightarrow K^*(1680)\bar{l}l$ and $B \rightarrow K^*(1410)\bar{l}l$ un-negligibly. But this situation will be ameliorated, if the decays $B_c \rightarrow D_{sJ}^{(*)}\bar{l}l$ are investigated. Compared with the $K_J^{(*)}$ s, the mass differences among the $D_{sJ}^{(*)}$ mesons are bigger and their widths are much narrower [22]. These features are helpful in reducing the interferences among the different channels. Hence in this paper, we are motivated to investigate the processes $B_c \rightarrow D_{sJ}^{(*)}\bar{l}l$.

In the previous works [23, 24], the process $B_c \rightarrow D_{s0}^*(2317)\bar{l}l$ was calculated including only the $b \rightarrow s\bar{l}l$ effects, whose typical Feynman diagrams are Box and Penguin (BP) diagrams, as plotted in figures 1 (a, b). However, besides the BP effects, the Annihilation (Ann) diagrams, as shown in figure 1 (c), also make un-negligible contributions. On one hand, both BP and Ann diagrams are of order $\mathcal{O}(\alpha_{em}G_f)$ and the ratio of their CKM matrix elements is $|V_{cb}^*V_{cs(d)}|/|V_{ts(d)}^*V_{tb}| \sim 1$. On the other hand, from figure 1 (c), we see that the color factors of Ann diagrams are 3 times larger than those of BP diagrams. Thus, when the decay $B_c \rightarrow D_{s0}^*(2317)\bar{l}l$ is analyzed, it is necessary to include the Ann effects.

In addition to the BP and Ann effects, the process $B_c \rightarrow D_{s0}^*(2317)\bar{l}l$ is also influenced by resonance cascade processes, such as $B_c \rightarrow D_{s0}^*(2317)J/\psi (\psi(2S)) \rightarrow D_{s0}^*(2317)\bar{l}l$. Their typical Feynman diagrams are illustrated in figures 1 (d, e). Transition amplitudes of these diagrams in the area $m_{\bar{l}l}^2 \sim m_{J/\psi (\psi(2S))}^2$ always become much larger than the BP and Ann ones. Hence, to avoid overwhelming the BP and Ann contributions, the regions around $m_{\bar{l}l}^2 \sim m_{J/\psi (\psi(2S))}^2$ should be experimentally removed. In ref. [23], the regions [25], which are defined through comparing the BP and color-suppressed (CS) cascade contributions, are employed. However, in the $B_c \rightarrow D_{s0}^*(2317)\bar{l}l$ process, both the color-favored (CF) and CS diagrams exist. Furthermore, the CF transition amplitudes are expected to be larger

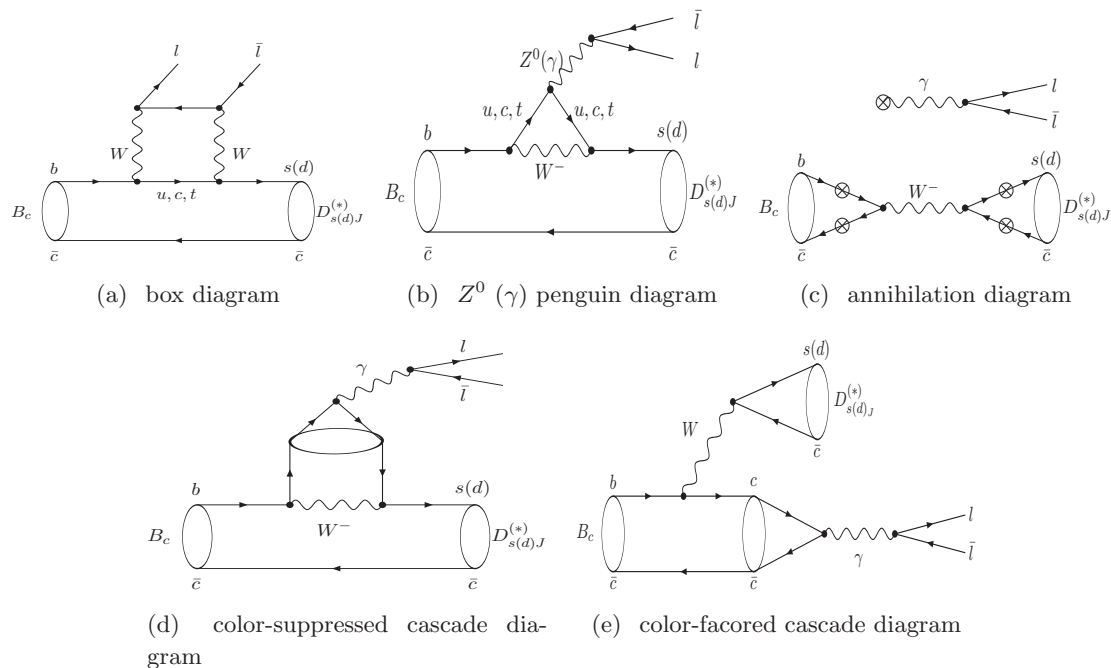


Figure 1. Typical diagrams of $B_c \rightarrow D_{s(d)J}^{(*)} l \bar{l}$ process. In annihilation diagrams (c) the photon can be emitted from each quark, denoted by \otimes , and decays to the lepton pair.

than the CS ones by a 3 times larger color factor approximately. Thus, it is necessary to redefine these regions with both CF and CS cascade influences.

So in this paper, we investigate $B_c \rightarrow D_{s_0}^*(2317) l \bar{l}$ transition including BP, Ann, CS and CF contributions. In addition, in order to give a more comprehensive discussion on the semi-leptonic rare decays of B_c , the processes $B_c \rightarrow D_{s_1}(2460, 2536) l \bar{l}$, $B_c \rightarrow D_{s_2}^*(2573) l \bar{l}$ and $B_c \rightarrow D_J^{(*)} l \bar{l}$ are also analyzed.

In our calculations, the low-energy effective theory is employed [26]. Within this method, the short distance information of transition amplitude is factorized into the Wilson coefficients, while the long distance effects are described by the matrix element which is an operator sandwiched by the initial and the final states. The Wilson coefficients in the SM can be attained perturbatively. But the matrix elements are of non-perturbative nature and in this paper we calculate them with the Bethe-Salpeter (BS) method [27]. In this method, the BS equation [28, 29] is employed to solve the wave functions for mesons, while the Mandelstam Formalism [30] is used to evaluate hadronic matrix elements. With such method, the hadronic matrix elements keep the relativistic effects from both the wave functions and the kinematics. In our previous paper [31], within the BS method, we calculated the $B_c \rightarrow D_{s,d}^{(*)} l \bar{l}$ rare transitions, whose final mesons are of S-wave states, and checked the gauge-invariance condition of the annihilation hadronic currents. In this paper, we investigate the processes $B_c \rightarrow D_{(s)J}^{(*)} l \bar{l}$, whose final mesons are of P-wave states, and furthermore, we give a more generalized conclusion: the annihilation hadronic currents obtained within the BS method satisfy the gauge-invariance condition, no matter what the J^P s of initial and final mesons are.

This paper is organized as follows. In section 2, we introduce the transition amplitudes corresponding to BP, Ann, CS and CF contributions and specify the involved hadronic matrix elements. Within section 3, we calculate these hadronic matrix elements through the Bethe-Salpeter method and express the results in terms of form factors. In section 4, using these form factors, we compute the observables, including dBr/dQ^2 , A_{LP} , A_{FB} and P_L . Section 5 is devoted to the discussions on the theoretical uncertainties. Finally, we summarize and conclude in section 6.

2 Transition amplitudes of BP, Ann, CS and CF contributions

In this section, we briefly review the transition amplitudes corresponding to BP, Ann, CS and CF effects. A more detailed introduction can be found in our previous paper [31].

According to low-energy effective theory [26], the transition amplitude describing the $b \rightarrow s(d)\bar{l}\bar{l}$ (or equivalently, BP) contribution is,

$$\mathcal{M}_{\text{BP}} = i \frac{G_F \alpha_{em}}{2\sqrt{2}\pi} V_{tb} V_{ts(d)}^* \left\{ \left[C_9^{\text{eff}} W_\mu - \frac{2m_b}{Q^2} C_7^{\text{eff}} W_\mu^T \right] \bar{l} \gamma^\mu l + C_{10} W_\mu \bar{l} \gamma^\mu \gamma_5 l \right\}, \quad (2.1)$$

where $Q = P_i - P_f$ and $P_{i(f)}$ stands for the momentum of the initial (final) meson. V_{tb} and $V_{ts(d)}$ denote the CKM matrix elements. C_{10} is the Wilson coefficient. $C_{7,9}^{\text{eff}}$ are the combinations of the Wilson coefficients which are multiplied by the same hadronic matrix elements. The numerical value of C_{10} and the explicit expressions of $C_{7,9}^{\text{eff}}$ can be found in ref. [32]. The hadronic matrix elements W_μ and W_μ^T are defined as

$$W_\mu = \langle f | \bar{s}(\bar{d}) \gamma_\mu (1 - \gamma_5) b | i \rangle, \quad W_\mu^T = \langle f | \bar{s}(\bar{d}) i \sigma_{\mu\nu} (P_i - P_f)^\nu (1 + \gamma_5) b | i \rangle, \quad (2.2)$$

where the definition $\sigma^{\mu\nu} = (i/2)[\gamma^\mu, \gamma^\nu]$ is used.

Based on the effective theory [26] and the factorization hypothesis [33], the transition amplitude describing the Ann effects is [31]

$$\mathcal{M}_{\text{Ann}} = V_{cb} V_{cs(d)}^* \frac{i \alpha_{em}}{Q^2} \frac{G_F}{2\sqrt{2}\pi} \left(\frac{C_1}{N_c} + C_2 \right) W_{\text{ann}}^\mu \bar{l} \gamma_\mu l, \quad (2.3)$$

where $C_{1,2}$ are the Wilson coefficients, whose values can be found in ref. [32]. The annihilation hadronic current W_{ann}^μ is defined as $W_{\text{ann}}^\mu = W_{1\text{ann}}^\mu + W_{2\text{ann}}^\mu + W_{3\text{ann}}^\mu + W_{4\text{ann}}^\mu$, where

$$\begin{aligned} W_{1\text{ann}}^\mu &= (-8\pi^2) \langle f | \bar{s}(\bar{d}) \gamma_\alpha (1 - \gamma_5) c | 0 \rangle \langle 0 | \bar{c} \gamma^\alpha (1 - \gamma_5) \frac{1}{\not{p}_{q_1} - m_{q_1} + i\epsilon} \left(-\frac{1}{3} \right) \gamma^\mu b | i \rangle, \\ W_{2\text{ann}}^\mu &= (-8\pi^2) \langle f | \bar{s}(\bar{d}) \gamma_\alpha (1 - \gamma_5) c | 0 \rangle \langle 0 | \bar{c} \left(\frac{2}{3} \right) \gamma^\mu \frac{1}{\not{p}_{q_2} - m_{q_2} + i\epsilon} \gamma^\alpha (1 - \gamma_5) b | i \rangle, \\ W_{3\text{ann}}^\mu &= (-8\pi^2) \langle f | \bar{s}(\bar{d}) \left(-\frac{1}{3} \right) \gamma^\mu \frac{1}{\not{p}_{q_3} - m_{q_3} + i\epsilon} \gamma_\alpha (1 - \gamma_5) c | 0 \rangle \langle 0 | \bar{c} \gamma^\alpha (1 - \gamma_5) b | i \rangle, \\ W_{4\text{ann}}^\mu &= (-8\pi^2) \langle f | \bar{s}(\bar{d}) \gamma_\alpha (1 - \gamma_5) \frac{1}{\not{p}_{q_4} - m_{q_4} + i\epsilon} \left(\frac{2}{3} \right) \gamma^\mu c | 0 \rangle \langle 0 | \bar{c} \gamma^\alpha (1 - \gamma_5) b | i \rangle. \end{aligned} \quad (2.4)$$

$p_{q_{1-4}}$ and $m_{q_{1-4}}$ are momenta and masses of the propagated quarks, respectively.

For the CS and CF cascade resonance effects, the transition amplitudes are [31]

$$\begin{aligned}\mathcal{M}_{\text{CS}} &= i \frac{9G_F}{2\sqrt{2}\alpha_{em}} V_{cb} V_{cs(d)}^* \left(C_1 + \frac{C_2}{N_c} \right) \left[\sum_{V=J/\psi, \psi(2S)} \frac{\Gamma(V \rightarrow \bar{l}l) M_V}{Q^2 - M_V^2 + i\Gamma_V M_V} \right] W_\mu \bar{l} \gamma^\mu l, \\ \mathcal{M}_{\text{CF}} &= i \frac{G_F \alpha_{em}}{2\sqrt{2}\pi} V_{cb} V_{cs(d)}^* \left(C_2 + \frac{C_1}{N_c} \right) W_{\text{CF}}^\mu \bar{l} \gamma_\mu l,\end{aligned}\tag{2.5}$$

where M_V and Γ_V are the mass and full width of the resonance meson, respectively. $\Gamma(V \rightarrow \bar{l}l)$ denotes the branching width of the transition $V \rightarrow \bar{l}l$. The resonance meson V stands for the particle J/ψ or $\psi(2S)$. The CF hadronic current W_{CF}^μ is defined as

$$W_{\text{CF}}^\mu = \sum_{V=J/\psi, \psi(2S)} \frac{-16\pi^2}{3M_V^2} \langle 0 | \bar{c} \gamma^\mu c | V \rangle \frac{i}{Q^2 - M_V^2 + i\Gamma_V M_V} \langle V | \bar{c} \gamma^\nu (1 - \gamma_5) b | i \rangle \langle f | \bar{s} (\bar{d}) \gamma_\nu (1 - \gamma_5) c | 0 \rangle.\tag{2.6}$$

Consequently, the total transition amplitude is

$$\mathcal{M}_{\text{Total}} = \mathcal{M}_{\text{BP}} + \mathcal{M}_{\text{Ann}} + \mathcal{M}_{\text{CS}} + \mathcal{M}_{\text{CF}}.\tag{2.7}$$

3 Hadronic transition matrix elements in the BS method

In section 2, the transition amplitudes of the $B_c \rightarrow D_{(s)J}^{(*)} \bar{l}l$ processes are introduced and the hadronic matrix elements $W_{(T)}$, W_{ann} and W_{CF} are defined. In this section, within the BS method, we show how to calculate these hadronic matrix elements. In section 3.1, we express the hadronic currents as the integrals of the wave functions. Section 3.2 is devoted to showing the wave functions of the mesons which are involved in this paper. Using these wave functions, we calculate the hadronic currents in section 3.3 and parameterize the results in terms of form factors in section 3.4. In section 3.5, we present the numerical results of the form factors.

3.1 General arguments on hadronic currents

In this part, we rewrite the hadronic currents as the integrals of the wave functions and present some general arguments.

According to the Mandelstam formalism [30], $W_{(T)}$ can be expressed as the integrals of the 4-dimensional BS wave functions. In the spirit of the instantaneous approximation [34], the integrations with respect to q_i^0 , where q_i represents the relative momentum between the quark and anti-quark of the initial meson, can be performed first. And then we have [27, 31]

$$\begin{aligned}W_\mu &= - \int \frac{d^3 \vec{q}_i}{(2\pi)^3} \text{Tr} \left\{ \frac{P_i}{M_i} \bar{\varphi}_f^{++} \gamma_\mu (1 - \gamma_5) \varphi_i^{++} \right\}, \\ W_T^\mu &= - \frac{1}{2} (P_i - P_f)_\nu (\mathcal{Y}_V^{\mu\nu} + \mathcal{Y}_A^{\nu\mu}),\end{aligned}\tag{3.1}$$

where the hadronic tensors $\mathcal{Y}_{V,A}^{\mu\nu}$ are defined as

$$\begin{aligned}\mathcal{Y}^{\mu\nu}_V &= - \int \frac{d^3\vec{q}_i}{(2\pi)^3} \text{Tr} \left\{ \frac{P_i}{M_i} \bar{\varphi}_f^{++} \gamma^\mu \gamma^\nu \varphi_i^{++} \right\}, \\ \mathcal{Y}^{\mu\nu}_A &= - \int \frac{d^3\vec{q}_i}{(2\pi)^3} \text{Tr} \left\{ \frac{P_i}{M_i} \bar{\varphi}_f^{++} \gamma^\mu \gamma^\nu \gamma_5 \varphi_i^{++} \right\}.\end{aligned}\tag{3.2}$$

The term φ_i^{++} in eqs. (3.1)–(3.2) denotes the positive energy part of the initial (final) wave function [34] and will be specified in the next subsection. In this paper we ignore the negative-energy parts since they give negligible contributions.

For W_{ann} , similar to the derivations of eq. (3.1), we have,¹

$$\begin{aligned}W_{1\text{ann}}^\mu(i \rightarrow f) &= \frac{8}{\pi^2} \left\{ \int \frac{d^3\vec{q}_i}{(2\pi)^3} \frac{2\mathcal{F}_{i0}^\nu(i)(\alpha_1^i P_i^\mu + q_a^\mu) - \mathcal{F}_{i+}^{\mu\nu}(i) - \mathcal{F}_{i-}^{\mu\nu}(i)}{M_i(Q^2 - 2Q \cdot (\alpha_1^i P_i + q_a) + i\epsilon)} \right\} \\ &\quad \times \left\{ \int \frac{d^3\vec{q}_f}{(2\pi)^3} \frac{\mathcal{F}_\nu^{f0}(f)}{M_f} \right\},\end{aligned}\tag{3.3}$$

$$\begin{aligned}W_{2\text{ann}}^\mu(i \rightarrow f) &= \frac{-16}{\pi^2} \left\{ \int \frac{d^3\vec{q}_i}{(2\pi)^3} \frac{2\mathcal{F}_{i0}^\nu(i)(-\alpha_2^i P_i^\mu + q_a^\mu) + \mathcal{F}_{i+}^{\mu\nu}(i) - \mathcal{F}_{i-}^{\mu\nu}(i)}{M_i(Q^2 + 2Q \cdot (-\alpha_2^i P_i + q_a) + i\epsilon)} \right\} \\ &\quad \times \left\{ \int \frac{d^3\vec{q}_f}{(2\pi)^3} \frac{\mathcal{F}_\nu^{f0}(f)}{M_f} \right\},\end{aligned}\tag{3.4}$$

$$\begin{aligned}W_{3\text{ann}}^\mu(i \rightarrow f) &= \frac{8}{\pi^2} \left\{ \int \frac{d^3\vec{q}_f}{(2\pi)^3} \frac{2\mathcal{F}_{f0}^\nu(f)(\alpha_1^f P_f^\mu + q_c^\mu) + \mathcal{F}_{f+}^{\mu\nu}(f) + \mathcal{F}_{f-}^{\mu\nu}(f)}{M_f(Q^2 + 2Q \cdot (\alpha_1^f P_f + q_c) + i\epsilon)} \right\} \\ &\quad \times \int \frac{d^3\vec{q}_i}{(2\pi)^3} \frac{\mathcal{F}_\nu^{i0}(i)}{M_i},\end{aligned}\tag{3.5}$$

$$\begin{aligned}W_{4\text{ann}}^\mu(i \rightarrow f) &= \frac{-16}{\pi^2} \left\{ \int \frac{d^3\vec{q}_f}{(2\pi)^3} \frac{-2\mathcal{F}_{f0}^\nu(f)(\alpha_2^f P_f^\mu - q_c^\mu) - \mathcal{F}_{f+}^{\mu\nu}(f) + \mathcal{F}_{f-}^{\mu\nu}(f)}{M_f(Q^2 + 2Q \cdot (\alpha_2^f P_f - q_c) + i\epsilon)} \right\} \\ &\quad \times \int \frac{d^3\vec{q}_i}{(2\pi)^3} \frac{\mathcal{F}_\nu^{i0}(i)}{M_i},\end{aligned}\tag{3.6}$$

where q_a is defined as $q_i - (P_i \cdot q_i / M_i^2) P_i$, while $q_c = q_f - (P_f \cdot q_f / M_f^2) P_f$. The coefficients $\alpha_{1,2}^{i,f}$ are given as $\alpha_1^i = m_b / (m_b + m_c)$, $\alpha_2^i = m_c / (m_b + m_c)$, $\alpha_1^f = m_{s(d)} / (m_{s(d)} + m_c)$, $\alpha_2^f = m_c / (m_{s(d)} + m_c)$, where $m_{b,c,s,d}$ are masses of the constituent quarks. The parameters $\mathcal{F}_{i0,i\pm}(i \rightarrow f)$ and $\mathcal{F}_{f0,f\pm}(i \rightarrow f)$ are defined as

$$\begin{aligned}\mathcal{F}_{i0}^\nu(i \rightarrow f) &= \text{Tr} \{ \varphi_i^{++} \gamma^\nu (1 - \gamma_5) \}, \quad \mathcal{F}_{i\pm}^{\mu\nu}(i \rightarrow f) = \frac{1}{2} \text{Tr} \{ \varphi_i^{++} \gamma^\nu (1 - \gamma_5) (\mathcal{Q} \gamma^\mu \pm \gamma^\mu \mathcal{Q}) \}, \\ \mathcal{F}_{f0}^\nu(i \rightarrow f) &= \text{Tr} \{ \bar{\varphi}_f^{++} \gamma^\nu (1 - \gamma_5) \}, \quad \mathcal{F}_{f\pm}^{\mu\nu}(i \rightarrow f) = \frac{1}{2} \text{Tr} \{ \bar{\varphi}_f^{++} \gamma^\nu (1 - \gamma_5) (\gamma^\mu \mathcal{Q} \pm \mathcal{Q} \gamma^\mu) \}.\end{aligned}\tag{3.7}$$

¹While deriving eqs. (3.3)–(3.6), we employ the weak binding hypothesis [34]. In this manner, the expansion $\omega_{1,2} \equiv \sqrt{m_{1,2}^2 - q_{a,c}^2} = m_{1,2} + \frac{-q_{a,c}^2}{2m_{1,2}} + \dots$ can be performed [34] and in this paper only the leading term is kept. Under this approximation, we have the relationships $(\alpha_1 \mathcal{P} + \not{q}_{P\perp} - m_1) \varphi_{i,f}^{++} \sim 0$ and $\varphi_{i,f}^{++} (\alpha_2 \mathcal{P} - \not{q}_{P\perp} + m_2) \sim 0$, which are quite useful to simplify W_{ann} .

Using eqs. (3.3)–(3.7), we now discuss the gauge invariant condition of the Ann hadronic currents calculated in BS method. One may note that examining whether W_{ann} satisfies the gauge invariant condition is equivalent to checking whether $W_{\text{ann}} \cdot Q$ is zero. If we multiply eqs. (3.3)–(3.6) by Q^μ , it is obvious that $(W_{1\text{ann}} \cdot Q) + (W_{2\text{ann}} \cdot Q)$ cancels $(W_{4\text{ann}} \cdot Q) + (W_{3\text{ann}} \cdot Q)$. Hence, we have $W_{\text{ann}} \cdot Q = 0$. This implies that the Ann hadronic currents in BS method indeed satisfy the gauge invariant condition. We stress that there is no need to specify the initial or final state in the process of obtaining $W_{\text{ann}} \cdot Q = 0$. Thus, our conclusion is quite general.

For W_{CF} , in this paper, we do not go into any details of their calculations, because W_{CF} s involved in the $B_c \rightarrow D_{(s)J}^{(*)} \mu \bar{\mu}$ transitions can be obtained from $W_{\text{CF}}(B_c \rightarrow D_{(s)}^{(*)} \mu \bar{\mu})_S$ by properly replacing the final decay constants. (We refer to ref. [31] for more details on $W_{\text{CF}}(B_c \rightarrow D_{(s)}^{(*)} \mu \bar{\mu})$ calculation.) The decay constants of the scalar and axial-vector mesons can be found in ref. [35]. But due to the angular momentum conservation condition, the longitudinal decay constants of the tensor mesons are zero. Hence, we have $W_{\text{CF}}(B_c \rightarrow D_{s_2}^*(2573)(D_2^*(2460)) \mu \bar{\mu}) = 0$.

3.2 Wave functions in BS method

In BS method, the meson is considered to be a bound state of two constituent quarks and can be described by the BS wave functions [28]. In the framework of instantaneous approximation [34], the time component of the BS wave functions' arguments can be integrated out and the BS equations are reduced to the Salpeter equations. By means of solving the Salpeter equations, we obtain the wave function [35–38] for each meson.

In the present work, the mesons $D_{s_0}^*(2317)$, $D_0^*(2400)$, $D_{s_2}^*(2573)$, $D_2^*(2460)$, $D_{s_1}(2460, 2536)$, $D_1(2420, 2430)$ and B_c are relevant. In the following paragraphs, their wave functions are introduced.

(1) Wave functions of $D_{s_0}^*(2317)$ and $D_0^*(2400)$. Based on ref. [22], J^P s of $D_{s_0}^*(2317)$ and $D_0^*(2400)$ mesons are 0^+ . In this paper, we consider them as 3P_0 states. In the BS approach, the positive energy wave function for 3P_0 state can be expressed as [39]

$$\varphi_{^3P_0}^{++} = a_1 \left(\not{q}_{P_\perp} + a_2 \frac{\not{P} \not{q}_{P_\perp}}{M} + a_3 + a_4 \frac{\not{P}}{M} \right), \quad (3.8)$$

where the parameters a_{1-4} can be found in ref. [39].

(2) Wave functions of $D_{s_2}^*(2573)$ and $D_2^*(2460)$. From ref. [22], J^P s of $D_{s_2}^*(2536)$ and $D_2^*(2460)$ mesons are 2^+ . In this paper, they are described as 3P_2 states. The positive energy wave function for 3P_2 state is [39]

$$\begin{aligned} \varphi_{^3P_2}^{++} = \epsilon_{\mu\nu}^T q_{P_\perp}^\nu \left\{ q_{P_\perp}^\mu \left[d_1 + d_2 \frac{\not{P}}{M} + d_3 \frac{\not{q}_{P_\perp}}{M} - d_4 \frac{\not{P} \not{q}_{P_\perp}}{M^2} \right] \right. \\ \left. + \gamma^\mu \left[d_5 + d_6 \frac{\not{P}}{M} + d_7 \frac{\not{q}_{P_\perp}}{M} + d_8 \frac{\not{P} \not{q}_{P_\perp}}{M^2} \right] \right\}, \end{aligned} \quad (3.9)$$

where $\epsilon_{\mu\nu}^T$ is the polarization tensor. The parameters d_{1-8} can be found in refs. [38, 39].

(3) Wave Functions of $D_{s1}(2460, 2536)$ and $D_1(2420, 2430)$. Unlike the mesons introduced above, $D_{s1}(2460, 2536)$ and $D_1(2420, 2430)$ can not be described by the pure $(2S+1)L_J$ states. Based on [40, 41], we consider them as the mixtures of the 1P_1 and 3P_1 states, namely,

$$\begin{aligned} \begin{pmatrix} |D_1(2430)\rangle \\ |D_1(2420)\rangle \end{pmatrix} &= \mathcal{A} \begin{pmatrix} |D_{1P_1}\rangle \\ |D_{3P_1}\rangle \end{pmatrix} \equiv \begin{pmatrix} \sin \alpha & \cos \alpha \\ \cos \alpha & -\sin \alpha \end{pmatrix} \begin{pmatrix} |D_{1P_1}\rangle \\ |D_{3P_1}\rangle \end{pmatrix}, \\ \begin{pmatrix} |D_{s1}(2460)\rangle \\ |D_{s1}(2536)\rangle \end{pmatrix} &= \mathcal{B} \begin{pmatrix} |D_{s^1P_1}\rangle \\ |D_{s^3P_1}\rangle \end{pmatrix} \equiv \begin{pmatrix} \sin \beta & \cos \beta \\ \cos \beta & -\sin \beta \end{pmatrix} \begin{pmatrix} |D_{s^1P_1}\rangle \\ |D_{s^3P_1}\rangle \end{pmatrix}, \end{aligned} \quad (3.10)$$

where $\alpha = \theta - \arctan(\sqrt{1/2})$ and $\beta = \theta_s - \arctan(\sqrt{1/2})$. Based on the experimental observation [42] and the discussions in ref. [41], the mixing angle $\theta = 5.7^\circ$ is used in this paper. Besides, according to the analysis in the quark potential model [43], $\theta_s = 7^\circ$ is employed.

From eq. (3.10), the wave functions of $D_{s1}(2460, 2536)$ and $D_1(2420, 2430)$ can be constructed from the ones of 1P_1 and 3P_1 states. In the BS method, the positive energy wave functions of 1P_1 and 3P_1 states [39] are

$$\begin{aligned} \varphi_{1P_1}^{++} &= b_1 \left(\epsilon_A \cdot q_{P_\perp} \right) \left(1 + b_2 \frac{\mathcal{P}}{M} + b_3 \not{q}_{P_\perp} - b_4 \frac{\mathcal{P} \not{q}_{P_\perp}}{M} \right) \gamma_5, \\ \varphi_{3P_1}^{++} &= i c_1 \epsilon_{\mu\nu\alpha\beta} P^\nu q_{P_\perp}^\alpha \epsilon_A^\beta \left(M \gamma^\mu + c_2 \gamma^\mu \mathcal{P} + c_3 \gamma^\mu \not{q}_{P_\perp} + c_4 \gamma^\mu \mathcal{P} \not{q}_{P_\perp} \right) / M^2, \end{aligned} \quad (3.11)$$

where ϵ_μ^A is the polarization vector of the axial-vector meson. The explicit expressions of b_{1-4} and c_{1-4} can be found in ref. [39] and their numerical values can be obtained by solving the Salpeter equations [35]. In the processes of solving the Salpeter equations, the masses of 1P_1 and 3P_1 states, namely, $M_{D_{(s)1P_1}}$ and $M_{D_{(s)3P_1}}$, are required. In analogy to the case of $\eta_1 - \eta_8$ mixing [44], we determine them from the following relationships [45, 46],

$$\begin{aligned} \mathcal{A}^\dagger \begin{pmatrix} M_{D_1(2430)}^2 & 0 \\ 0 & M_{D_1(2420)}^2 \end{pmatrix} \mathcal{A} &= \begin{pmatrix} M_{D_{1P_1}}^2 & \delta \\ \delta & M_{D_{3P_1}}^2 \end{pmatrix}, \\ \mathcal{B}^\dagger \begin{pmatrix} M_{D_{s1}(2460)}^2 & 0 \\ 0 & M_{D_{s1}(2536)}^2 \end{pmatrix} \mathcal{B} &= \begin{pmatrix} M_{D_{s^1P_1}}^2 & \delta_s \\ \delta_s & M_{D_{s^3P_1}}^2 \end{pmatrix}, \end{aligned} \quad (3.12)$$

where $M_{D_1(2420,2430)}$ and $M_{D_{s1}(2460,2536)}$ stand for the physical masses and we take them from ref. [22].

(4) Wave function of B_c . The B_c meson is considered as a 1S_0 state, whose the positive energy wave function can be written as [36],

$$\varphi_{1S_0}^{++} = e_1 \left[e_2 + \frac{\mathcal{P}}{M} + \not{q}_{P_\perp} e_3 + \frac{\not{q}_{P_\perp} \mathcal{P} - \mathcal{P} \not{q}_{P_\perp}}{2M} e_4 \right] \gamma_5. \quad (3.13)$$

where the parameters e_{1-4} can be found in ref. [36].

3.3 Calculations of hadronic matrix elements

In this part, we calculate the hadronic currents through the formalism introduced above. Since W^μ s have been investigated extensively in our previous papers [39, 47–51], here we do not introduce the W^μ calculations but pay more attentions to $W_{T,ann}^\mu$ s. Please recall that W_T^μ s have been expressed in combinations of $\mathcal{Y}_{V,A}^{\mu\nu}$ s within eq. (3.1), while in eqs. (3.3)–(3.6), W_{ann}^μ s are written in terms of $\mathcal{F}_{i,f0(\pm)}$ s. Hence, in order to obtain $W_{T,ann}^\mu$, it is convenient to compute $\mathcal{Y}_{V,A}^{\mu\nu}$ s and $\mathcal{F}_{i,f0(\pm)}$ s first of all. From their definitions in eq. (3.2) and eq. (3.7), we see that the calculations of $\mathcal{Y}_{V,A}^{\mu\nu}$ s and $\mathcal{F}_{i,f0(\pm)}$ s are channel-dependent and the channels under our consideration include $P \rightarrow S, T, A$ transitions, where P, S, T, A are the abbreviations for pseudo-scalar, scalar, tensor, axial-vector mesons, respectively.

3.3.1 Hadronic matrix elements of $P \rightarrow S$ processes

First, we introduce the details of the $\mathcal{Y}_{V,A}^{\mu\nu}(P \rightarrow S)$ estimations. We have expressed $\mathcal{Y}_{V,A}^{\mu\nu}$ s as the overlapping integrals of $\varphi_{i,f}^{++}$ s in eq. (3.2). In the $P \rightarrow S$ processes, the initial wave function φ_i^{++} corresponds to $\varphi_{1S_0}^{++}$, while φ_f^{++} should be $\varphi_{3P_0}^{++}$. The expressions of $\varphi_{1S_0}^{++}$ and $\varphi_{3P_0}^{++}$ are given in eq. (3.13) and eq. (3.8), respectively. Substituting eqs. (3.8), (3.13) into eq. (3.2), the hadronic matrix elements $\mathcal{Y}_{V,A}^{\mu\nu}$ s can be obtained. In light of the forbidden parity, we have $\mathcal{Y}_V^{\mu\nu}(P \rightarrow S) = 0$, while for $\mathcal{Y}_A^{\mu\nu}(P \rightarrow S)$, it reads

$$\begin{aligned} \mathcal{Y}_A^{\mu\nu}(P \rightarrow S) = & \int \frac{d^3\vec{q}}{(2\pi)^3} \frac{-4a_1e_1}{M_f M_i} \{ M_i [g^{\mu\nu} (q_a \cdot q_b a_2 e_3 e_f + e_4 M_f q_a \cdot q_b + a_4 e_4 P_f \cdot q_a + a_4 e_2 e_f \\ & - a_3 M_f) + q_b^\mu (q_a^\nu a_2 e_3 e_f + q_a^\nu e_4 M_f + a_2 P_f^\nu) - q_a^\mu (q_b^\nu a_2 e_3 e_f + q_b^\nu e_4 M_f + a_4 e_4 P_f^\nu)] \\ & - a_2 e_3 g^{\mu\nu} P_f \cdot q_a P_i \cdot q_b - P_i^\mu [q_b^\nu (e_2 M_f - a_2 e_3 P_f \cdot q_a) + P_f^\nu (a_2 e_3 q_a \cdot q_b + a_4 e_2) \\ & + a_3 e_3 M_f q_a^\nu] + P_f^\mu [q_a^\nu (a_4 e_4 M_i - a_2 e_3 P_i \cdot q_b) + P_i^\nu (a_2 e_3 q_a \cdot q_b + a_4 e_2) - a_2 M_i q_b^\nu] \\ & - a_2 e_3 q_b^\mu P_i^\nu P_f \cdot q_a + a_2 e_3 q_a^\mu P_f^\nu P_i \cdot q_b + a_3 e_3 M_f q_a^\mu P_i^\nu + e_2 M_f g^{\mu\nu} P_i \cdot q_b + e_2 M_f q_b^\mu P_i^\nu \}, \end{aligned} \quad (3.14)$$

where the definition of q_a has been given in section 3.1, while q_b is the relative momentum of the final meson. Due to the spectator approximation, the retarded relationship between q_a and q_b reads [27]

$$q_b^\mu = q_a + \alpha_2^f P_f^\mu - \alpha_2^f E_f P_i / M_i. \quad (3.15)$$

Now we turn to the discussions of $\mathcal{F}_{i,f0(\pm)}(P \rightarrow S)$ s. In eq. (3.7), $\mathcal{F}_{i0(\pm)}$ s are written in terms of φ_i^{++} s, while $\mathcal{F}_{f0(\pm)}$ s are shown in the integrals of φ_f^{++} s. Similar to the calculations of $\mathcal{Y}_{V,A}^{\mu\nu}(P \rightarrow S)$ s, $\varphi_{i(f)}^{++}$ corresponds to $\varphi_{1S_0(3P_0)}^{++}$. So we have

$$\begin{aligned} \mathcal{F}_{i0}^\nu(P \rightarrow S) &= 4e_1 (e_3 M_i q_a + P_i)^\nu, \\ \mathcal{F}_{i+}^{\mu\nu}(P \rightarrow S) &= 4e_1 [-g^{\nu\mu} (e_3 M_i Q \cdot q_a + Q \cdot P_i) + Q^\nu (e_3 M_i q_a^\mu + P_i^\mu) + e_3 M_i Q^\mu q_a^\nu + Q^\mu P_i^\nu], \\ \mathcal{F}_{i-}^{\mu\nu}(P \rightarrow S) &= 4ie_1 (e_3 M_i \epsilon^{\nu\mu Q q_a} + \epsilon^{\nu\mu Q P_i}), \\ \mathcal{F}_{f0}^\nu(P \rightarrow S) &= 4a_1 (a_4 P_f + M_f q_c)^\nu, \\ \mathcal{F}_{f+}^{\mu\nu}(P \rightarrow S) &= 4a_1 \left\{ -g^{\nu\mu} (a_4 Q \cdot P_f + M_f Q \cdot q_c) + Q^\nu (a_4 P_f^\mu + M_f q_c^\mu) + a_4 Q^\mu P_f^\nu + M_f Q^\mu q_c^\nu \right\}, \\ \mathcal{F}_{f-}^{\mu\nu}(P \rightarrow S) &= -4ia_1 (a_4 \epsilon^{\nu\mu Q P_f} + M_f \epsilon^{\nu\mu Q q_c}). \end{aligned} \quad (3.16)$$

3.3.2 Hadronic matrix elements of $P \rightarrow T$ processes

Here we deal with $\mathcal{Y}_{V,A}^{\mu\nu}$ in the $P \rightarrow T$ processes. The calculations of $\mathcal{Y}_{V,A}^{\mu\nu}(P \rightarrow T)$ are similar to the ones of $\mathcal{Y}_{V,A}^{\mu\nu}(P \rightarrow S)$, except replacing the final wave function $\varphi_{3P_0}^{++}$ by $\varphi_{3P_2}^{++}$. The expression of $\varphi_{3P_2}^{++}$ can be found in eq. (3.9). Hence, we have

$$\begin{aligned}\mathcal{Y}_V^{\mu\nu}(P \rightarrow T) &= \int \frac{d^3\vec{q}}{(2\pi)^3} \frac{-4ie_1}{M_f^2 M_i^2} \epsilon_{\alpha\beta}^T q_b^\beta \{ \mathcal{F}_{V1}^{\alpha\mu\nu} + \mathcal{F}_{V2}^{\alpha\mu\nu} + \mathcal{F}_{V3}^{\alpha\mu\nu} + \mathcal{F}_{V4}^{\alpha\mu\nu} + \mathcal{F}_{V5}^{\alpha\mu\nu} + \mathcal{F}_{V6}^{\alpha\mu\nu} + \mathcal{F}_{V7}^{\alpha\mu\nu} \}, \\ \mathcal{Y}_A^{\mu\nu}(P \rightarrow T) &= \int \frac{d^3\vec{q}}{(2\pi)^3} \frac{-4e_1}{M_f^2 M_i} \epsilon_{\alpha\beta}^T q_b^\beta \{ -e_3 \mathcal{F}_{A1}^{\alpha\mu\nu} - e_2 M_i \mathcal{F}_{A2}^{\alpha\mu\nu} - e_4 M_i \mathcal{F}_{A3}^{\alpha\mu\nu} \}.\end{aligned}\quad (3.17)$$

The expressions of $\mathcal{F}_{Vl}^{\alpha\mu\nu}$ and $\mathcal{F}_{Ak}^{\alpha\mu\nu}$, where $l = 1, \dots, 7$ and $k = 1, 2, 3$, are presented in appendix A.

Next, we pay attentions to $\mathcal{F}_{i0(\pm)}(P \rightarrow T)$ s. From eq. (3.7), we see that $\mathcal{F}_{i0(\pm)}(P \rightarrow T)$ s are the same as $\mathcal{F}_{i0(\pm)}(P \rightarrow S)$ s, due to the identical initial meson B_c in the decays $P \rightarrow S, T$. The discussions of $\mathcal{F}_{i0(\pm)}(P \rightarrow S)$ s have been performed in section 3.3.1. But for $\mathcal{F}_{f0(\pm)}(P \rightarrow T)$ s, the situations are different. They should be calculated through eq. (3.7), with the final wave functions φ_f^{++} being $\varphi_{3P_2}^{++}$. After factoring the polarization tensor out, we have

$$\begin{aligned}\mathcal{F}_{f0}^\nu(P \rightarrow T) &= \mathcal{E}_{f0}^{\nu\delta}({}^3P_2) \epsilon_{\delta\sigma}^T q_c^\sigma / M_f, & \mathcal{F}_{f+}^{\mu\nu}(P \rightarrow T) &= \mathcal{E}_{f+}^{\mu\nu\delta}({}^3P_2) \epsilon_{\delta\sigma}^T q_c^\sigma / M_f, \\ \mathcal{F}_{f-}^{\mu\nu}(P \rightarrow T) &= \mathcal{E}_{f-}^{\mu\nu\delta}({}^3P_2) \epsilon_{\delta\sigma}^T q_c^\sigma / M_f,\end{aligned}\quad (3.18)$$

where $\mathcal{E}_{f0, f\pm}({}^3P_2)$ are defined as

$$\begin{aligned}\mathcal{E}_{f0}^{\nu\delta}({}^3P_2) &= 8 \left\{ (d_2 M_f - d_8) P_f^\nu q_c^\delta + M_f \left(d_3 q_c^\nu q_c^\delta + d_5 g^{\delta\nu} M_f \right) + id_8 \epsilon^{\nu\delta P_f q_c} \right\}, \\ \mathcal{E}_{f+}^{\mu\nu\delta}({}^3P_2) &= 4M_f q_c^\delta \left[-g^{\nu\mu} (d_3 Q \cdot q_c + d_2 Q \cdot P_f) + Q^\nu \left(d_3 q_c^\mu + d_2 P_f^\mu \right) + d_3 Q^\mu q_c^\nu + d_2 Q^\mu P_f^\nu \right] \\ &\quad - 2id_8 \left[-2iq_c^\delta \left(-g^{\nu\mu} Q \cdot P_f + Q^\mu P_f^\nu + Q^\nu P_f^\mu \right) - 2g^{\nu\mu} \epsilon^{\delta Q P_f q_c} + 2Q^\nu \epsilon^{\delta\mu P_f q_c} + Q^\delta \epsilon^{\nu\mu P_f q_c} \right. \\ &\quad \left. - 2P_f^\mu \epsilon^{\nu\delta Q q_c} + 2q_c^\mu \epsilon^{\nu\delta Q P_f} \right] + 4d_5 M_f^2 \left(Q^\nu g^{\delta\mu} - Q^\delta g^{\nu\mu} + Q^\mu g^{\nu\delta} \right), \\ \mathcal{E}_{f-}^{\mu\nu\delta}({}^3P_2) &= 2id_8 \left\{ -2g^{\delta\mu} \epsilon^{\nu Q P_f q_c} + 2q_c^\nu \left[\epsilon^{\delta\mu Q P_f} + i \left(Q^\delta P_f^\mu - g^{\delta\mu} Q \cdot P_f \right) \right] \right. \\ &\quad \left. - 2P_f^\nu \left[\epsilon^{\delta\mu Q q_c} + i \left(Q^\delta q_c^\mu - g^{\delta\mu} Q \cdot q_c \right) \right] + 2g^{\nu\delta} \left[\epsilon^{\mu Q P_f q_c} + i \left(q_c^\mu Q \cdot P_f - P_f^\mu Q \cdot q_c \right) \right] \right. \\ &\quad \left. + Q^\delta \epsilon^{\nu\mu P_f q_c} + 2 \left(q_c^\delta \epsilon^{\nu\mu Q P_f} + Q^\mu \epsilon^{\nu\delta P_f q_c} + Q \cdot P_f \epsilon^{\nu\delta\mu q_c} - Q \cdot q_c \epsilon^{\nu\delta\mu P_f} \right) \right\} \\ &\quad - 4iM_f q_c^\delta \left(d_3 \epsilon^{\nu\mu Q q_c} + d_2 \epsilon^{\nu\mu Q P_f} \right) - 4id_5 M_f^2 \epsilon^{\nu\delta\mu Q}.\end{aligned}\quad (3.19)$$

3.3.3 Hadronic matrix elements of $P \rightarrow A$ processes

Due to the mixing nature of the final mesons as formulated in eq. (3.10), the calculations of $\mathcal{Y}_{V,A}^{\mu\nu}(P \rightarrow A)$ s and $\mathcal{F}_{i, f0(\pm)}(P \rightarrow A)$ s are different from the cases of $P \rightarrow S$ and $P \rightarrow T$. In order to obtain $\mathcal{Y}_{V,A}^{\mu\nu}(P \rightarrow A)$ s and $\mathcal{F}_{i, f0(\pm)}(P \rightarrow A)$ s, first of all, we compute $\mathcal{Y}_{V,A}^{\mu\nu}(P \rightarrow A_{3P_1, 1P_1})$ s and $\mathcal{F}_{i, f0(\pm)}(P \rightarrow A_{3P_1, 1P_1})$ s. And then, based on the mixing relationships in eq. (3.10), we combine the results of $P \rightarrow A_{3P_1}$ and $P \rightarrow A_{1P_1}$.

For $\mathcal{Y}_{V,A}^{\mu\nu}(P \rightarrow A_{3P_1,1P_1})$ s, we calculate them from eq. (3.2), with the initial wave function φ_i^{++} being $\varphi_{1S_0}^{++}$ and the final one φ_f^{++} being $\varphi_{3P_1,1P_1}^{++}$. The expressions of $\varphi_{3P_1,1P_1}^{++}$ are given in eq. (3.11), while the initial ones $\varphi_{1S_0}^{++}$ is shown in eq. (3.13). The results of $\mathcal{Y}_{V,A}^{\mu\nu}(P \rightarrow A_{3P_1,1P_1})$ s read

$$\begin{aligned}
 \mathcal{Y}_V^{\mu\nu}(P \rightarrow A_{3P_1}) &= \int \frac{d^3\vec{q}}{(2\pi)^3} \frac{-8c_1c_4e_1}{M_f^2M_i^2} \epsilon^{\nu P_f q_b \epsilon_A} \left[e_4 (M_i^2 \epsilon^{\mu P_f q_a q_b} + 2P_i^\mu \epsilon^{P_f P_i q_a q_b} - 2P_f \cdot P_i \epsilon^{\mu P_i q_a q_b} \right. \\
 &\quad \left. + 2P_i \cdot q_b \epsilon^{\mu P_f P_i q_a} - e_2 M_i \epsilon^{\mu P_f P_i q_b} \right], \\
 \mathcal{Y}_A^{\mu\nu}(P \rightarrow A_{3P_1}) &= \int \frac{d^3\vec{q}}{(2\pi)^3} \frac{-8ic_1e_1}{M_f^2M_i} \epsilon^{\nu P_f q_b \epsilon_A} \left\{ q_b^\mu [M_i (c_4 e_4 P_f \cdot q_a + 2c_3 M_f^2) + c_4 e_2 P_f \cdot P_i] \right. \\
 &\quad \left. - P_f^\mu [c_4 (e_4 M_i q_a \cdot q_b + e_2 P_i \cdot q_b) - 2c_2 M_i] + M_f (e_4 M_i q_a^\mu + e_2 P_i^\mu) \right\}, \\
 \mathcal{Y}_V^{\mu\nu}(P \rightarrow A_{1P_1}) &= \int \frac{d^3\vec{q}}{(2\pi)^3} \frac{-4b_1e_1q_b \cdot \epsilon_A}{M_f M_i} \left\{ M_i [g^{\mu\nu} (e_4 b_3 M_f q_a \cdot q_b + e_4 b_2 P_f \cdot q_a + M_f) - e_4 q_a^\mu \right. \\
 &\quad (b_3 M_f q_b^\nu + b_2 P_f^\nu) + q_b^\mu (b_3 e_4 M_f q_a^\nu + b_4 P_f^\nu)] - b_4 e_3 g^{\mu\nu} P_f \cdot q_a P_i \cdot q_b + b_4 e_3 g^{\mu\nu} q_a \cdot q_b P_f \cdot P_i \\
 &\quad - P_i^\mu [q_b^\nu (b_3 e_2 M_f - b_4 e_3 P_f \cdot q_a) + P_f^\nu (b_4 e_3 q_a \cdot q_b + b_2 e_2) - e_3 M_f q_a^\nu] + P_f^\mu [q_a^\nu (b_2 e_4 M_i \\
 &\quad - b_4 e_3 P_i \cdot q_b) + P_i^\nu (b_4 e_3 q_a \cdot q_b + b_2 e_2) - b_4 M_i q_b^\nu] + b_4 e_3 q_a^\nu q_b^\mu P_f \cdot P_i - b_4 e_3 q_a^\mu q_b^\nu P_f \cdot P_i \\
 &\quad - b_4 e_3 q_b^\mu P_i^\nu P_f \cdot q_a + b_4 e_3 q_a^\mu P_f^\nu P_i \cdot q_b - e_3 M_f q_a^\mu P_i^\nu + b_3 e_2 M_f g^{\mu\nu} P_i \cdot q_b + b_2 e_2 g^{\mu\nu} P_f \cdot P_i \\
 &\quad \left. + b_3 e_2 M_f q_b^\mu P_i^\nu \right\}, \\
 \mathcal{Y}_A^{\mu\nu}(P \rightarrow A_{1P_1}) &= \int \frac{d^3\vec{q}}{(2\pi)^3} \frac{4ib_1e_1q_b \cdot \epsilon_A}{M_f M_i^2} \left\{ M_i \left[b_4 e_3 \left(-g^{\mu\nu} \epsilon^{P_f P_i q_a q_b} - P_f^\mu \epsilon^{\nu P_i q_a q_b} \right. \right. \right. \\
 &\quad \left. \left. + P_i^\mu \epsilon^{\nu P_f q_a q_b} + q_b^\mu \epsilon^{\nu P_f P_i q_a} + P_f^\nu \epsilon^{\mu P_i q_a q_b} - P_i^\nu \epsilon^{\mu P_f q_a q_b} - q_b^\nu \epsilon^{\mu P_f P_i q_a} + P_f \cdot P_i \epsilon^{\mu\nu q_a q_b} \right. \right. \\
 &\quad \left. \left. + P_f \cdot q_a \epsilon^{\mu\nu P_i q_b} + P_i \cdot q_b \epsilon^{\mu\nu P_f q_a} \right) + M_f (b_3 e_2 \epsilon^{\mu\nu P_i q_b} - e_3 \epsilon^{\mu\nu P_i q_a}) + (b_4 e_3 q_a \cdot q_b \right. \\
 &\quad \left. - b_2 e_2) \epsilon^{\mu\nu P_f P_i} \right] - M_i^2 (e_4 b_3 M_f \epsilon^{\mu\nu q_a q_b} - e_4 b_2 \epsilon^{\mu\nu P_f q_a} + b_4 \epsilon^{\mu\nu P_f q_b}) + b_4 (e_3 M_i q_a^\mu \\
 &\quad + 2P_i^\mu) \epsilon^{\nu P_f P_i q_b} - b_4 (e_3 M_i q_a^\nu + 2P_i^\nu) \epsilon^{\mu P_f P_i q_b} + 2 [e_4 (b_3 M_f P_i^\nu \epsilon^{\mu P_i q_a q_b} - b_3 M_f P_i^\mu \epsilon^{\nu P_i q_a q_b} \\
 &\quad - \epsilon^{\mu\nu P_i q_a} (b_3 M_f P_i \cdot q_b + b_2 P_f \cdot P_i) + b_2 P_i^\mu (-\epsilon^{\nu P_f P_i q_a}) + b_2 P_i^\nu \epsilon^{\mu P_f P_i q_a}) \\
 &\quad \left. + b_4 P_f \cdot P_i \epsilon^{\mu\nu P_i q_b} + b_4 P_i \cdot q_b \epsilon^{\mu\nu P_f P_i} \right\}.
 \end{aligned} \tag{3.20}$$

For $\mathcal{F}_{i0(\pm)}(P \rightarrow A_{3P_1,1P_1})$ s, we see that they are identical to $\mathcal{F}_{i0(\pm)}(P \rightarrow S)$ s. But as to $\mathcal{F}_{f0(\pm)}(P \rightarrow A_{3P_1,1P_1})$ s, we need to compute them by substituting $\varphi_{3P_1,1P_1}^{++}$ into eq. (3.7). The results read

$$\begin{aligned}
 \mathcal{F}_{f0}^\alpha(A_{1P_1}) &= 4b_1 q_c \cdot \epsilon_A (b_3 M_f q_c^\alpha + b_2 P_f^\alpha), \\
 \mathcal{F}_{f+}^{\mu\alpha}(A_{1P_1}) &= \frac{4b_1 q_c \cdot \epsilon_A}{M_f} \left[b_3 M_f (-g^{\alpha\mu} Q \cdot q_c + Q^\mu q_c^\alpha + Q^\alpha q_c^\mu) + b_2 (-g^{\alpha\mu} Q \cdot P_f + Q^\mu P_f^\alpha + Q^\alpha P_f^\mu) \right], \\
 \mathcal{F}_{f-}^{\mu\alpha}(A_{1P_1}) &= -\frac{4ib_1 q_c \cdot \epsilon_A (b_3 M_f \epsilon^{\alpha\mu Q q_c} + b_2 \epsilon^{\alpha\mu Q P_f})}{M_f}, \\
 \mathcal{F}_{f0}^\alpha(A_{3P_1}) &= 4c_1 [c_4 (q_c^\alpha M_f q_c \cdot \epsilon_A - q_c^2 \epsilon_A^\alpha) - i \epsilon^{\alpha P_f q_c \epsilon_A}],
 \end{aligned}$$

$$\begin{aligned}
 \mathcal{F}_{f+}^{\mu\alpha}(A_{3P_1}) &= \frac{1}{M_f} 4c_1 \{c_4 M_f [q_c \cdot \epsilon_A (-g^{\alpha\mu} Q \cdot q_c + Q^\mu q_c^\alpha + Q^\alpha q_c^\mu) - q_c^2 (-g^{\alpha\mu} Q \cdot \epsilon_A \\
 &\quad + Q^\mu \epsilon_A^\alpha + Q^\alpha \epsilon_A^\mu)] - i [g^{\alpha\mu} (-\epsilon^{QP_f q_c \epsilon_A}) + Q^\alpha \epsilon^{\mu P_f q_c \epsilon_A} + Q^\mu \epsilon^{\alpha P_f q_c \epsilon_A}]\}, \\
 \mathcal{F}_{f-}^{\mu\alpha}(A_{3P_1}) &= \frac{1}{M_f^2} 4c_1 \left\{ M_f \left[\epsilon_A^\alpha (q_c^\mu Q \cdot P_f - P_f^\mu Q \cdot q_c) + q_c^\alpha (P_f^\mu Q \cdot \epsilon_A - \epsilon_A^\mu Q \cdot P_f) \right. \right. \\
 &\quad \left. \left. + P_f^\alpha (\epsilon_A^\mu Q \cdot q_c - q_c^\mu Q \cdot \epsilon_A) \right] + i c_4 \left[(q_c^\mu P_f^\alpha - q_c^\alpha P_f^\mu) \epsilon^{QP_f q_c \epsilon_A} + \epsilon^{\mu P_f q_c \epsilon_A} (q_c^\alpha Q \cdot P_f \right. \right. \\
 &\quad \left. \left. - P_f^\alpha Q \cdot q_c) + \epsilon^{\alpha P_f q_c \epsilon_A} (P_f^\mu Q \cdot q_c - q_c^\mu Q \cdot P_f) \right] \right\}. \tag{3.21}
 \end{aligned}$$

Finally, with the results above and the mixing relationship in eq. (3.10), we can calculate the hadronic matrix elements of the physical processes from

$$\begin{aligned}
 \begin{pmatrix} \mathcal{Y}_{V,A}^{\mu\nu}(B_c \rightarrow D_1(2430)) \\ \mathcal{Y}_{V,A}^{\mu\nu}(B_c \rightarrow D_1(2420)) \end{pmatrix} &= \mathcal{A} \begin{pmatrix} \mathcal{Y}_{V,A}^{\mu\nu}(B_c \rightarrow D_{1P_1}) \\ \mathcal{Y}_{V,A}^{\mu\nu}(B_c \rightarrow D_{3P_1}) \end{pmatrix}, \\
 \begin{pmatrix} \mathcal{Y}_{V,A}^{\mu\nu}(B_c \rightarrow D_{s1}(2460)) \\ \mathcal{Y}_{V,A}^{\mu\nu}(B_c \rightarrow D_{s1}(2536)) \end{pmatrix} &= \mathcal{B} \begin{pmatrix} \mathcal{Y}_{V,A}^{\mu\nu}(B_c \rightarrow D_{s^1 P_1}) \\ \mathcal{Y}_{V,A}^{\mu\nu}(B_c \rightarrow D_{s^3 P_1}) \end{pmatrix}, \\
 \begin{pmatrix} \mathcal{F}_{f0(\pm)}(B_c \rightarrow D_1(2430)) \\ \mathcal{F}_{f0(\pm)}(B_c \rightarrow D_1(2420)) \end{pmatrix} &= \mathcal{A} \begin{pmatrix} \mathcal{F}_{f0(\pm)}(B_c \rightarrow D_{1P_1}) \\ \mathcal{F}_{f0(\pm)}(B_c \rightarrow D_{3P_1}) \end{pmatrix}, \\
 \begin{pmatrix} \mathcal{F}_{f0(\pm)}(B_c \rightarrow D_{s1}(2460)) \\ \mathcal{F}_{f0(\pm)}(B_c \rightarrow D_{s1}(2536)) \end{pmatrix} &= \mathcal{B} \begin{pmatrix} \mathcal{F}_{f0(\pm)}(B_c \rightarrow D_{s^1 P_1}) \\ \mathcal{F}_{f0(\pm)}(B_c \rightarrow D_{s^3 P_1}) \end{pmatrix}. \tag{3.22}
 \end{aligned}$$

During our calculations of eq. (3.22), to avoid the kinematic confusion, we consider M_f in eqs. (3.20)–(3.21) as the physical mass of the final meson. (In this paper, the masses of 1P_1 and 3P_1 states introduced in Eq (3.12) are used only in solving the BS equations.) This approximation can also be found in the investigations of $B \rightarrow K_1(1270, 1400)\bar{l}l$ [52–56].

3.4 The definitions of form factors

In the previous parts, we show how to calculate the hadronic currents. In order to show their results conveniently, here we parameterize the hadronic matrix elements in terms of the form factors. In this paper, we do not define the form factors of W_{CFs} , because as introduced in section 3.1, $W_{\text{CF}}^\mu(P \rightarrow S, A)$ can be obtained from $W_{\text{CF}}^\mu(P \rightarrow P, V)$ by some trivial replacements, while $W_{\text{CF}}^\mu(P \rightarrow T) = 0$. Hence, in the following paragraphs, we pay more attentions to the form factors of $W_{(T)}$ and W_{anns} .

In the case of the $P \rightarrow S\bar{l}l$ transitions, according to the Lorentz symmetry and the gauge invariant condition of the Ann currents discussed in section 3.1, we have

$$\begin{aligned}
 W^\mu(P \rightarrow S) &= F_z^S \left(P_+^\mu - \frac{P_+ \cdot Q}{Q^2} Q^\mu \right) + F_0^S \frac{P_+ \cdot Q}{Q^2} Q^\mu, \\
 W_T^\mu(P \rightarrow S) &= \frac{-F_T^S}{M_i + M_f} \{ Q^2 P_+^\mu - (P_+ \cdot Q) Q^\mu \}, \\
 W_{\text{ann}}^\mu(P \rightarrow S) &= B_z^S \{ Q^2 P_+^\mu - (P_+ \cdot Q) Q^\mu \}, \tag{3.23}
 \end{aligned}$$

where $P_+ \equiv P_i + P_f$ and $F_z^S, F_0^S, F_T^S, B_z^S$ are form factors.

Similarly, for $P \rightarrow T\bar{l}\bar{l}$ transitions, the definitions are shown as

$$\begin{aligned}
 W^\mu(P \rightarrow T) &= \frac{iV^T}{(M_i + M_f)M_f} \epsilon_{\alpha\beta}^T Q^\beta \epsilon^{\mu\alpha Q P_+} - 2A_0^T \frac{\epsilon_T^{\alpha\beta} Q_\beta Q_\alpha}{Q^2} Q^\mu - \frac{M_i + M_f}{M_f} A_1^T (\epsilon_T^{\mu\alpha} Q_\alpha \\
 &\quad - \frac{\epsilon_T^{\alpha\beta} Q_\beta Q_\alpha}{Q^2} Q^\mu) + A_2^T \frac{\epsilon_T^{\alpha\beta} Q_\beta Q_\alpha}{M_f(M_i + M_f)} \left\{ P_+^\mu - \frac{P_+ \cdot Q}{Q^2} Q^\mu \right\}, \\
 W_T^\mu(P \rightarrow T) &= -i \frac{T_1^T}{M_f} \epsilon_{\alpha\beta}^T Q^\beta \epsilon^{\mu\alpha Q P_+} + \frac{T_2^T}{M_f} \left\{ P_+ \cdot Q \epsilon_T^{\mu\beta} Q_\beta - (\epsilon_T^{\alpha\beta} Q_\beta Q_\alpha) P_+^\mu \right\} \\
 &\quad + \frac{T_3^T}{M_f} (\epsilon_T^{\alpha\beta} Q_\beta Q_\alpha) \left\{ Q^\mu - \frac{Q^2}{P_+ \cdot Q} P_+^\mu \right\}, \\
 W_{\text{ann}}^\mu(P \rightarrow T) &= (M_i - M_f) \left\{ T_{1\text{ann}}^T \frac{M_i^2}{M_f} \left(\epsilon_T^{\mu\alpha} Q_\alpha - \frac{Q^\alpha Q^\beta \epsilon_{\alpha\beta}^T}{Q^2} Q^\mu \right) + \frac{T_{\text{zann}}^T}{M_f} \epsilon_T^{\alpha\beta} Q_\alpha Q_\beta (P_+^\mu \right. \\
 &\quad \left. - \frac{P_+ \cdot Q}{Q^2} Q^\mu) + \frac{1}{2} i \frac{V_{\text{ann}}^T}{M_f} \epsilon_{\alpha\beta}^T Q^\beta \epsilon^{\mu\alpha Q P_+} \right\}, \tag{3.24}
 \end{aligned}$$

where $V^T, A_1^T, A_2^T, A_0^T, T_1^T, T_2^T, T_3^T, T_{1\text{ann}}^T, T_{\text{zann}}^T$ and V_{ann}^T are the form factors.

As to $P \rightarrow A\bar{l}\bar{l}$ decays, the definitions take the following forms,

$$\begin{aligned}
 W^\mu(P \rightarrow A) &= \frac{iV^A}{M_i + M_f} \epsilon^{\mu\epsilon_A Q P_+} - 2M_f A_0^A \frac{\epsilon_A \cdot Q}{Q^2} Q^\mu - (M_i + M_f) A_1^A \left(\epsilon_A^\mu - \frac{\epsilon_A \cdot Q}{Q^2} Q^\mu \right) \\
 &\quad + A_2^A \frac{\epsilon_A \cdot Q}{M_i + M_f} \left\{ P_+^\mu - \frac{P_+ \cdot Q}{Q^2} Q^\mu \right\}, \\
 W_T^\mu(P \rightarrow A) &= -iT_1^A \epsilon^{\mu\epsilon_A Q P_+} + T_2^A \left\{ P_+ \cdot Q \epsilon_A^\mu - (\epsilon_A \cdot Q) P_+^\mu \right\} \\
 &\quad + T_3^A (\epsilon_A \cdot Q) \left\{ Q^\mu - \frac{Q^2}{P_+ \cdot Q} P_+^\mu \right\}, \\
 W_{\text{ann}}^\mu(P \rightarrow A) &= (M_i - M_f) \left\{ T_{1\text{ann}}^A M_i^2 \left(\epsilon_A^\mu - \frac{Q \cdot \epsilon_A}{Q^2} Q^\mu \right) + T_{\text{zann}}^A Q \cdot \epsilon_A \left(P_+^\mu - \frac{P_+ \cdot Q}{Q^2} Q^\mu \right) \right. \\
 &\quad \left. + \frac{1}{2} i V_{\text{ann}}^A \epsilon^{\mu\epsilon_A Q P_+} \right\}, \tag{3.25}
 \end{aligned}$$

where $V^A, A_1^A, A_2^A, A_0^A, T_1^A, T_2^A, T_3^A, T_{1\text{ann}}^A, T_{\text{zann}}^A$ and V_{ann}^A are the form factors.

3.5 Numerical results of form factors

In this part, we present the numerical results of form factors and the according discussions.

3.5.1 Parameters in the calculations

Here we specify the involved parameters. First, the masses and the lifetimes of B_c and $D_{(s)J}^{(*)}$ are required in our calculations and we take their values from ref. [22]. Second, the BS-inputs are also needed, which include the Cornell-Potential-Parameters (CPPs) and the masses of the constituent quarks. The CPPs can be found in ref. [57]. The masses of the constituent quarks are taken as $m_b = 4.96$ GeV, $m_c = 1.62$ GeV, $m_s = 0.5$ GeV and $m_d = 0.311$ GeV [47].

3.5.2 Results and discussions on form factors

From the aforementioned parameters and the derivations in section 3.3, the form factors can be evaluated. In the following paragraphs, we will show and discuss them.

In figure 3(a), the form factors of $W_{(T)}^\mu(B_c \rightarrow D_{s0}^*(2317))$ are presented. These form factors are all positively related to Q^2 . This behavior can be understood from the facts that 1) as shown in eqs. (3.1)–(3.2), our hadronic currents $W_{(T)}^\mu$ s are obtained from the integrals over the overlapping regions of the initial and final wave functions and 2) due to the retarded relationship in eq. (3.15), the overlapping regions grow with increase in the variable Q^2 .

In recent years, $W_{(T)}^\mu(B_c \rightarrow D_{s0}^*(2317))$ have also been calculated in the three-point QCD sum rules [23] and light-cone quark model [24]. The definitions of the $W_{(T)}^\mu$ form factors in refs. [23, 24] are different from the ones in this paper. But if the same definitions are taken, the absolute values of our form factors are comparable with theirs.

Figure 3(b) shows the form factors of $W_{\text{ann}}^\mu(B_c \rightarrow D_{s0}^*(2317))$. We see that B_z^S are complex. The reason is that in the calculations of the W_{ann} , the quark propagators are involved, as shown in eqs. (3.3)–(3.6). In order to deal with these propagators, we separate them into two parts: the principal value terms and δ function ones. The real part of B_z^S comes from the principal value terms, while its imaginary part is caused by δ function terms.²

Figures 4(a, b) display the results of $W_{(T)}^\mu(B_c \rightarrow D_{s2}^*(2573))$. Similar to $W_{(T)}^\mu(B_c \rightarrow D_{s0}^*(2317))$, the form factors of $W_{(T)}^\mu(B_c \rightarrow D_{s2}^*(2573))$ also increase monotonically as Q^2 grows. This similarity comes from the facts that both $W_{(T)}^\mu(B_c \rightarrow D_{s0}^*(2317))$ and $W_{(T)}^\mu(B_c \rightarrow D_{s2}^*(2573))$ are evaluated by eqs. (3.1)–(3.2).

In figures 4(c, d), the Ann form factors of $B_c \rightarrow D_{s2}^*(2573)\bar{l}\bar{l}$ process are plotted. One may note that the absolute values of these form factors are quite smaller than the ones of $W_{\text{ann}}^\mu(B_c \rightarrow D_{s0}^*(2317))$. To see how this happens, one should recall that the Ann currents W_{ann} are the sums of the terms $W_{\text{ann}1, \dots, \text{ann}4}$ s. In the case of $W_{\text{ann}}^\mu(B_c \rightarrow D_{s0}^*(2317))$, the four terms all contribute. But as to $W_{\text{ann}}^\mu(B_c \rightarrow D_{s2}^*(2573))$, the vanishing decay constant of the final meson forbids the $W_{\text{ann}1, \text{ann}2}$ contributions and leaves only $W_{\text{ann}3, \text{ann}4}$ terms. Compared with the sums of $W_{\text{ann}1}$ and $W_{\text{ann}2}$, the contributions of $W_{\text{ann}3}$ and $W_{\text{ann}4}$ are fairly suppressed.³ Thus, we see the smaller $W_{\text{ann}}^\mu(B_c \rightarrow D_{s2}^*(2573))$ form factors in figures 4(c, d).

In figures 5(a, b) and figures 6(a, b), we plot the BP form factors of $B_c \rightarrow D_{s1}(2460, 2536)\bar{l}\bar{l}$. First, we see that the form factors of $W_{(T)}^\mu(B_c \rightarrow D_{s1}(2460, 2536))$ are not of the same sign. To understand this feature, recall that in order to calculate $W_{(T)}^\mu(B_c \rightarrow D_{s1}(2460, 2536))$, the hadronic currents $W_{(T)}(B_c \rightarrow D_{s^1 P_1, ^3 P_1})$ are first evalu-

²The monotonicity of the BP form factors and complexity of the Ann form factors can also be found in the case of $B_c \rightarrow D_{(s)}^{(*)}\mu\bar{\mu}$ processes [31]. And in ref. [31], there is a more detailed discussion on them.

³The reason of this suppression is that $W_{\text{ann}3}$ and $W_{\text{ann}4}$ correspond to the diagrams where the virtual photons are emitted from the final quarks. Under the non-relativistic limit, the propagated quarks of these diagrams are highly off-shell and therefore when calculating the amplitudes of these diagrams, the denominators are considerably large. Even though the relativistic effects are included, this kind of suppression is still not obviously ameliorated.

ated and then we mix the results according to the mixing relationship in eq. (3.22). The form factors of $W_{(T)}(B_c \rightarrow D_{s^1 P_1, 3 P_1})$ are all of the same sign. But in the mixing step, we need to evaluate the sums and differences of the $W_{(T)}(B_c \rightarrow D_{s^1 P_1, 3 P_1})$ form factors. Hence, as illustrated in figures 5 (a, b) and figures 6 (a, b), the form factors with the different signs emerge.

Second, from figures 6 (a, b), one may note that the absolute values of V^A , A_1^A , T_1^A and T_2^A are much smaller than those of $A_{0,2}^A$ and T_3^A . This feature implies that the hadronic matrix element $W_{(T)}(B_c \rightarrow D_{s1}(2536)_\perp)$ obtained in the BS method is suppressed significantly compared with $W_{(T)}(B_c \rightarrow D_{s1}(2536)_\parallel)$. Here $D_{s1}(2536)_\perp(\parallel)$ stands for the final meson $D_{s1}(2536)$ which is transversely (longitudinally) polarized.

Figures 5 (c, d) and figures 6 (c, d) present the Ann form factors of $B_c \rightarrow D_{s1}(2460, 2536)\bar{l}l$. Due to the suppressions from the small decay constant of $D_{s1}(2536)$ [35], we see that the form factors corresponding to $W_{\text{ann}}(B_c \rightarrow D_{s1}(2536))$ are much smaller than those of $W_{\text{ann}}(B_c \rightarrow D_{s1}(2460))$.

In figures 7–10, we illustrate the form factors of $B_c \rightarrow D_J^{(*)}\bar{l}l$ decays. The form factors of $W_{(T),\text{ann}}(B_c \rightarrow D_J^{(*)})$ behave similarly to the $W_{(T),\text{ann}}(B_c \rightarrow D_{sJ}^{(*)})$ ones. This is because 1) as discussed in section 3.3, $W_{(T),\text{ann}}(B_c \rightarrow D_J^{(*)})$ and $W_{(T),\text{ann}}(B_c \rightarrow D_{sJ}^{(*)})$ are calculated within the same formalism and 2) in the BS method, due to the constituent mass relationship $m_s \sim m_d \ll m_c$, the wave functions of $D_J^{(*)}$ are quite comparable with the $D_{sJ}^{(*)}$ ones.

4 The observables

In the previous section, we calculate the hadronic matrix elements within the BS method and express the results in terms of the form factors. Using these form factors, the total amplitude $\mathcal{M}_{\text{Total}}$ in eq. (2.7) can be estimated. From the obtained total amplitude, in this section, we evaluate the physical observables.

4.1 The calculations of observables

In this part, we employ the helicity amplitude method [32] to calculate observables.

First of all, we need to split the total transition amplitudes as

$$\mathcal{M}_{\text{Total}} \equiv \mathcal{M}_1^\mu \bar{l} \gamma_\mu l + \mathcal{M}_2^\mu \bar{l} \gamma_\mu \gamma_5 l, \quad (4.1)$$

where $\mathcal{M}_{1(2)}^\mu$ can be determined by matching eq. (2.7) to the equation above.

And then by projecting $M_{1(2)}^\mu$ to the helicity components $\epsilon_H^\mu(t, 0, \pm 1)$, the helicity amplitudes can be obtained, that is [32],

$$H_{t, \pm, 0}^{1(2)} = \epsilon_H^\mu(t, \pm, 0) \cdot M_{1(2)}^\mu. \quad (4.2)$$

The explicit expressions of $\epsilon_H^\mu(t, 0, \pm 1)$ are specified in appendix B.

Finally, according to the derivations in ref. [32], the differential branching fractions dBr/dQ^2 , the forward-backward asymmetries A_{FB} , the longitudinal polarizations of the

final mesons P_L and the leptonic longitudinal polarization asymmetries A_{LP_L} can be expressed in terms of helicity amplitudes, which are

$$\begin{aligned}
 \frac{dBr}{dQ^2} &= \frac{1}{(2\pi)^3 \Gamma_{B_c}} \frac{\lambda^{1/2} Q^2}{24M_{B_c}^3} \sqrt{1 - \frac{4m_l^2}{Q^2}} \mathcal{M}_H^2, \\
 A_{FB} &= \frac{3}{4} \sqrt{1 - \frac{4m_l^2}{Q^2}} \frac{2}{\mathcal{M}_H^2} \left\{ \text{Re} \left(H_+^{(1)} H_+^{\dagger(2)} \right) - \text{Re} \left(H_-^{(1)} H_-^{\dagger(2)} \right) \right\}, \\
 P_L &= \frac{1}{\mathcal{M}_H^2} \left\{ H_0^{(1)} H_0^{\dagger(1)} \left(1 + \frac{2m_l^2}{Q^2} \right) + H_0^{(2)} H_0^{\dagger(2)} \left(1 - \frac{4m_l^2}{Q^2} \right) + \frac{2m_l^2}{Q^2} 3H_t^{(2)} H_t^{\dagger(2)} \right\}, \\
 A_{LP_L} &\equiv \frac{dBr_{h=-1/2}/dQ^2 - dBr_{h=1/2}/dQ^2}{dBr_{h=-1/2}/dQ^2 + dBr_{h=1/2}/dQ^2} \\
 &= \sqrt{1 - \frac{4m_l^2}{Q^2}} \frac{2}{\mathcal{M}_H^2} \left\{ \text{Re} \left(H_+^{(1)} H_+^{\dagger(2)} \right) + \text{Re} \left(H_-^{(1)} H_-^{\dagger(2)} \right) + \text{Re} \left(H_0^{(1)} H_0^{\dagger(2)} \right) \right\}, \quad (4.3)
 \end{aligned}$$

where h denotes the helicity of l^- , while the denotation $\lambda = (M_i^2 - M_f^2)^2 + Q^2(Q^2 - 2M_i^2 - 2M_f^2)$ is employed. And the definition of \mathcal{M}_H is

$$\begin{aligned}
 \mathcal{M}_H^2 &= \left(H_+^{(1)} H_+^{\dagger(1)} + H_-^{(1)} H_-^{\dagger(1)} + H_0^{(1)} H_0^{\dagger(1)} \right) \left(1 + \frac{2m_l^2}{Q^2} \right) + \\
 &\quad \left(H_+^{(2)} H_+^{\dagger(2)} + H_-^{(2)} H_-^{\dagger(2)} + H_0^{(2)} H_0^{\dagger(2)} \right) \left(1 - \frac{4m_l^2}{Q^2} \right) + \frac{2m_l^2}{Q^2} 3H_t^{(2)} H_t^{\dagger(2)}. \quad (4.4)
 \end{aligned}$$

Plugging the helicity amplitudes $H_{t,\pm,0}^{1(2)}$ into eq. (4.3), the observables are obtained.

4.2 Numerical results of the observables

Within figures 11–18, the numerical values of the observables are presented in the solid (or dash-dot) lines, while their theoretical uncertainties are illustrated in the pale green (or pink) areas. In this part, we lay stress on the introductions of numerical results of the observables. And in next section, the systematic discussions on the theoretical uncertainties will be shown.

When the numerical values of observables are calculated in this paper, we have considered the BP, Ann, CS and CF diagrams. In order to show their influences clearly, for each channel, we plot 1) the observables where only BP contributions are considered, 2) the ones where BP and CS effects are contained, 3) the ones with BP and Ann influences and 4) the ones including the BP, Ann, CS and CF diagrams. In the following paragraphs, their comparisons and discussions will be presented.

4.2.1 The observables of $B_c \rightarrow D_{s0}^*(2317)\mu\bar{\mu}$ decays

In figures 11 (a, b), the differential branching fractions of $B_c \rightarrow D_{s0}^*(2317)\mu\bar{\mu}$ process are illustrated.

For dBr/dQ^2 which includes only BP contributions, as shown in the dash-dot line of figure 11 (a), we see that dBr/dQ^2 is biggest around $Q^2 \sim 10.5 \text{ GeV}^2$ and suppressed

considerably at the end points. This is similar to the result in ref. [24] but quite different from the one in ref. [23]. If the Ann effects are added, as plotted in the dash-dot line of figure 11 (b), dBr/dQ^2 is enhanced un-negligibly around $Q \sim 12.5 \text{ GeV}^2$.

For dBr/dQ^2 which contains BP and CS effects, as plotted in the solid line of figure 11 (a), because of the Breit-Wigner propagators in C_9^{CS} , the significant enlargements emerge around the resonance regions. If the Ann and CF diagrams are included, as displayed in solid line of figure 11 (b), dBr/dQ^2 around $Q^2 \sim M_{J/\psi}^2$ continues enlarging. But in light of the node structure of the $\psi(2S)$ wave function, which leads to the cancellations in the $W_{\text{CF}}(B_c \rightarrow D_{s0}^*(2317)\psi(2S) \rightarrow D_{s0}^*(2317)\mu\bar{\mu})$ calculation, dBr/dQ^2 around $Q^2 \sim M_{\psi(2S)}^2$ changes imperceptibly. This feature can also be found in the processes $B_c \rightarrow D_{(s)}\mu\bar{\mu}$ [31].

In figures 11 (c, d), we illustrate A_{LPL} s of the $B_c \rightarrow D_{s0}^*(2317)\mu\bar{\mu}$ process.

For A_{LPL} which includes only BP diagrams, as shown in dash-dot line of figure 11 (c), we note that $A_{LPL} \sim -1$ in the region $Q^2 \in [2, 15] \text{ GeV}^2$. In order to see how this happens, note that due to the relationship $C_9^{\text{eff}} \sim C_{10} \gg 2m_b C_7^{\text{eff}}/(M_i + M_f)$, $\mathcal{M}_{\text{BP}}^L$ contributes to \mathcal{M}_{BP} dominantly. (Hereafter, $\mathcal{M}_{\text{BP(ann)}}^{L(R)}$ s stand for the BP (or Ann) amplitudes whose final leptons are all left (or right) handed.) This makes that for the relativistically boosted μ^\pm , $dBr_{h=+1/2}/dQ^2$ s are much bigger than $dBr_{h=-1/2}/dQ^2$ s over the domain $Q^2 \in [2, 15] \text{ GeV}^2$. Hence, from the definition of A_{LPL} in eq. (4.3), we have $A_{LPL} \sim -1$. This feature can also be found in the decays $B_c \rightarrow D_{(s)}^{(*)}\mu\bar{\mu}$ [31].

If the Ann effects are added, as given in dash-dot line of figure 11 (d), A_{LPL} deviates from -1 strongly over the low Q^2 area, while in the high Q^2 region, this kind of deviation becomes weaker. To understand this feature, recall that the real part of Ann form factor $\Re[B_{\text{zann}}^S]$ is positive within the low Q^2 domain but turns negative when $Q^2 \geq 12 \text{ GeV}^2$, as shown in figure 3 (b). When $\Re[B_{\text{zann}}^S] > 0$, $\mathcal{M}_{\text{ann}}^L$ interferes destructively with $\mathcal{M}_{\text{BP}}^L$, making $dBr_{h=+1/2}/dQ^2$ suppressed. But if $\Re[B_{\text{zann}}^S] < 0$, there are constructive interferences between $\mathcal{M}_{\text{ann}}^L$ and $\mathcal{M}_{\text{BP}}^L$, leading to the enhanced $dBr_{h=+1/2}/dQ^2$. Hence, based on eq. (4.3), A_{LPL} should be quite larger than -1 in the low Q^2 domain but become smaller with the increase in Q^2 .

Once the BP, Ann, CS and CF contributions are all considered, as seen in solid line of figure 11 (d), one may find that $A_{LPL} \sim -1$ in the low Q^2 region. This is due to the cancellations between Ann and CF transition amplitudes.

4.2.2 The observables of $B_c \rightarrow D_{s2}^*(2573)\mu\bar{\mu}$ decays

Figures 12 (a–h) depict observables of the $B_c \rightarrow D_{s2}^*(2573)\mu\bar{\mu}$ transition. Considering $W_{\text{CF}}(B_c \rightarrow D_{s2}^*(2573)) = 0$ as discussed in section 3.1, the $B_c \rightarrow D_{s2}^*(2573)\mu\bar{\mu}$ process does not receive any contributions from the CF diagrams. Hence, in figures 12 (a–h), we do not illustrate the observables which include CF effects.

Within figures 12 (a, b), we plot dBr/dQ^2 s as the functions of Q^2 . First, we see that $dBr/dQ^2(B_c \rightarrow D_{s2}^*(2573)\mu\bar{\mu})$ s are much bigger than $dBr/dQ^2(B_c \rightarrow D_{s0}^*(2317)\mu\bar{\mu})$ s around the $Q^2 \sim 0 \text{ GeV}^2$ point. To understand this behavior, note that 1) from eq. (4.3), dBr/dQ^2 s are almost proportional to the sum of $H_{\pm,0}^{(1,2)} H_{\pm,0}^{\dagger(1,2)}$ s and 2) in the low Q^2 area,

the transverse contributions $H_{\pm}^{(1,2)}H_{\pm}^{\dagger(1,2)}$ s can be enhanced significantly by the γ propagators. For $B_c \rightarrow D_{s_2}^*(2573)\mu\bar{\mu}$ decay, both $H_0^{(1,2)}H_0^{\dagger(1,2)}$ s and $H_{\pm}^{(1,2)}H_{\pm}^{\dagger(1,2)}$ s contribute. But in $B_c \rightarrow D_{s_0}^*(2317)\mu\bar{\mu}$ process, only $H_0^{(1,2)}H_0^{\dagger(1,2)}$ s participate. Hence, around the $Q^2 \sim 0$ GeV² point, there are enhancements in $dBr/dQ^2(B_c \rightarrow D_{s_2}^*(2573)\mu\bar{\mu})$ but not in $dBr/dQ^2(B_c \rightarrow D_{s_0}^*(2317)\mu\bar{\mu})$. Second, from figures 12 (a, b), one may note that dBr/dQ^2 including the BP and Ann effects deviates imperceptibly from the one with only BP contribution. This is because that as plotted in figures 4 (c, d), the Ann form factors are quite small, which suppresses \mathcal{M}_{ann} considerably so that the Ann contributions are much less than the BP ones. Hence, as illustrated in figures 12 (a, b), dBr/dQ^2 s show the insensitivities to the Ann diagrams.

Figures 12 (c, d) are devoted to presenting the results of $A_{LPL}(B_c \rightarrow D_{s_2}^*(2573)\mu\bar{\mu})$. When the BP (and CS) effects are included, we see the similarities between $A_{LPL}(B_c \rightarrow D_{s_2}^*(2573)\mu\bar{\mu})$ s and $A_{LPL}(B_c \rightarrow D_{s_0}^*(2317)\mu\bar{\mu})$ s. If the Ann contributions are added, in analogy to the case of $dBr/dQ^2(B_c \rightarrow D_{s_2}^*(2573)\mu\bar{\mu})$ s, $A_{LPL}(B_c \rightarrow D_{s_2}^*(2573)\mu\bar{\mu})$ s also change slightly.

In figures 12 (e, f), we display A_{FBS} of the $B_c \rightarrow D_{s_2}^*(2573)\mu\bar{\mu}$ process. In figure 12 (e), we see that A_{FBS} are positive over the high Q^2 domain (except the resonance regions), while due to suppressions from the γ penguin diagrams, A_{FBS} turn negative in the low Q^2 region. Once the Ann influences are taken into account, likewise for $dBr(B_c \rightarrow D_{s_2}^*(2573)\mu\bar{\mu})/dQ^2$ s and $A_{LPL}(B_c \rightarrow D_{s_2}^*(2573)\mu\bar{\mu})$ s, A_{FBS} behave insensitively to Ann effects.

Figures 12 (g, h) show the results of $P_L(B_c \rightarrow D_{s_2}^*(2573)\mu\bar{\mu})$ s. When only the BP diagrams are contained, P_L is positively related to Q^2 in the low Q^2 region but inversely to Q^2 in the high Q^2 domain. If the Ann effects are added, P_L s change negligibly.

4.2.3 The observables of $B_c \rightarrow D_{s_1}(2460)\mu\bar{\mu}$ decays

Figures 13 (a–h) present the observables of $B_c \rightarrow D_{s_1}(2460)\mu\bar{\mu}$ process. When the BP (and CS) contributions are under consideration, the $B_c \rightarrow D_{s_1}(2460)\mu\bar{\mu}$ observables are similar to those of $B_c \rightarrow D_{s_2}^*(2573)\mu\bar{\mu}$ decays.

But once the CF and Ann effects are included, the $B_c \rightarrow D_{s_1}(2460)\mu\bar{\mu}$ observables behave quite sensitively. More specifically, we see that 1) in figures 13 (c, d), A_{LPL} which includes the BP (and CS) diagrams is negative in the low Q^2 region. But if the CF and Ann contributions are taken account of, A_{LPL} turns positive; 2) in figures 13 (a, b), $dBr/dQ^2(B_c \rightarrow D_{s_1}(2460)\mu\bar{\mu})$ s around $Q^2 = M_{J/\psi}^2$ are enlarged considerably by the CF contributions; 3) in figures 13 (e–h), P_L s and A_{FBS} are suppressed fairly after the Ann and CF effects are added.

These sensitive behaviors imply that the CF and Ann contributions play important roles in the $B_c \rightarrow D_{s_1}(2460)\mu\bar{\mu}$ process. Therefore, when the observables of $B_c \rightarrow D_{s_1}(2460)\mu\bar{\mu}$ transition are calculated, besides the BP and CS Feynman diagrams, it is necessary to include the CF and Ann diagrams.

4.2.4 The observables of $B_c \rightarrow D_{s_1}(2536)\mu\bar{\mu}$ decays

In figures 14 (a–h), the observables of the decay $B_c \rightarrow D_{s_1}(2536)\mu\bar{\mu}$ are illustrated. The behaviors of these observables are very different from those in the $B_c \rightarrow D_{s_1}(2460)\mu\bar{\mu}$ process.

First, we see that if only the BP contribution is considered, $dBr/dQ^2(B_c \rightarrow D_{s1}(2536)\mu\bar{\mu})$ is much smaller than $dBr/dQ^2(B_c \rightarrow D_{s1}(2460)\mu\bar{\mu})$. To understand this smallness, note that, as discussed in section 3.5.2, the BP form factors of the $B_c \rightarrow D_{s1}(2536)\mu\bar{\mu}$ process have different signs. This makes that when $\mathcal{M}_{BP}(B_c \rightarrow D_{s1}(2536)\mu\bar{\mu})$ is calculated, the cancelations emerge between the positive BP form factors and the negative ones. Hence, as shown in figures 13, 14(a), $dBr/dQ^2(B_c \rightarrow D_{s1}(2536)\mu\bar{\mu}) \ll dBr/dQ^2(B_c \rightarrow D_{s1}(2460)\mu\bar{\mu})$.

Second, we see that when only BP Feynman diagrams are included, $A_{FB} \sim 0$ and $P_L \sim 1$ within the area $Q^2 \in [1, 6] \text{ GeV}^2$. To see how this happens, we note that as concluded in section 3.5.2, the hadronic current $W_{(T)}(B_c \rightarrow D_{s1}(2536)_\perp)$ obtained in BS method is much smaller than $W_{(T)}(B_c \rightarrow D_{s1}(2536)_\parallel)$. This implies that, if only BP effects are considered, the transverse helicity amplitudes in the $B_c \rightarrow D_{s1}(2536)\mu\bar{\mu}$ decay are considerably suppressed compared with the longitudinal ones, namely, $H_\pm^{(1,2)} \ll H_0^{(1,2)}$. Hence, according to the expressions of A_{FB} and P_L in eq. (4.3), over the domain $Q^2 \in [1, 6] \text{ GeV}^2$, $|A_{FB}|$ has a quite small value, while P_L almost equals one.

Third, if the Ann and CF influences are contained, the $B_c \rightarrow D_{s1}(2536)\mu\bar{\mu}$ observables show the insensitivities. This is because the decay constant of $D_{s1}(2536)$ is fairly small, which suppresses \mathcal{M}_{ann} and \mathcal{M}_{CF} strongly so that the BP contributions are quite bigger than the others. Hence, as illustrated in figures 14(a–h), when the Ann and CF diagrams are added, there are no obvious deviations in the $B_c \rightarrow D_{s1}(2536)\mu\bar{\mu}$ observables outside the resonance regions.

4.2.5 The observables of $B_c \rightarrow D_J^{(*)}\mu\bar{\mu}$ decays

In figures 15–18(a, b), the differential branching fractions of $B_c \rightarrow D_J^{(*)}\mu\bar{\mu}$ are displayed. One may note that $dBr(B_c \rightarrow D_J^{(*)}\mu\bar{\mu})/dQ^2$ s are much smaller than $dBr(B_c \rightarrow D_{sJ}^{(*)}\mu\bar{\mu})/dQ^2$ s. We attribute this smallness to their suppressed CKM matrix elements. More specifically, for $B_c \rightarrow D_{sJ}^{(*)}\mu\bar{\mu}$, the CKM matrix element of BP diagrams is $V_{tb}V_{ts}^* \sim -A\lambda^2$ [22], while the one corresponding to Ann, CS and CF effects is $V_{cb}V_{cs}^* \sim A\lambda^2$ [22]. But as to $B_c \rightarrow D_J^{(*)}\mu\bar{\mu}$, the CKM matrix element for BP diagrams is $V_{tb}V_{td}^* \sim A\lambda^3$ [22], while the one of Ann, CS and CF contributions is $V_{cb}V_{cd}^* \sim -A\lambda^3$ [22]. Hence, when $dBr/dQ^2(B_c \rightarrow D_J^{(*)}\mu\bar{\mu})$ s are calculated, the small parameter λ suppresses their numerical values.

In figures 15(c, d) and figures 16–18(c–h), the A_{LPLS} , A_{FBS} and P_L s of $B_c \rightarrow D_J^{(*)}\mu\bar{\mu}$ are shown. We see that these observables behave similarly to those in $B_c \rightarrow D_{sJ}^{(*)}\mu\bar{\mu}$ decays. The reasons are 1) in the present work, the Feynman diagrams corresponding to $B_c \rightarrow D_J^{(*)}\mu\bar{\mu}$ are analogous to those of the $B_c \rightarrow D_{sJ}^{(*)}\mu\bar{\mu}$ processes; 2) as shown in section 3.5.2, the $B_c \rightarrow D_J^{(*)}\mu\bar{\mu}$ form factors are quite similar to the $B_c \rightarrow D_{sJ}^{(*)}\mu\bar{\mu}$ ones.

4.3 The experimentally excluded regions and integrated branching fractions

Using the results of dBr/dQ^2 s, as shown in figures 11–18(a, b), now we define the experimentally excluded regions. According to the sensitivities to the CF effects, the decays $B_c \rightarrow D_{(s)J}^{(*)}\mu\bar{\mu}$ fall into two categories. The first category includes $B_c \rightarrow D_0^*(2400)(D_{s0}^*(2317))\mu\bar{\mu}$,

Modes	$Br^{\text{BP+Ann}}$	$Br^{\text{BP+Ann+CS+CF}}$
$B_c \rightarrow D_0^*(2400)\mu\bar{\mu}$	$8.9_{-2.3}^{+2.8} \times 10^{-11}$	$1.1_{-0.4}^{+0.5} \times 10^{-10}$
$B_c \rightarrow D_{s0}^*(2317)\mu\bar{\mu}$	$4.0_{-1.1}^{+1.4} \times 10^{-9}$	$5.4_{-2.0}^{+2.5} \times 10^{-9}$
$B_c \rightarrow D_1(2420)\mu\bar{\mu}$	$8.3_{-1.5}^{+1.9} \times 10^{-10}$	$7.1_{-1.7}^{+1.7} \times 10^{-10}$
$B_c \rightarrow D_1(2430)\mu\bar{\mu}$	$1.2_{-0.2}^{+0.5} \times 10^{-9}$	$9.7_{-2.0}^{+4.5} \times 10^{-10}$
$B_c \rightarrow D_{s1}(2460)\mu\bar{\mu}$	$4.7_{-1.3}^{+1.2} \times 10^{-8}$	$4.5_{-1.2}^{+1.1} \times 10^{-8}$
$B_c \rightarrow D_{s1}(2536)\mu\bar{\mu}$	$3.7_{-0.9}^{+0.4} \times 10^{-8}$	$3.4_{-1.0}^{+0.5} \times 10^{-8}$
$B_c \rightarrow D_2^*(2460)\mu\bar{\mu}$	$9.5_{-2.1}^{+2.6} \times 10^{-10}$	$9.8_{-2.7}^{+3.2} \times 10^{-10}$
$B_c \rightarrow D_{s2}^*(2573)\mu\bar{\mu}$	$4.5_{-1.0}^{+1.3} \times 10^{-8}$	$4.7_{-1.4}^{+1.7} \times 10^{-8}$

Table 1. Branching ratio for each channel.

$B_c \rightarrow D_{s1}(2460)\mu\bar{\mu}$ and $B_c \rightarrow D_1(2430)\mu\bar{\mu}$ channels, which are quite sensitive to the CF contributions. Through comparing dBr/dQ^2 s which contain only BP and Ann effects with the ones which include BP, Ann, CS and CF contributions, we define their experimentally excluded region as

$$\text{Region : } Q^2 > 5 \text{ GeV}^2. \tag{4.5}$$

The second category contains $B_c \rightarrow D_2^*(2460)(D_{s2}^*(2573))\mu\bar{\mu}$, $B_c \rightarrow D_{s1}(2536)\mu\bar{\mu}$ and $B_c \rightarrow D_1(2420)\mu\bar{\mu}$ transitions, which are not sensitive to the CF contributions. So their experimentally excluded area is defined as

$$\text{Region : } Q^2 > 7 \text{ GeV}^2. \tag{4.6}$$

Based on the experimentally excluded regions introduced above, the integrated branching fractions are calculated and shown in table 1. As seen in table 1, the branching fractions including BP and Ann effects are comparable with the ones containing both BP, Ann, CF and CS contributions. This implies that our experimentally excluded regions defined in eqs. (4.5), (4.6) are workable.

5 Discussions

5.1 Estimations of the theoretical uncertainties

In the previous section, the numerical results of the $B_c \rightarrow D_{(s)}^{(*)}J\mu\bar{\mu}$ observables are discussed. In this part, we discuss their theoretical uncertainties.

In this paper, we estimate the theoretical uncertainties of the observables including two aspects. First, the theoretical errors from hadronic matrix elements are considered. Recall that our hadronic currents are calculated in the BS method and the obtained form factors are dependent on the numerical values of the BS inputs. In order to estimate the according

systematic uncertainties, we calculate the observables with changing the BS inputs by $\pm 5\%$. Second, the systematic errors aroused by the factorization hypothesis are included. In the derivations of $\mathcal{M}_{\text{Ann,CS,CF}}$, the factorization hypothesis [33] is employed. In this method, in order to include the non-factorizable contributions, the number of colors N_c in the expression $(C_1/N_c + C_2)$ or $(C_1 + C_2/N_c)$ is treated as an adjustable parameter which should be determined by fitting the experimental data [58–61]. But since that the present experimental data on B_c meson is still rare so that this parameter can not be obtained at the moment, we calculate the observables with $N_c = 3$ but change the numerical values of N_c within the region $[2, \infty]$ for estimating systematic uncertainties brought by factorization hypothesis.

Actually, in recent years, several methods, dealing with the non-factorizable contributions more systematically, have been devoted to investigating the B_c decays, such as perturbative QCD approach (PQCD) [62, 63] and QCD factorization (QCDF) [64]. However, the channels in which the PQCD and QCDF are workable must have energetic final particles. Moreover as to $B_c \rightarrow D_{(s)J}^{(*)} l \bar{l}$, the final mesons have small recoil momenta in the high Q^2 domain. Hence, in this paper, we choose to employ the factorization method [33]. Similar situations can also be found in the calculations of $B_c \rightarrow D_{(s)}^{(*)} l \bar{l}$ [32, 65–73] in which the factorization method has to be used extensively to account for the non-factorizable effects.

Here we stress that using the factorization assumption to deal with the non-factorizable effects is a temporary way in the early stage of investigating the rare B_c decays. A more systematical method is important and necessary. Hence, more work in the future is required.

5.2 Testing the hadronic matrix elements

In the previous subsection, by changing the BS inputs within $\pm 5\%$, we estimate the theoretical uncertainties from hadronic currents. Strictly speaking, this only measures parts of the uncertainties, because the systematic uncertainties from the approximations made within the BS method are not considered. Considering that this kind of uncertainties are rather difficult to be systematically estimated, in fact, we do not control the hadronic uncertainties confidently.⁴ Hence, testing whether the hadronic currents are properly evaluated is important.

From eq. (2.1), we see that within the transition amplitude \mathcal{M}_{BP} , the hadronic currents are multiplied by the Wilson coefficients $C_{7,9}^{\text{eff}}, C_{10}$ which are sensitive to NP. This makes that from the observables of $B_c \rightarrow D_{(s)J}^{(*)} l \bar{l}$, it is quite involved to tell whether each hadronic current is correctly estimated. Hence, in order to test them, it is beneficial to analyze the channels in which the short distance interactions are not sensitive to NP and the hadronic matrix elements are similar or identical to the ones participating in $B_c \rightarrow D_{(s)J}^{(*)} l \bar{l}$.

First, we pay attentions to the decays $B_c \rightarrow D_J^{(*)} \mu \bar{\nu}_\mu$. The processes $B_c \rightarrow D_J^{(*)} \mu \bar{\nu}_\mu$ are induced by the transitions $b \rightarrow u \mu \bar{\nu}_\mu$. From the experiences of B decays, $b \rightarrow u \mu \bar{\nu}_\mu$ is dominated by the SM contributions [22]. In the SM, the according amplitude reads $M(B_c \rightarrow D_J^{(*)} \mu \bar{\nu}_\mu) = -i V_{ub}^* \frac{4G_f}{\sqrt{2}} \langle D_J^{(*)} | \bar{u} \gamma^\alpha (1 - \gamma_5) b | B_c \rangle \bar{l}_\mu \gamma_\alpha (1 - \gamma_5) l_\nu$. In light of the isospin

⁴To our knowledge, most (maybe all) of models, which are employed to calculate the hadronic matrix elements, suffer from this problem.

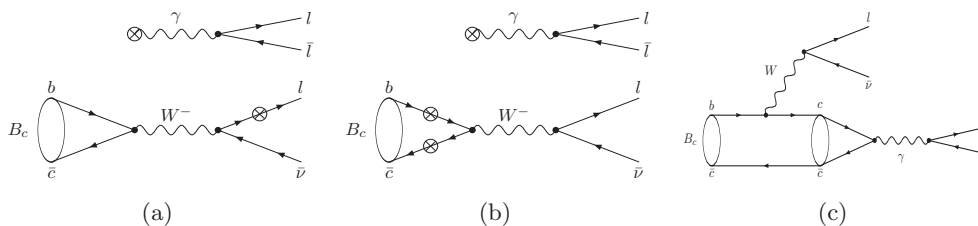


Figure 2. Typical diagrams of $B_c \rightarrow \bar{l}l\bar{\nu}$.

symmetry of u and d quarks, $\langle D_J^{(*)} | \bar{u}\gamma^\alpha(1 - \gamma_5)b | B_c \rangle_s$ are almost identical to $\langle D_J^{(*)} | \bar{d}\gamma^\alpha(1 - \gamma_5)b | B_c \rangle_s$. Hence, by means of investigating the $B_c \rightarrow D_J^{(*)} \mu \bar{\nu}_\mu$ observables experimentally, we can test the form factors of $\langle D_J^{(*)} | \bar{d}\gamma^\alpha(1 - \gamma_5)b | B_c \rangle$. In our previous paper [39], the decays $B_c \rightarrow D_J^{(*)} \mu \bar{\nu}_\mu$ have been calculated.

Second, we turn to investigating $B_c \rightarrow l_A \bar{l}_A l_B \bar{\nu}_B$, whose typical diagrams are illustrated in figure 2. For figure 2(a), the according hadronic matrix element is $\langle 0 | \bar{c}\gamma_\mu(1 - \gamma_5)b | B_c \rangle$, which can be obtained from the future experimental data on pure leptonic decays $B_c \rightarrow l\bar{l}$. As to figure 2(b), the according hadronic matrix elements are the same as $W_{1\text{ann}} + W_{2\text{ann}}$ in eq. (2.4), except the absence of $\langle f | \bar{s}(\bar{d})\gamma_\nu(1 - \gamma_5)c | 0 \rangle$. Likewise, for figure 2(c), its hadronic current is similar to W_{CF} in eq. (2.6), except lacking $\langle f | \bar{s}(\bar{d})\gamma_\nu(1 - \gamma_5)c | 0 \rangle$. Hence, through experimentally detecting $B_c \rightarrow l_A \bar{l}_A l_B \bar{\nu}_B$, we can examine the hadronic currents $W_{1\text{ann}} + W_{2\text{ann}}$ and W_{CF} . (or, parts of $W_{1\text{ann}} + W_{2\text{ann}}$ and W_{CF} .) Considering that in this paper we focus on the calculations of $B_c \rightarrow D_{(s)J}^{(*)} l \bar{l}$, we do not show the results of $B_c \rightarrow l_A \bar{l}_A l_B \bar{\nu}_B$ here but put them into our future work.

However, for the other hadronic matrix elements W_T , $W_{3\text{ann}}$, $W_{4\text{ann}}$ and $W(B_c \rightarrow D_{sJ}^{(*)})$, the ideal channels to examine them are difficult to find unless extra hypothesis is introduced. Hence, we attempt to test them in an indirect way: we use the same framework and the same set of inputs as the ones, which are used to calculate W_T , $W_{3\text{ann}}$, $W_{4\text{ann}}$ and $W(B_c \rightarrow D_{sJ}^{(*)})$, to investigate the processes $B_s \rightarrow D_{sJ}^* \mu \bar{\nu}$, $B \rightarrow D_J^* \mu \bar{\nu}$ and $B_c \rightarrow \chi_{cJ} \mu \bar{\nu}$. The reasons for choosing these channels are that 1) these channels are induced by $b \rightarrow c(u)\mu\bar{\nu}$ transitions, which are dominated by SM contributions from experiences of $B_{(s)}$ decays [22]; 2) unlike the non-leptonic decays, these semi-leptonic processes do not suffer from the theoretical uncertainties from the factorization problem. In our previous papers [50, 74], the processes $B_s \rightarrow D_{sJ}^* \mu \bar{\nu}$, $B \rightarrow D_J^* \mu \bar{\nu}$ were calculated, while in ref. [51], $B_c \rightarrow \chi_{cJ} \mu \bar{\nu}$ were analyzed.

In the paragraphs above, the channels $B_c \rightarrow D_J^{(*)} \mu \bar{\nu}_\mu$, $B_c \rightarrow l_A \bar{l}_A l_B \bar{\nu}_B$, $B_s \rightarrow D_{sJ}^* \mu \bar{\nu}$, $B \rightarrow D_J^* \mu \bar{\nu}$ and $B_c \rightarrow \chi_{cJ} \mu \bar{\nu}$ are recommended in order to test our hadronic matrix elements. At present, only the experimental results on $B \rightarrow D_J^* \mu \bar{\nu}$ [22] are available and most of them are comparable with our theoretical results [50, 74] within the systemic errors. If in the future more experimental results on the $B_{c,s}$ decays are reported, we can continue examining our hadronic matrix elements. Once the deviations appear between our predictions on $B_c \rightarrow D_J^{(*)} \mu \bar{\nu}_\mu$, $B_c \rightarrow l_A \bar{l}_A l_B \bar{\nu}_B$, $B_s \rightarrow D_{sJ}^* \mu \bar{\nu}$, $B \rightarrow D_J^* \mu \bar{\nu}$, $B_c \rightarrow \chi_{cJ} \mu \bar{\nu}$ and the future experimental observations, we need to check whether these deviations come from 1) the BS inputs or the approximations of the BS method; 2) our assumption that $D_{(s)J}^{(*)}$ can be categorized as the conventional charmed(-strange) meson family.

In order to examine the BS inputs and the approximations of the BS method, we should pay attentions to the $B_{c,s,u,d} \rightarrow D_{s,d,u}^{(*)}(\eta_c, J/\psi)\mu\bar{\nu}$ decays whose final mesons are of S-wave states. In our previous papers [48, 75], the observables of the processes $B_{(s)} \rightarrow D_{(s)}^{(*)}\mu\bar{\nu}$ are estimated and the results are in good agreements with the experimental observations [22]. In ref. [76], the $B_c \rightarrow J/\psi(\eta_c)\mu\bar{\nu}$ are analyzed and we expect that these channels can be tested by the future experimental data. If our results deviate from the future data, constraining our BS inputs or modifying BS method is required.

In this work, we take all the $D_{(s)J}^{(*)}$ mesons as the conventional charmed(-strange) mesons. However, there are still controversies on the natures of $D_{s0}^*(2317)$ and $D_{s1}(2460)$ mesons (A recent review on this problem can be found in ref. [77].) For examining whether $D_{s0}^*(2317)$ and $D_{s1}(2460)$ mesons are pure $c\bar{s}$ states, we need to lay stress on their electromagnetic and strong decays. If the future data implies that this assumption is not suitable, we should modify our wave functions describing $D_{(s)J}^{(*)}$ mesons.

6 Conclusion

In this paper, including the BP, Ann, CS and CF contributions, we re-analyze the process $B_c \rightarrow D_{s0}^*(2317)\mu\bar{\mu}$ and first calculate the decays $B_c \rightarrow D_{s1}(2460, 2536)\mu\bar{\mu}$, $B_c \rightarrow D_{s2}^*(2573)\mu\bar{\mu}$ and $B_c \rightarrow D_J^*(\mu\bar{\mu})$. Their results are illustrated in figures 11–18. And our conclusions contain

1. If only BP effects are considered, our results on the $B_c \rightarrow D_{s0}^*(2317)\mu\bar{\mu}$ transition are agreeable with the ones in ref. [24] but quite different from the ones in ref. [23]. Once Ann, CS and CF Feynman diagrams are contained, the $B_c \rightarrow D_{s0}^*(2317)\mu\bar{\mu}$ observables change considerably, as shown in figures 11 (a-d).
2. As plotted in figures 14, 18 (a-h), the observables of the $B_c \rightarrow D_{s1}(2536)(D_1(2430))\mu\bar{\mu}$ processes behave quite sensitively to the Ann and CF influences. This makes that when these channels are analyzed, besides the BP and CS diagrams, it is necessary to include the Ann and CF ones.
3. Unlike the case of $B_c \rightarrow D_{s1}(2536)(D_1(2430))\mu\bar{\mu}$, the observables of the $B_c \rightarrow D_{s2}^*(2573)\mu\bar{\mu}$, $B_c \rightarrow D_2^*(2460)\mu\bar{\mu}$, $B_c \rightarrow D_{s1}(2536)\mu\bar{\mu}$ and $B_c \rightarrow D_1(2420)\mu\bar{\mu}$ processes are influenced by Ann and CF diagrams slightly. Hence, if only BP effects are interesting, these channels offer purer laboratories than the $B_c \rightarrow D_{s1}(2536)(D_1(2430))\mu\bar{\mu}$ processes.

Acknowledgments

Our gratitude are expressed to Ramesh Verma (Punjabi University) and Hai-Yang Cheng (Institute of Physics, Academia Sinica) with whom we had very important and helpful discussions on the mixing natures of the axial vector mesons. This work is supported in part by the National Natural Science Foundation of China (NSFC) under Grant Nos. 11175051, 11347193, 11175151 and 11235005, in part by the Fundamental Research

Funds for the Central Universities, Program for Innovation Research of Science in Harbin Institute of Technology, and in part by the Program for New Century Excellent Talents in University (NCET) by Ministry of Education of P. R. China (Grant No. NCET-13-0991).

A Definitions of $\mathcal{F}_{V1-7}^\alpha$ and $\mathcal{F}_{A1-3}^\alpha$

Here we present the explicit expressions of $\mathcal{F}_{V1-7}^\alpha$ and $\mathcal{F}_{A1-3}^\alpha$.

$$\begin{aligned} \mathcal{F}_{V1}^\alpha = & d_8 e_4 M_i^2 (-g^{\mu\nu}) \epsilon^{\alpha P_f q_a q_b} + d_8 \epsilon^{\alpha P_f P_i q_b} (2e_4 (q_a^\nu P_i^\mu - q_a^\mu P_i^\nu) + e_2 M_i g^{\mu\nu}) + \epsilon^{\alpha P_f P_i q_a} (d_6 e_3 \\ & M_f M_i g^{\mu\nu} - 2d_8 e_4 (g^{\mu\nu} P_i \cdot q_b + q_b^\mu P_i^\nu - q_b^\nu P_i^\mu)) + \epsilon^{\alpha P_i q_a q_b} (d_7 e_3 M_f M_i g^{\mu\nu} + \\ & 2d_8 e_4 (g^{\mu\nu} P_f \cdot P_i - P_f^\nu P_i^\mu + P_f^\mu P_i^\nu)). \end{aligned} \quad (\text{A.1})$$

$$\begin{aligned} \mathcal{F}_{V2}^\alpha = & -M_i \epsilon^{\mu\alpha P_f q_a} (d_8 e_4 M_i q_b^\nu + d_6 e_3 M_f P_i^\nu) - d_8 M_i (e_4 M_i q_a^\nu + e_2 P_i^\nu) \epsilon^{\mu\alpha P_f q_b} + M_i \epsilon^{\mu\alpha q_a q_b} \\ & (d_7 e_3 M_f P_i^\nu - d_8 e_4 M_i P_f^\nu) + \epsilon^{\mu\alpha P_f P_i} (-2P_i^\nu (d_8 e_4 q_a \cdot q_b + d_6 M_f) + q_a^\nu (2d_8 e_4 P_i \cdot q_b \\ & P_i \cdot q_b - d_6 e_3 M_f M_i) + d_8 e_2 M_i q_b^\nu) + \epsilon^{\mu\alpha P_i q_a} (e_3 M_f M_i (d_7 q_b^\nu + d_6 P_f^\nu) - 2e_4 (d_8 (P_f^\nu P_i \cdot q_b \\ & - q_b^\nu P_f \cdot P_i) + d_5 M_f^2 P_i^\nu)) + \epsilon^{\mu\alpha P_i q_b} (P_i^\nu (2d_7 M_f - 2d_8 e_4 P_f \cdot q_a) + q_a^\nu (d_7 e_3 M_f M_i \\ & + 2d_8 e_4 P_f \cdot P_i) + d_8 e_2 M_i P_f^\nu). \end{aligned} \quad (\text{A.2})$$

$$\begin{aligned} \mathcal{F}_{V3}^\alpha = & M_i \epsilon^{\mu P_f q_a q_b} (d_8 e_4 M_i g^{\alpha\nu} - d_4 e_3 q_b^\alpha P_i^\nu) + \epsilon^{\mu P_f P_i q_a} (2e_4 (q_b^\alpha (d_8 - d_2 M_f) P_i^\nu + d_8 (g^{\alpha\nu} P_i \cdot q_b \\ & - q_b^\nu P_i^\alpha)) - e_3 M_i (d_4 q_b^\alpha q_b^\nu + d_6 M_f g^{\alpha\nu})) + \epsilon^{\mu P_i q_a q_b} (e_3 M_i (d_4 q_b^\alpha P_f^\nu - d_7 M_f g^{\alpha\nu}) - 2e_4 (d_3 \\ & M_f q_b^\alpha P_i^\nu + d_8 (g^{\alpha\nu} P_f \cdot P_i - P_f^\nu P_i^\alpha))) + \epsilon^{\mu P_f P_i q_b} (-q_a^\nu (d_4 e_3 M_i \epsilon_1 \cdot q_b + 2d_8 e_4 \alpha \cdot P_i) \\ & - 2(d_4 - d_8 e_4) q_a^\alpha P_i^\nu - d_8 e_2 M_i g^{\alpha\nu}). \end{aligned} \quad (\text{A.3})$$

$$\begin{aligned} \mathcal{F}_{V4}^\alpha = & M_i \epsilon^{\nu\alpha P_f q_a} (d_8 e_4 M_i q_b^\mu + d_6 e_3 M_f P_i^\mu) + d_8 M_i (e_4 M_i q_a^\mu + e_2 P_i^\mu) \epsilon^{\nu\alpha P_f q_b} + M_i \epsilon^{\nu\alpha q_a q_b} (d_8 e_4 \\ & M_i P_f^\mu - d_7 e_3 M_f P_i^\mu) + \epsilon^{\nu\alpha P_f P_i} (2P_i^\mu (d_8 e_4 q_a \cdot q_b + d_6 M_f) + q_a^\mu (d_6 e_3 M_f M_i - 2d_8 e_4 P_i \cdot q_b) \\ & - d_8 e_2 M_i q_b^\mu) + \epsilon^{\nu\alpha P_i q_a} (2e_4 (d_8 (P_f^\mu P_i \cdot q_b - q_b^\mu P_f \cdot P_i) + d_5 M_f^2 P_i^\mu) - e_3 M_f M_i (d_7 q_b^\mu \\ & + d_6 P_f^\mu)) + \epsilon^{\nu\alpha P_i q_b} (2P_i^\mu (d_8 e_4 P_f \cdot q_a - d_7 M_f) - q_a^\mu (d_7 e_3 M_f M_i + 2d_8 e_4 P_f \cdot P_i) \\ & - d_8 e_2 M_i P_f^\mu). \end{aligned} \quad (\text{A.4})$$

$$\begin{aligned} \mathcal{F}_{V5}^\alpha = & \epsilon^{\nu P_f P_i q_b} (M_i (d_4 e_3 q_a^\mu q_b^\alpha + d_8 e_2 g^{\alpha\mu}) + 2P_i^\mu (d_4 q_b^\alpha - d_8 e_4 q_a^\alpha) + 2d_8 e_4 q_a^\mu P_i^\alpha) + M_i \epsilon^{\nu P_f q_a q_b} \\ & (d_4 e_3 q_b^\alpha P_i^\mu - d_8 e_4 M_i g^{\alpha\mu}) + \epsilon^{\nu P_f P_i q_a} (2e_4 (q_b^\alpha (d_2 M_f - d_8) P_i^\mu + d_8 (q_b^\mu P_i^\alpha - g^{\alpha\mu} P_i \cdot q_b)) \\ & + e_3 M_i (d_4 q_b^\alpha q_b^\mu + d_6 M_f g^{\alpha\mu})) + \epsilon^{\nu P_i q_a q_b} (e_3 M_i (d_7 M_f g^{\alpha\mu} - d_4 q_b^\alpha P_f^\mu) + 2e_4 (d_3 M_f q_b^\alpha P_i^\mu \\ & + d_8 (g^{\alpha\mu} P_f \cdot P_i - P_f^\mu P_i^\alpha))). \end{aligned} \quad (\text{A.5})$$

$$\begin{aligned} \mathcal{F}_{V6}^\alpha = & M_i \epsilon^{\mu\nu\alpha P_f} (M_i (d_8 e_4 q_a \cdot q_b + d_6 M_f) + d_8 e_2 P_i \cdot q_b) + \epsilon^{\mu\nu\alpha P_i} (-2(P_f \cdot P_i (d_8 e_4 q_a \cdot q_b \\ & + d_6 M_f) + d_7 M_f P_i \cdot q_b) + M_f M_i (d_5 e_2 M_f - e_3 (d_7 q_a \cdot q_b + d_6 P_f \cdot q_a)) + 2d_8 e_4 P_f \cdot q_a P_i \cdot q_b) \\ & - M_f M_i \epsilon^{\mu\nu\alpha q_a} (e_3 (d_7 P_i \cdot q_b + d_6 P_f \cdot P_i) + d_5 e_4 M_f M_i) - M_i \epsilon^{\mu\nu\alpha q_b} (M_i (d_8 e_4 P_f \cdot q_a \\ & - d_7 M_f) + d_8 e_2 P_f \cdot P_i). \end{aligned} \quad (\text{A.6})$$

$$\begin{aligned} \mathcal{F}_{V7}^\alpha = & M_i \epsilon^{\mu\nu P_f q_b} (M_i (d_8 e_4 q_a^\alpha - d_4 q_b^\alpha) + d_8 e_2 P_i^\alpha) + \epsilon^{\mu\nu P_f P_i} (2P_i^\alpha (d_8 e_4 q_a \cdot q_b + d_6 M_f) \\ & + q_a^\alpha (d_6 e_3 M_f M_i - 2d_8 e_4 P_i \cdot q_b) + q_b^\alpha (M_i (d_4 e_3 q_a \cdot q_b + e_2 (d_2 M_f - d_8)) + 2d_4 P_i \cdot q_b)) \\ & + M_i \epsilon^{\mu\nu P_f q_a} (q_b^\alpha (d_4 e_3 P_i \cdot q_b + e_4 M_i (d_8 - d_2 M_f)) + d_6 e_3 M_f P_i^\alpha) + \epsilon^{\mu\nu P_i q_a} (q_b^\alpha (2e_4 \end{aligned} \quad (\text{A.7})$$

$$\begin{aligned}
 & (d_3 M_f P_i \cdot q_b + (d_2 M_f - d_8) P_f \cdot P_i) - e_3 M_f M_i (d_1 M_f + d_7)) + 2d_5 e_4 M_f^2 P_i^\alpha + \epsilon^{\mu\nu P_i q_b} \\
 & (q_b^\alpha (M_i (d_4 e_3 P_f \cdot q_a - d_3 e_2 M_f) + 2d_4 P_f \cdot P_i) + 2P_i^\alpha (d_8 e_4 P_f \cdot q_a - d_7 M_f) - q_a^\alpha (d_7 e_3 M_f M_i \\
 & + 2d_8 e_4 P_f \cdot P_i)) + M_i \epsilon^{\mu\nu q_a q_b} (q_b^\alpha (d_3 e_4 M_f M_i + d_4 e_3 P_f \cdot P_i) - d_7 e_3 M_f P_i^\alpha).
 \end{aligned}$$

$$\begin{aligned}
 \mathcal{F}_{A1}^\alpha = & -d_7 M_f (-q_a^\nu g^{\alpha\mu} P_i \cdot q_b + q_a^\mu g^{\alpha\nu} P_i \cdot q_b - q_a^\alpha g^{\mu\nu} P_i \cdot q_b + g^{\alpha\mu} P_i^\nu q_a \cdot q_b - g^{\alpha\nu} P_i^\mu q_a \cdot q_b \quad (\text{A.8}) \\
 & + g^{\mu\nu} P_i^\alpha q_a \cdot q_b + q_a^\mu q_b^\alpha P_i^\nu - q_a^\nu q_b^\alpha P_i^\mu - q_a^\alpha q_b^\mu P_i^\nu + q_a^\nu q_b^\mu P_i^\alpha + q_a^\alpha q_b^\nu P_i^\mu - q_a^\mu q_b^\nu P_i^\alpha) \\
 & + d_4 q_b^\alpha (g^{\mu\nu} q_a \cdot q_b P_f \cdot P_i - g^{\mu\nu} P_f \cdot q_a P_i \cdot q_b + q_a^\nu q_b^\mu P_f \cdot P_i - q_a^\mu q_b^\nu P_f \cdot P_i - q_b^\mu P_i^\nu P_f \cdot q_a \\
 & + q_b^\nu P_i^\mu P_f \cdot q_a + q_a^\mu P_f^\nu P_i \cdot q_b - q_a^\nu P_f^\mu P_i \cdot q_b - P_f^\nu P_i^\mu q_a \cdot q_b + P_f^\mu P_i^\nu q_a \cdot q_b) + d_1 M_f^2 q_b^\alpha \\
 & (- (q_a^\mu P_i^\nu - q_a^\nu P_i^\mu)) - d_6 M_f (-q_a^\alpha g^{\mu\nu} P_f \cdot P_i - q_a^\nu g^{\alpha\mu} P_f \cdot P_i + q_a^\mu g^{\alpha\nu} P_f \cdot P_i \\
 & + g^{\alpha\mu} P_i^\nu P_f \cdot q_a - g^{\alpha\nu} P_i^\mu P_f \cdot q_a + g^{\mu\nu} P_i^\alpha P_f \cdot q_a + q_a^\alpha P_f^\nu P_i^\mu - q_a^\nu P_f^\mu P_i^\alpha - q_a^\mu P_f^\nu P_i^\alpha + q_a^\nu P_f^\mu P_i^\alpha).
 \end{aligned}$$

$$\begin{aligned}
 \mathcal{F}_{A2}^\alpha = & d_2 M_f q_b^\alpha (-g^{\mu\nu} P_f \cdot P_i + P_f^\nu P_i^\mu - P_f^\mu P_i^\nu) - d_3 M_f q_b^\alpha (g^{\mu\nu} P_i \cdot q_b + q_b^\mu P_i^\nu - q_b^\nu P_i^\mu) - d_8 \quad (\text{A.9}) \\
 & (-q_b^\alpha g^{\mu\nu} P_f \cdot P_i - q_b^\nu g^{\alpha\mu} P_f \cdot P_i + q_b^\mu g^{\alpha\nu} P_f \cdot P_i + P_f^\nu g^{\alpha\mu} P_i \cdot q_b - P_f^\mu g^{\alpha\nu} P_i \cdot q_b + q_b^\alpha P_f^\nu P_i^\mu \\
 & - q_b^\nu P_f^\mu P_i^\alpha - q_b^\mu P_f^\nu P_i^\alpha + q_b^\nu P_f^\mu P_i^\alpha) + d_1 M_f^2 (-q_b^\alpha) g^{\mu\nu} - d_7 M_f (q_b^\nu g^{\alpha\mu} - q_b^\mu g^{\alpha\nu} + q_b^\alpha g^{\mu\nu}) \\
 & - d_4 q_b^\alpha (q_b^\mu P_f^\nu - q_b^\nu P_f^\mu) - d_5 M_f^2 (g^{\alpha\mu} P_i^\nu - g^{\alpha\nu} P_i^\mu + g^{\mu\nu} P_i^\alpha) - d_6 M_f (P_f^\nu g^{\alpha\mu} - P_f^\mu g^{\alpha\nu}).
 \end{aligned}$$

$$\begin{aligned}
 \mathcal{F}_{A3}^\alpha = & d_2 M_f q_b^\alpha (-g^{\mu\nu} P_f \cdot q_a + q_a^\mu P_f^\nu - q_a^\nu P_f^\mu) - d_3 M_f q_b^\alpha (g^{\mu\nu} q_a \cdot q_b + q_a^\nu q_b^\mu - q_a^\mu q_b^\nu) \quad (\text{A.10}) \\
 & - d_8 (-q_b^\alpha g^{\mu\nu} P_f \cdot q_a - q_b^\nu g^{\alpha\mu} P_f \cdot q_a + q_b^\mu g^{\alpha\nu} P_f \cdot q_a + P_f^\nu g^{\alpha\mu} q_a \cdot q_b - P_f^\mu g^{\alpha\nu} q_a \cdot q_b \\
 & + q_a^\mu q_b^\alpha P_f^\nu - q_a^\nu q_b^\alpha P_f^\mu - q_a^\alpha q_b^\mu P_f^\nu + q_a^\alpha q_b^\nu P_f^\mu) + d_5 M_f^2 (- (q_a^\nu g^{\alpha\mu} - q_a^\mu g^{\alpha\nu} + q_a^\alpha g^{\mu\nu})).
 \end{aligned}$$

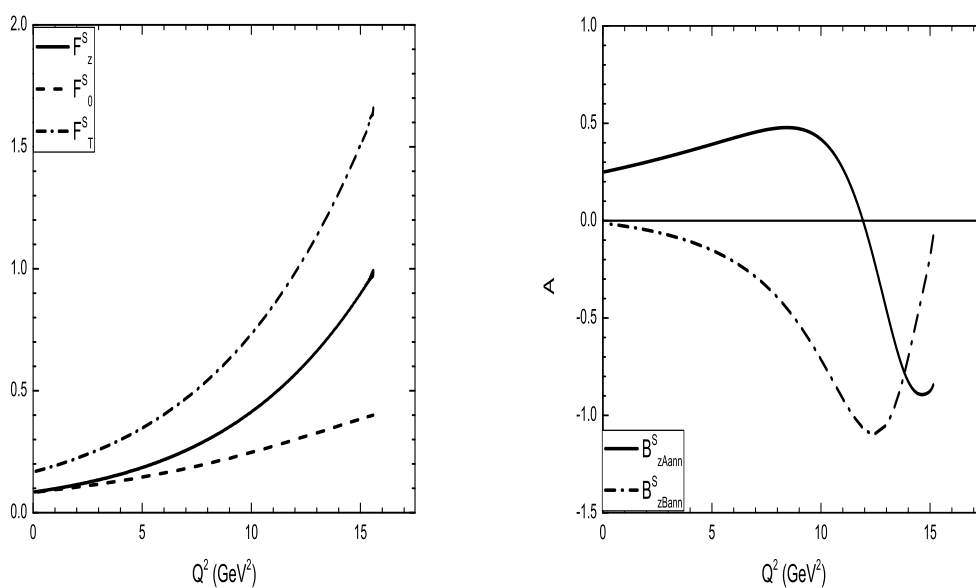
B Definitions of P_i , P_f , ϵ_A , ϵ_T and ϵ_H^μ

During calculating the physical observables, we must specify the P_i , P_f , ϵ_A , ϵ_T and ϵ_H^μ . In the initial meson rest frame, we have $P_i^\alpha = (M_i, 0, 0, 0)$ and $P_f^\alpha = (E_f, 0, 0, P_f^3)$. The polarization vectors ϵ_A^α are chosen as $\epsilon_A^\alpha(\pm 1) = \frac{1}{\sqrt{2}}(0, \pm 1, +i, 0)$ and $\epsilon_A^\alpha(0) = \frac{1}{M_f}(-P_f^3, 0, 0, -E_f)$. The polarization tensors $\epsilon_T^{\alpha\beta}$ can be constructed in terms of the polarization vectors ϵ_A^α , which are written as

$$\begin{aligned}
 \epsilon_T^{\alpha\beta}(\pm 2) &= \epsilon_A(\pm 1)^\alpha \epsilon_A(\pm 1)^\beta, \\
 \epsilon_T^{\alpha\beta}(\pm 1) &= \sqrt{\frac{1}{2}} \left\{ \epsilon_A(\pm 1)^\alpha \epsilon_A(0)^\beta + \epsilon_A(0)^\alpha \epsilon_A(\pm 1)^\beta \right\}, \quad (\text{B.1}) \\
 \epsilon_T^{\alpha\beta}(0) &= \sqrt{\frac{1}{6}} \left\{ \epsilon_A(+1)^\alpha \epsilon_A(-1)^\beta + \epsilon_A(-1)^\alpha \epsilon_A(+1)^\beta \right\} + \sqrt{\frac{2}{3}} \epsilon_A(0)^\alpha \epsilon_A(0)^\beta.
 \end{aligned}$$

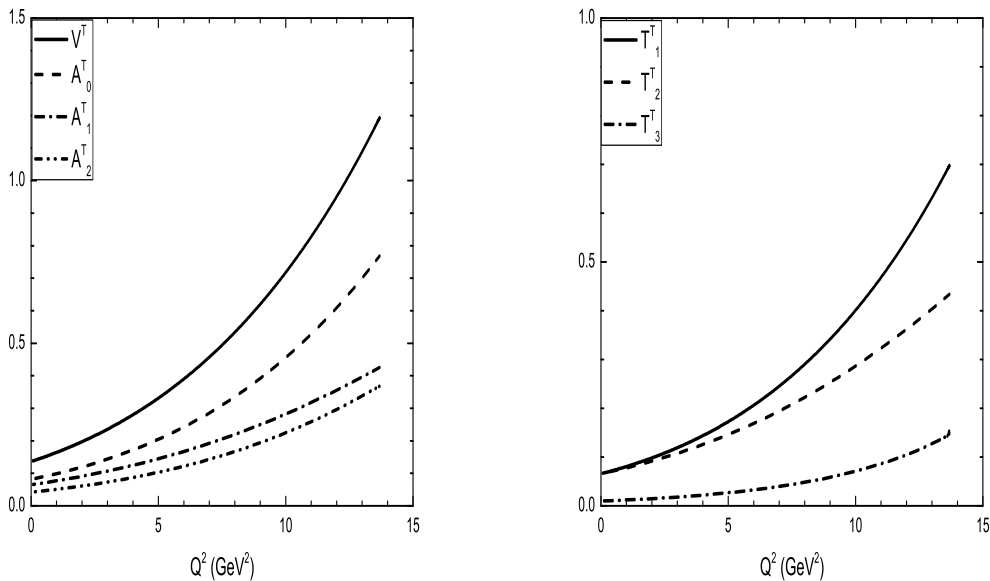
Besides, we define the helicity amplitudes as [32]

$$\begin{aligned}
 \epsilon_H^\mu(t) &= \frac{1}{\sqrt{Q^2}} (M_i - E_f, 0, 0, -P_f^3), \\
 \epsilon_H^\mu(\pm 1) &= \frac{1}{\sqrt{2}} (0, \mp 1, +i, 0), \quad (\text{B.2}) \\
 \epsilon_H^\mu(0) &= \frac{1}{\sqrt{Q^2}} (-P_f^3, 0, 0, M_i - E_f).
 \end{aligned}$$

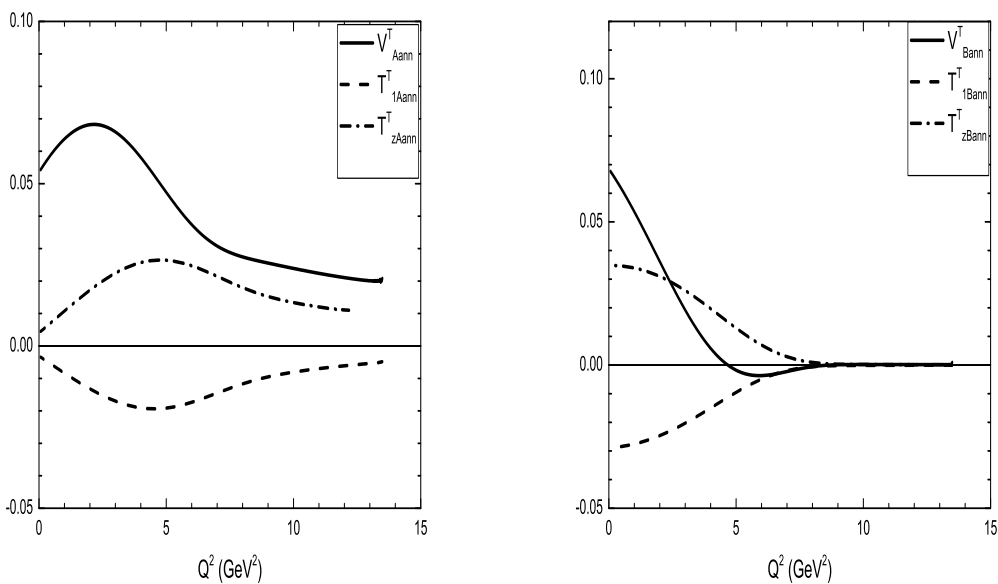


(a) Form-Factors of W^μ and W_T^μ induced by penguin and box diagrams (b) Form-Factors of W_{ann}^μ induced by annihilation diagrams

Figure 3. Form-Factors of $B_c \rightarrow D_{s0}^*(2317)l\bar{l}$, where B_{zAann}^S stands for $\text{Re}[B_{zann}^S]$, while B_{zBann}^S denotes $\text{Im}[B_{zann}^S]$.

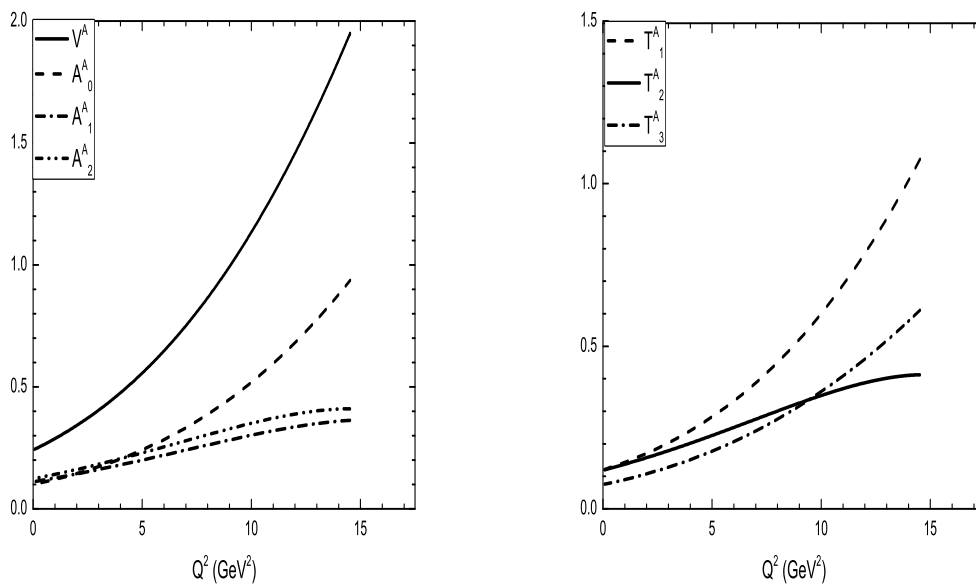


(a) Form-factors of W^μ induced by Z^0 penguin and (b) Form-factors of W_T^μ induced by γ penguin diagrams

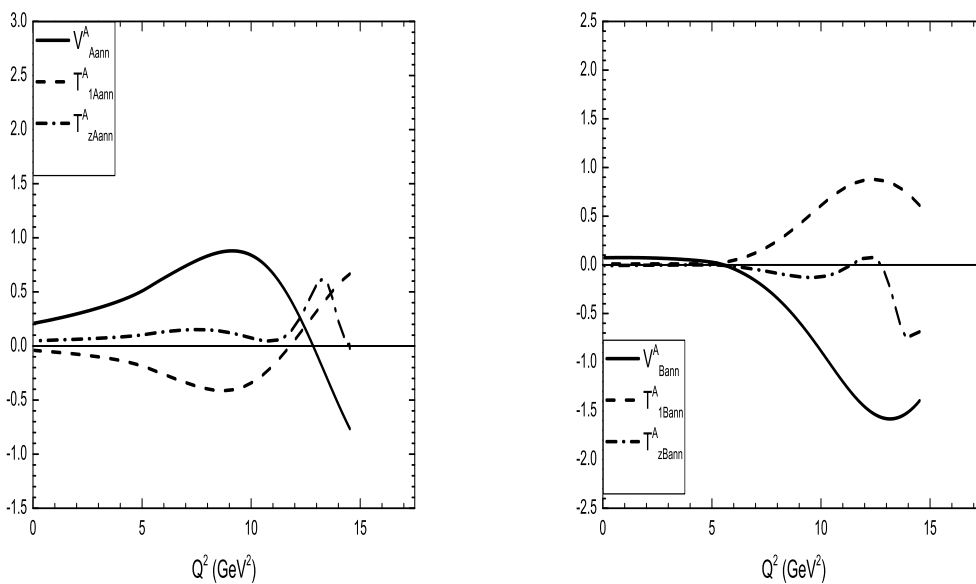


(c) Real parts of W_{ann}^μ Form-Factors induced by annihilation diagrams (d) Imaginary parts of W_{ann}^μ Form-Factors induced by annihilation diagrams

Figure 4. Form-factors of $B_c \rightarrow D_{s2}^* l \bar{l}$, where V_{Aann}^T and $T_{1,z\text{Aann}}^T$ stand for $\text{Re}[V_{\text{ann}}^T]$ and $\text{Re}[T_{1,z\text{ann}}^T]$, respectively, while V_{Bann}^T and $T_{1,z\text{Bann}}^T$ denote $\text{Im}[V_{\text{ann}}^T]$ and $\text{Im}[T_{1,z\text{ann}}^T]$.

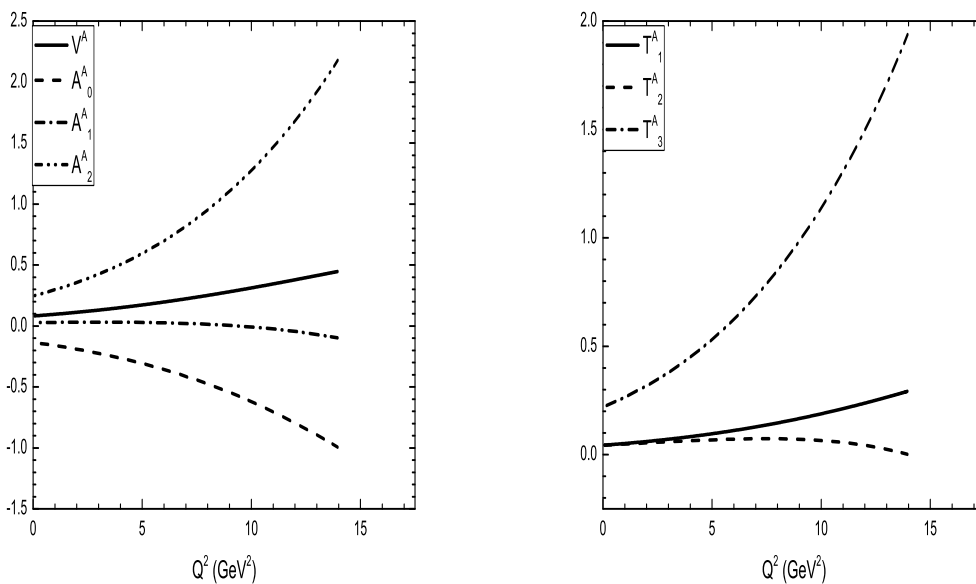


(a) Form-factors of W^μ induced by Z^0 penguin and (b) Form-factors of W_T^μ induced by γ penguin diagrams

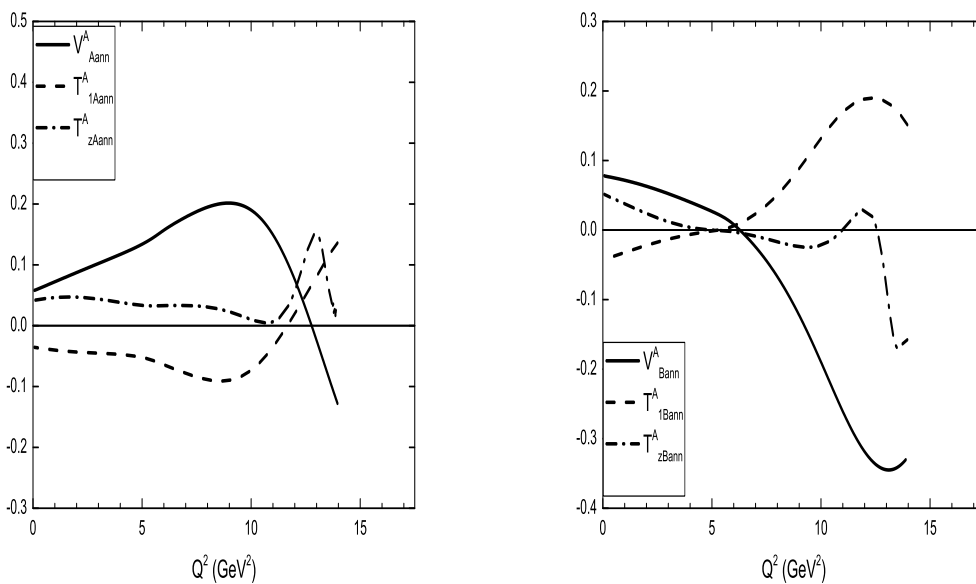


(c) Real parts of W_{ann}^μ Form-Factors induced by annihilation diagrams and (d) Imaginary parts of W_{ann}^μ Form-Factors induced by annihilation diagrams

Figure 5. Form-factors of $B_c \rightarrow D_{s1}(2460)l\bar{l}$, where $V_{A\text{ann}}^A$ and $T_{1,zA\text{ann}}^A$ stand for $\text{Re}[V_{\text{ann}}^A]$ and $\text{Re}[T_{1,z\text{ann}}^A]$, respectively, while $V_{B\text{ann}}^A$ and $T_{1,zB\text{ann}}^A$ denote $\text{Im}[V_{\text{ann}}^A]$ and $\text{Im}[T_{1,z\text{ann}}^A]$.

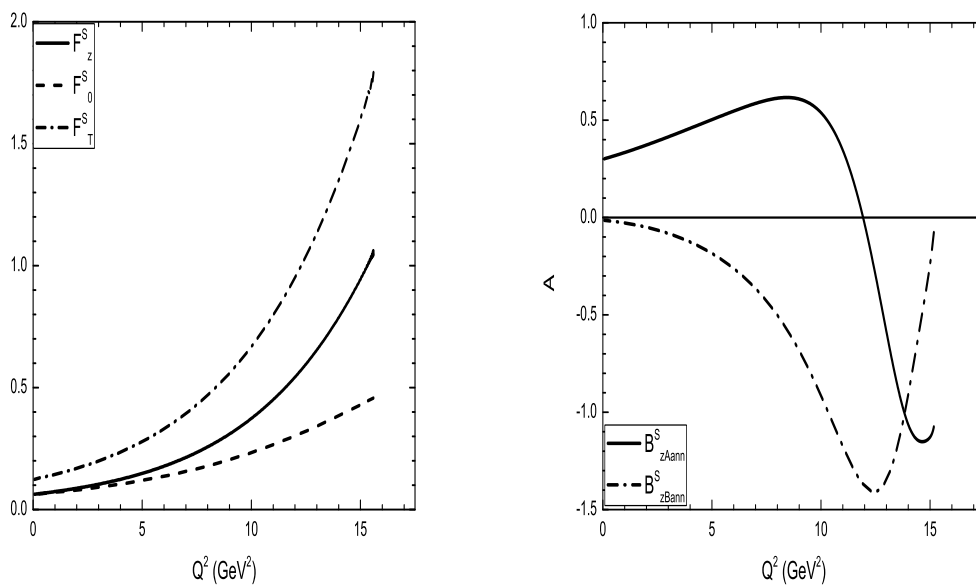


(a) Form-factors of W^μ induced by Z^0 penguin and (b) Form-factors of W_T^μ induced by γ penguin diagrams



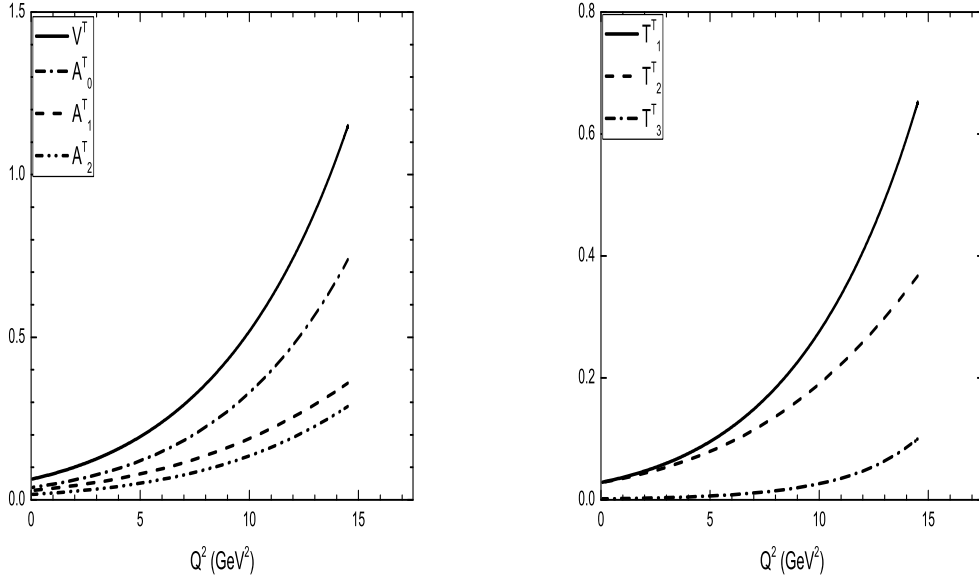
(c) Real parts of W_{ann}^μ Form-Factors induced by an- (d) Imaginary parts of W_{ann}^μ Form-Factors induced by annihilation diagrams

Figure 6. Form-factors of $B_c \rightarrow D_{s1}(2536)l\bar{l}$, where $V_{A\text{ann}}^A$ and $T_{1,zA\text{ann}}^A$ stand for $\text{Re}[V_{\text{ann}}^A]$ and $\text{Re}[T_{1,z\text{ann}}^A]$, respectively, while $V_{B\text{ann}}^A$ and $T_{1,zB\text{ann}}^A$ denote $\text{Im}[V_{\text{ann}}^A]$ and $\text{Im}[T_{1,z\text{ann}}^A]$.

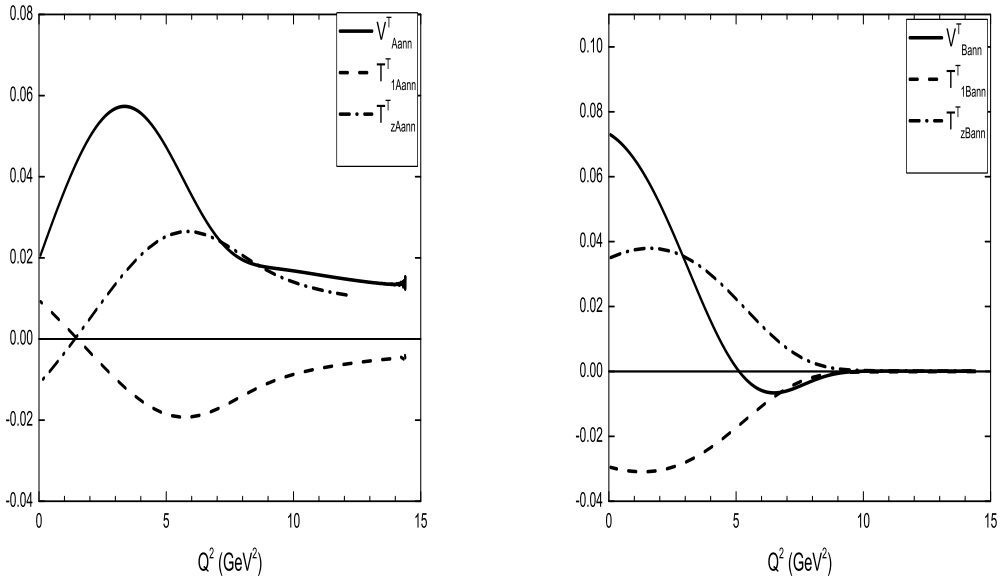


(a) Form-Factors of W^μ and W_T^μ induced by penguin (b) Form-Factors of W_{ann}^μ induced by annihilation and box diagrams

Figure 7. Form-Factors of $B_c \rightarrow D_0^*(2400)l\bar{l}$, where B_{zAann}^S stands for $\text{Re}[B_{zann}^S]$, while B_{zBann}^S denotes $\text{Im}[B_{zann}^S]$.

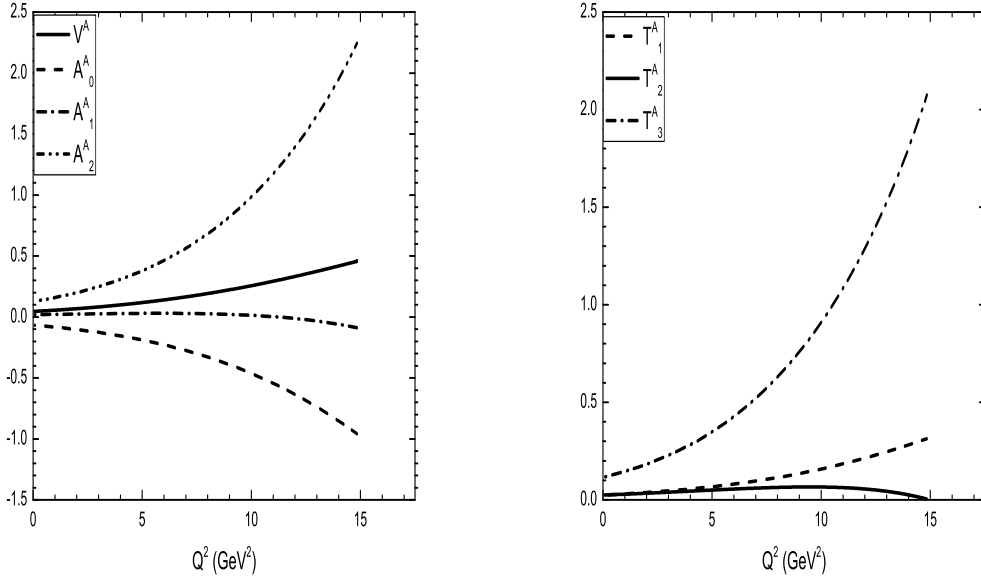


(a) Form-factors of W^μ induced by Z^0 penguin and (b) Form-factors of W_T^μ induced by γ penguin diagrams

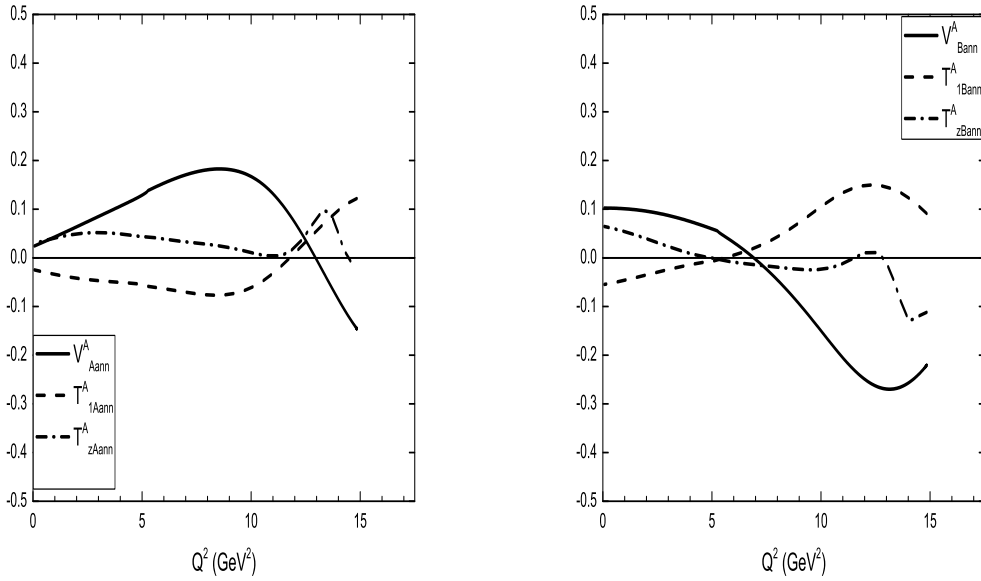


(c) Real parts of W_{ann}^μ Form-Factors induced by an- (d) Imaginary parts of W_{ann}^μ Form-Factors induced by annihilation diagrams

Figure 8. Form-factors of $B_c \rightarrow D_2^*(2460)l\bar{l}$, where V_{Aann}^T and $T_{1,z\text{Aann}}^T$ stand for $\text{Re}[V_{\text{ann}}^T]$ and $\text{Re}[T_{1,z\text{ann}}^T]$, respectively, while V_{Bann}^T and $T_{1,z\text{Bann}}^T$ denote $\text{Im}[V_{\text{ann}}^T]$ and $\text{Im}[T_{1,z\text{ann}}^T]$.

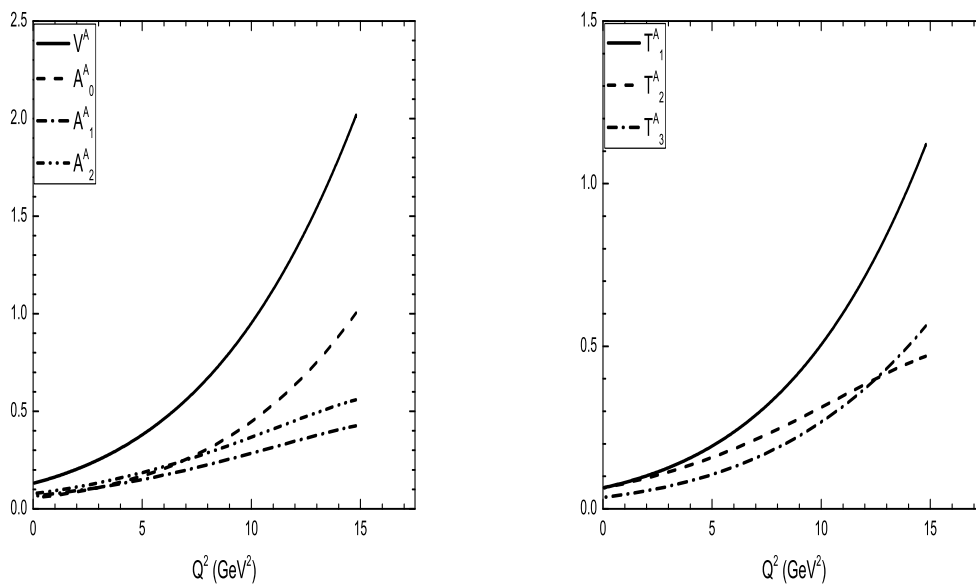


(a) Form-factors of W^μ induced by Z^0 penguin and (b) Form-factors of W_T^μ induced by γ penguin diagrams

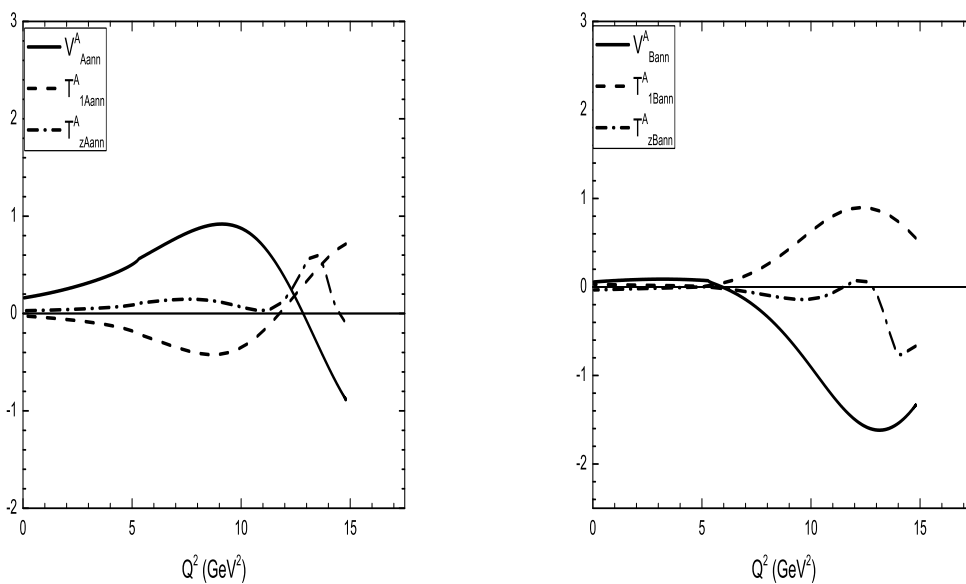


(c) Real parts of W_{ann}^μ Form-Factors induced by an- (d) Imaginary parts of W_{ann}^μ Form-Factors induced by annihilation diagrams

Figure 9. Form-factors of $B_c \rightarrow D_1(2420)\bar{l}l$, where $V_{A\text{ann}}^A$ and $T_{1,zA\text{ann}}^A$ stand for $\text{Re}[V_{\text{ann}}^A]$ and $\text{Re}[T_{1,z\text{ann}}^A]$, respectively, while $V_{B\text{ann}}^A$ and $T_{1,zB\text{ann}}^A$ denote $\text{Im}[V_{\text{ann}}^A]$ and $\text{Im}[T_{1,z\text{ann}}^A]$.

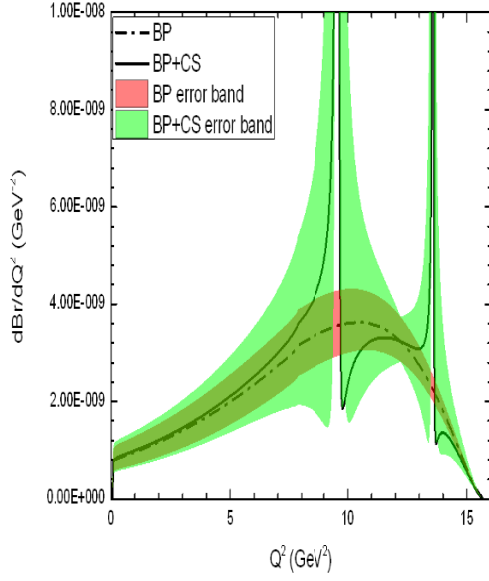


(a) Form-factors of W^μ induced by Z^0 penguin and (b) Form-factors of W_T^μ induced by γ penguin diagrams

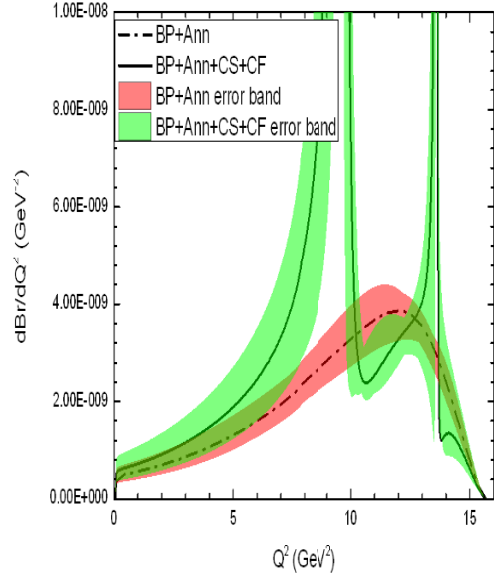


(c) Real parts of W_{ann}^μ Form-Factors induced by annihilation diagrams (d) Imaginary parts of W_{ann}^μ Form-Factors induced by annihilation diagrams

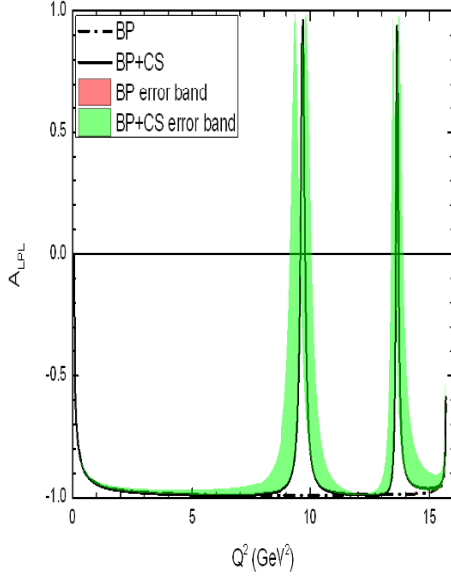
Figure 10. Form-factors of $B_c \rightarrow D_1(2430)\bar{l}l$, where V_{Aann}^A and $T_{1,z\text{Aann}}^A$ stand for $\text{Re}[V_{\text{ann}}^A]$ and $\text{Re}[T_{1,z\text{ann}}^A]$, respectively, while V_{Bann}^A and $T_{1,z\text{Bann}}^A$ denote $\text{Im}[V_{\text{ann}}^A]$ and $\text{Im}[T_{1,z\text{ann}}^A]$.



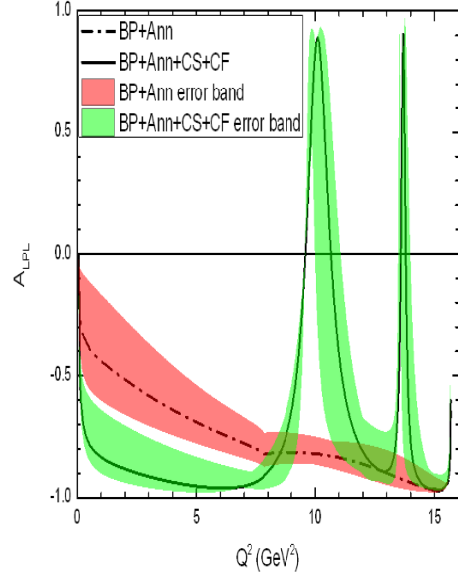
(a) Differential branching fraction



(b) Differential branching fraction

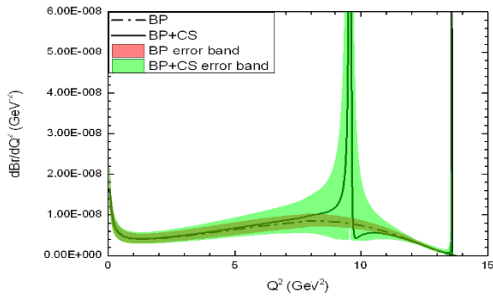


(c) Leptonic longitudinal polarization asymmetry

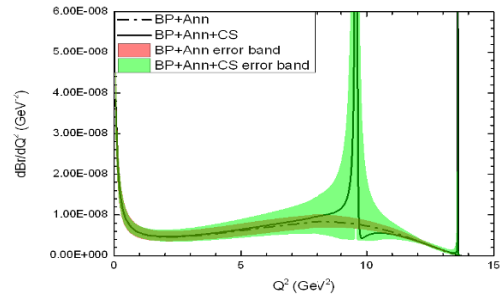


(d) Leptonic longitudinal polarization asymmetry

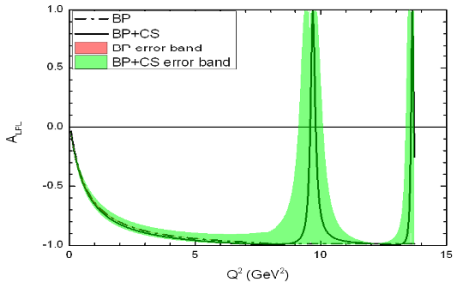
Figure 11. Observables of $B_c \rightarrow D_{s0}^*(2317)\mu\bar{\mu}$.



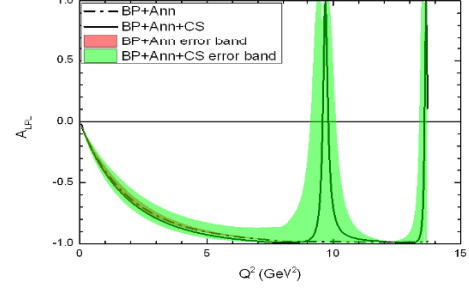
(a) Differential branching fraction



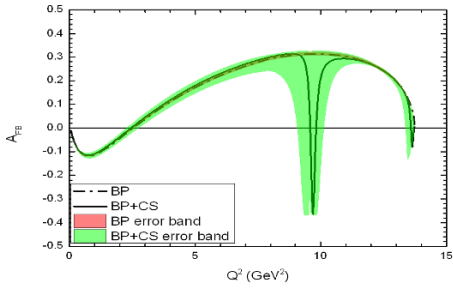
(b) Differential branching fraction



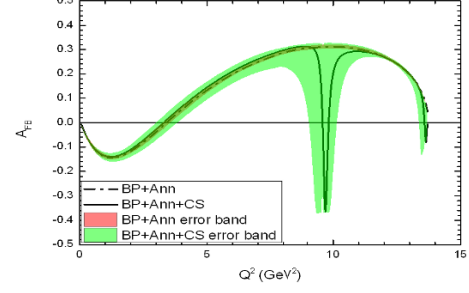
(c) Leptonic longitudinal polarization asymmetry



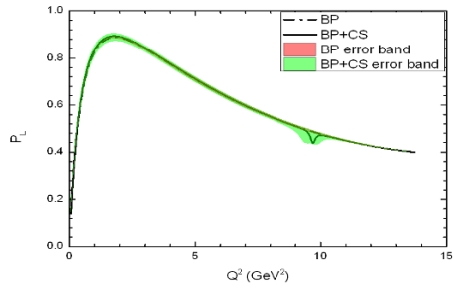
(d) Leptonic longitudinal polarization asymmetry



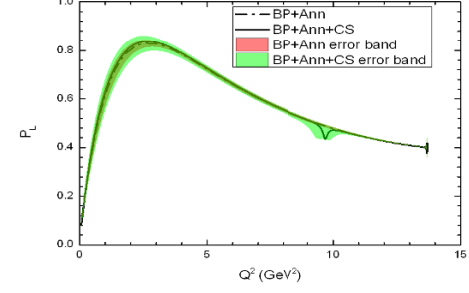
(e) Forward-backward asymmetry



(f) Forward-backward asymmetry

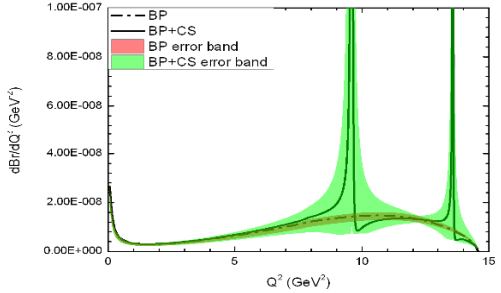


(g) Longitudinal polarization of the meson

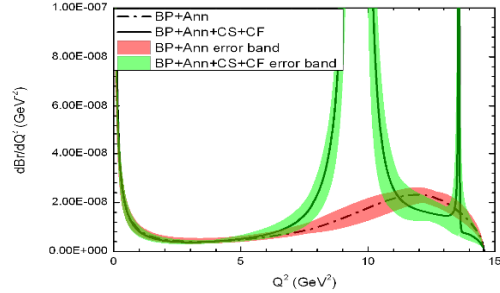


(h) Longitudinal polarization of the final meson

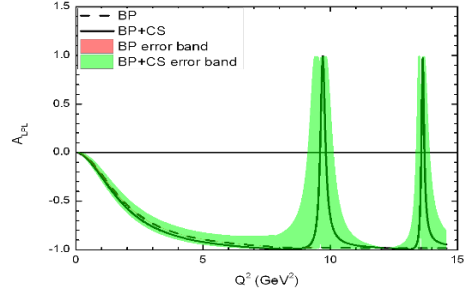
Figure 12. Observables of $B_c \rightarrow D_{s2}^*(2573)\mu\bar{\mu}$.



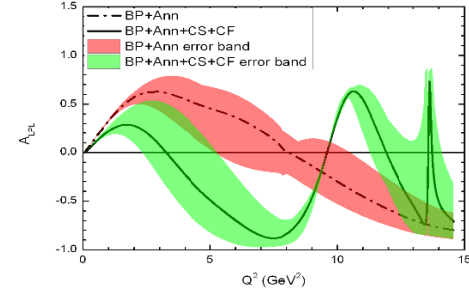
(a) Differential branching fraction



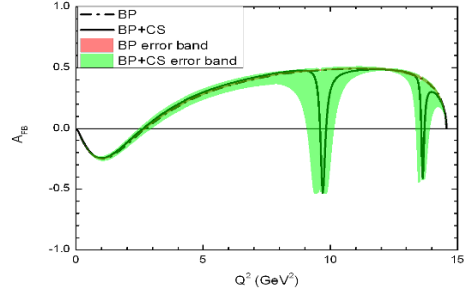
(b) Differential branching fraction



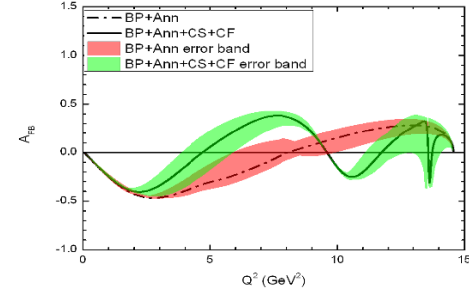
(c) Leptonic longitudinal polarization asymmetry



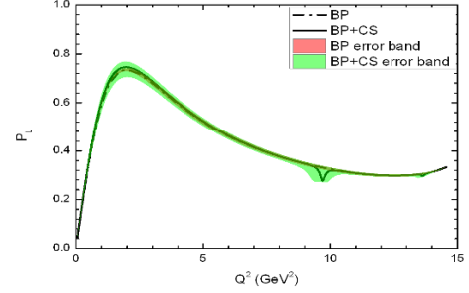
(d) Leptonic longitudinal polarization asymmetry



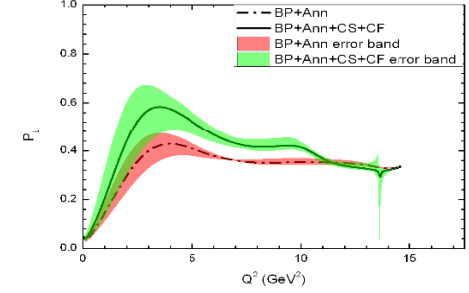
(e) Forward-backward asymmetry



(f) Forward-backward asymmetry

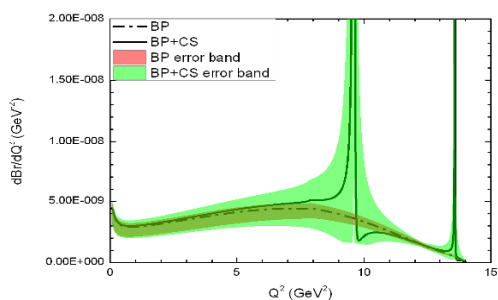


(g) Longitudinal polarization of the meson

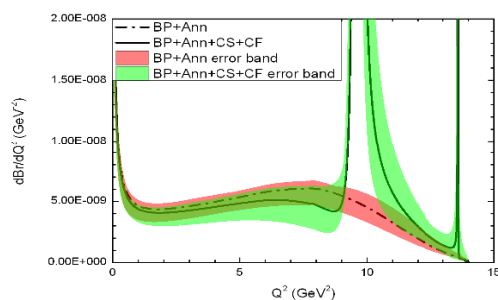


(h) Longitudinal polarization of the final meson

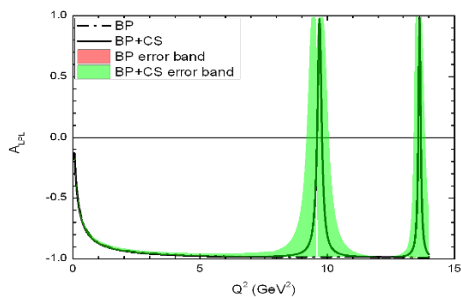
Figure 13. Observables of $B_c \rightarrow D_{s1}(2460)\mu\bar{\mu}$.



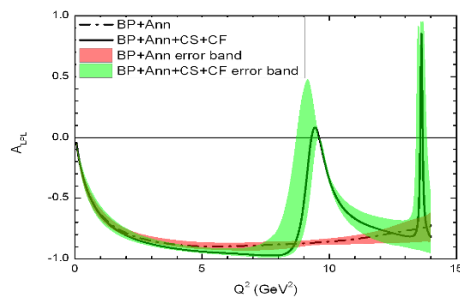
(a) Differential branching fraction



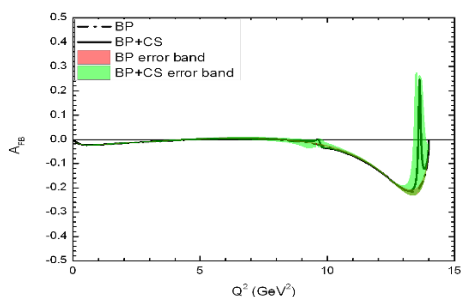
(b) Differential branching fraction



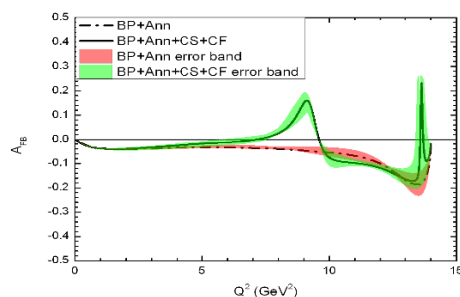
(c) Leptonic longitudinal polarization asymmetry



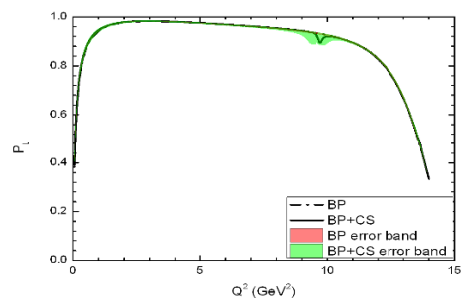
(d) Leptonic longitudinal polarization asymmetry



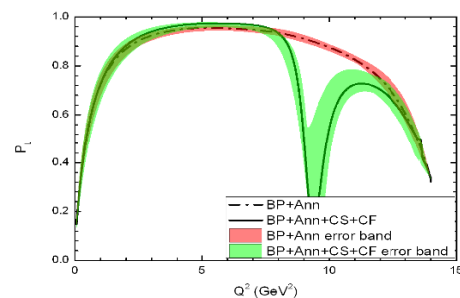
(e) Forward-backward asymmetry



(f) Forward-backward asymmetry

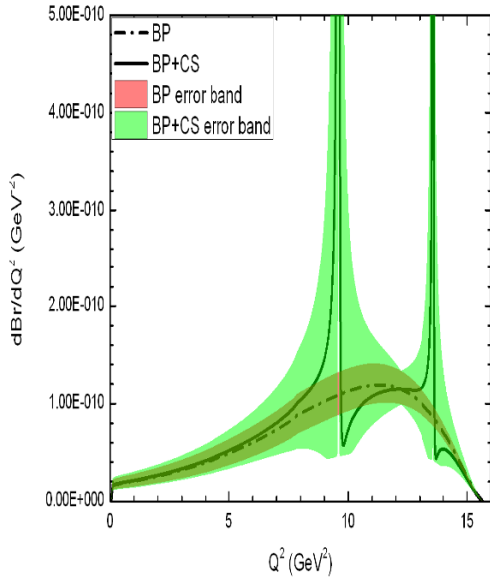


(g) Longitudinal polarization of the meson

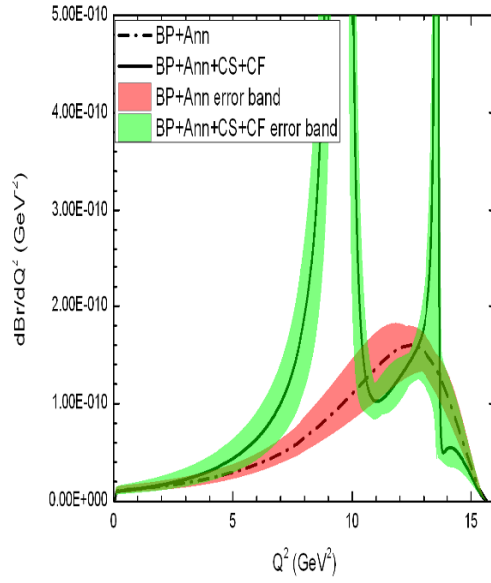


(h) Longitudinal polarization of the final meson

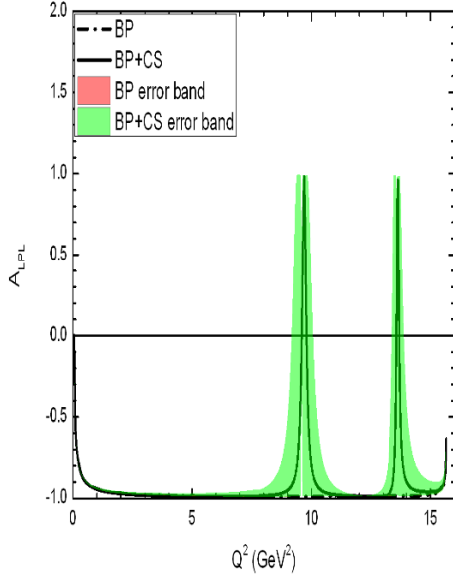
Figure 14. Observables of $B_c \rightarrow D_{s1}(2536)\mu\bar{\mu}$.



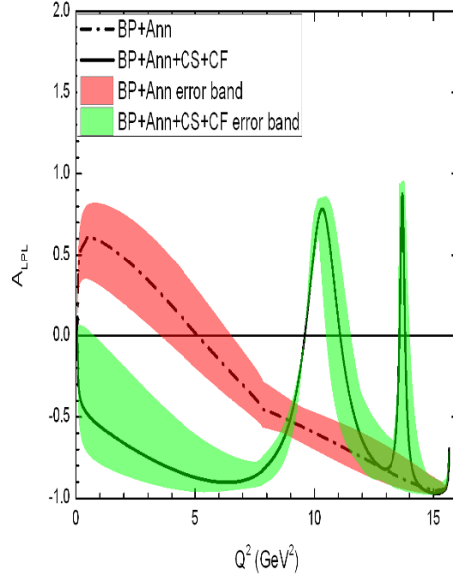
(a) Differential branching fraction



(b) Differential branching fraction

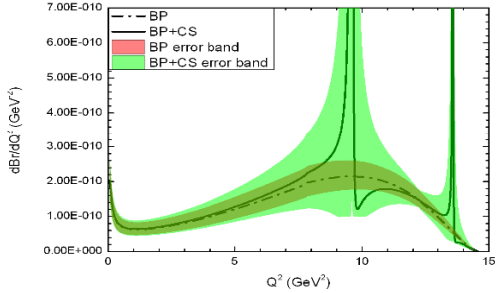


(c) Leptonic longitudinal polarization asymmetry

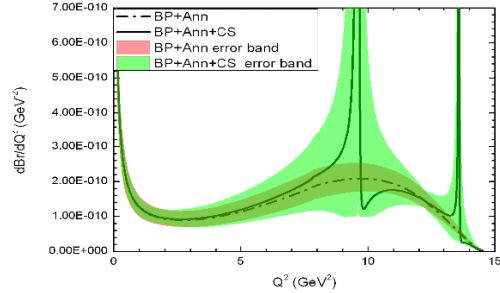


(d) Leptonic longitudinal polarization asymmetry

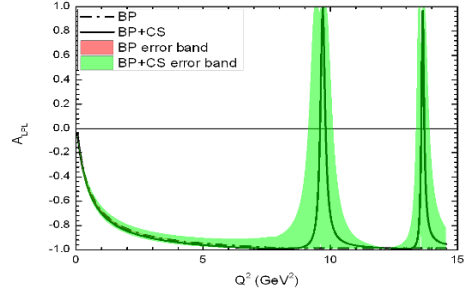
Figure 15. Observables of $B_c \rightarrow D_0^*(2400)\mu\bar{\mu}$.



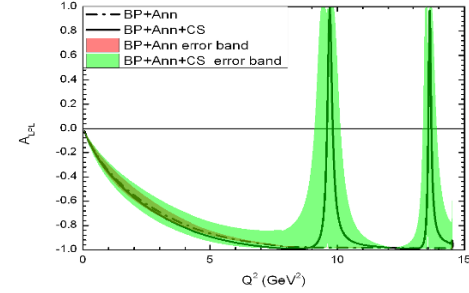
(a) Differential branching fraction



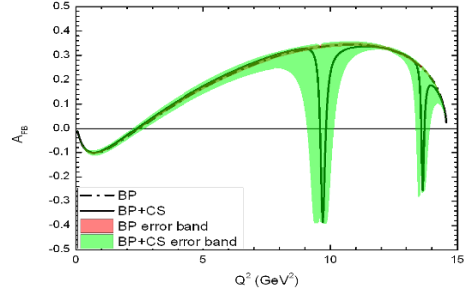
(b) Differential branching fraction



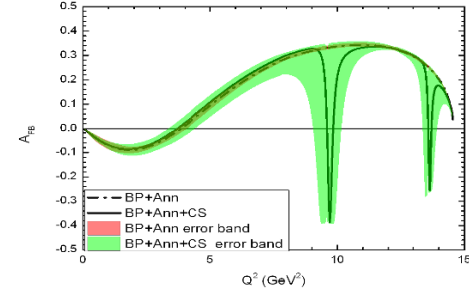
(c) Leptonic longitudinal polarization asymmetry



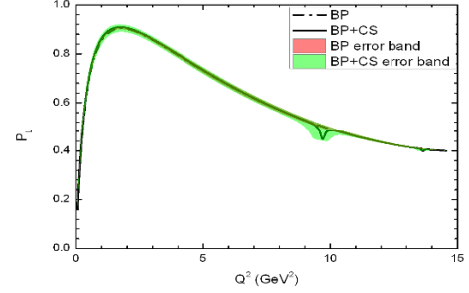
(d) Leptonic longitudinal polarization asymmetry



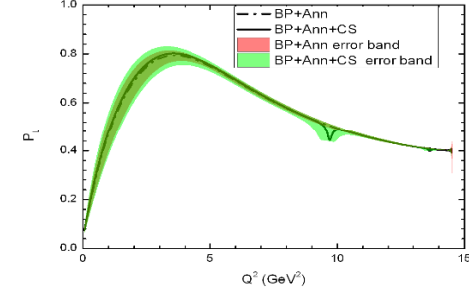
(e) Forward-backward asymmetry



(f) Forward-backward asymmetry

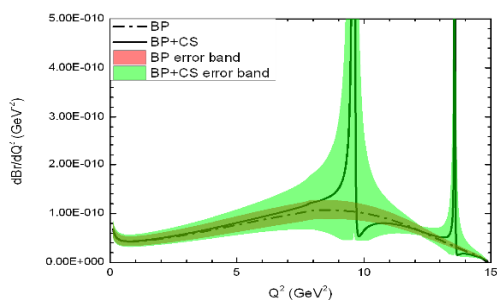


(g) Longitudinal polarization of the meson

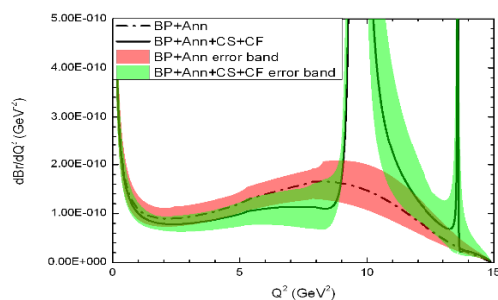


(h) Longitudinal polarization of the final meson

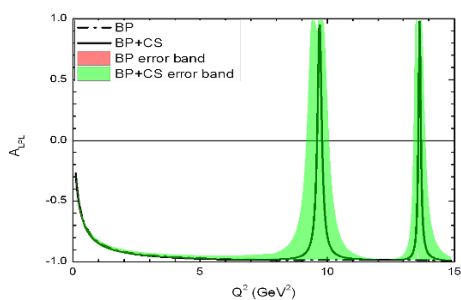
Figure 16. Observables of $B_c \rightarrow D_2^*(2460)\mu\bar{\nu}$.



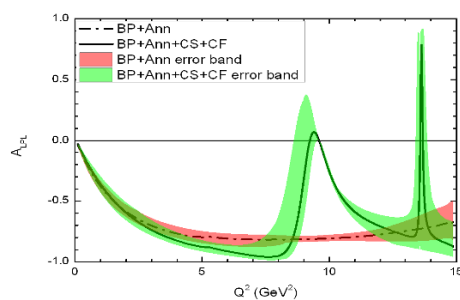
(a) Differential branching fraction



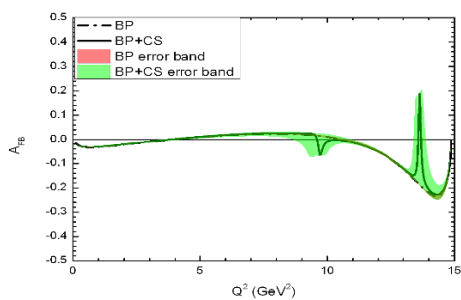
(b) Differential branching fraction



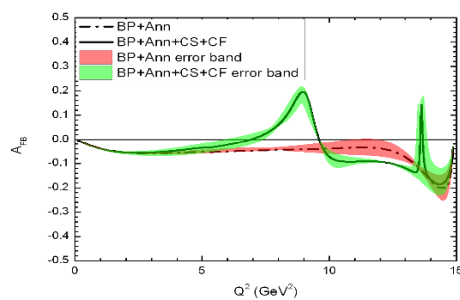
(c) Leptonic longitudinal polarization asymmetry



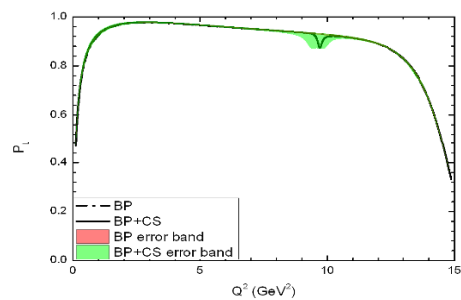
(d) Leptonic longitudinal polarization asymmetry



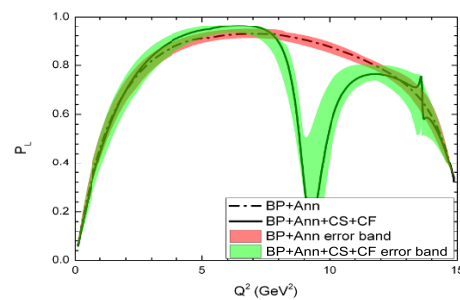
(e) Forward-backward asymmetry



(f) Forward-backward asymmetry

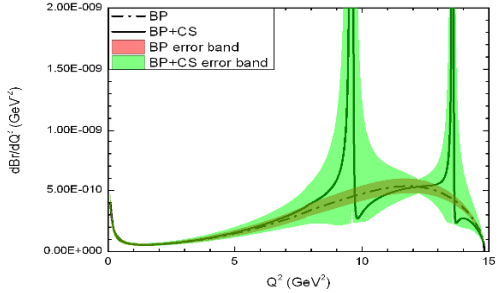


(g) Longitudinal polarization of the meson

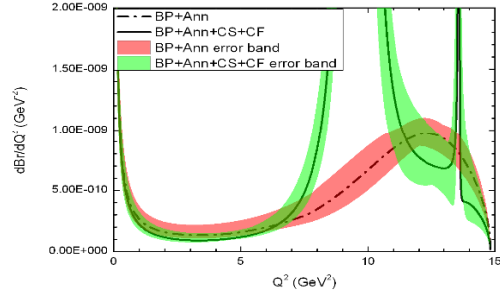


(h) Longitudinal polarization of the final meson

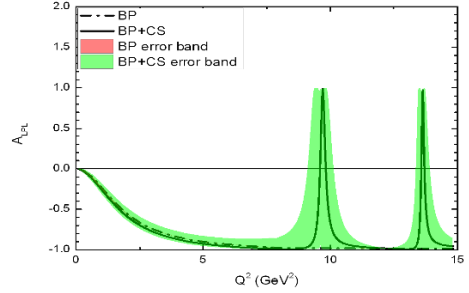
Figure 17. Observables of $B_c \rightarrow D_1(2420)\mu\bar{\mu}$.



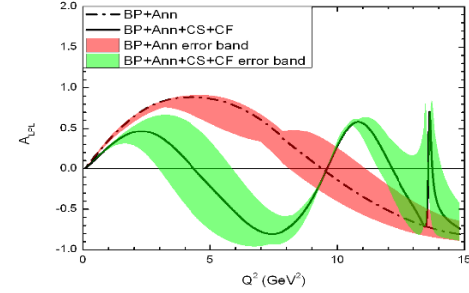
(a) Differential branching fraction



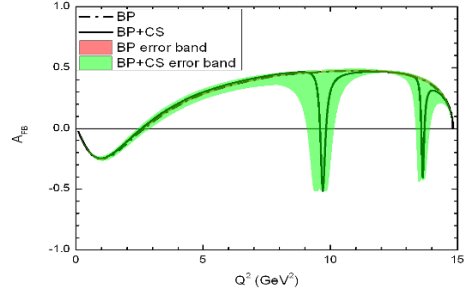
(b) Differential branching fraction



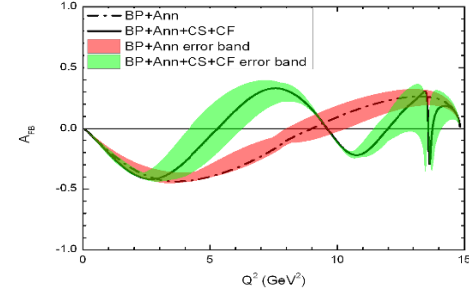
(c) Leptonic longitudinal polarization asymmetry



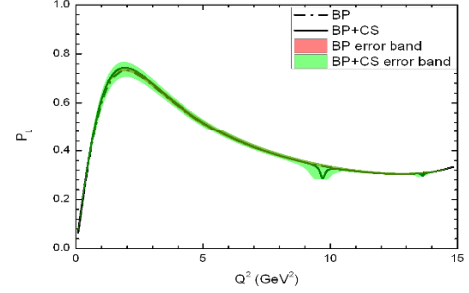
(d) Leptonic longitudinal polarization asymmetry



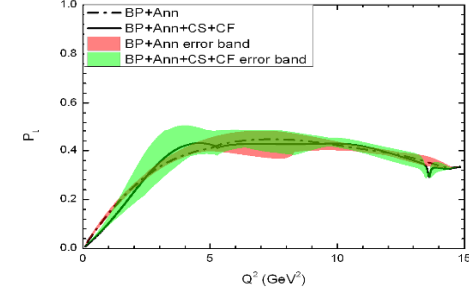
(e) Forward-backward asymmetry



(f) Forward-backward asymmetry



(g) Longitudinal polarization of the meson



(h) Longitudinal polarization of the final meson

Figure 18. Observables of $B_c \rightarrow D_1(2430)\mu\bar{\mu}$.

Open Access. This article is distributed under the terms of the Creative Commons Attribution License ([CC-BY 4.0](https://creativecommons.org/licenses/by/4.0/)), which permits any use, distribution and reproduction in any medium, provided the original author(s) and source are credited.

References

- [1] T.M. Aliev, M. Savci and K.-C. Yang, *Tensor form factors of $B \rightarrow K_1$ transition from QCD light cone sum rules*, *Phys. Lett. B* **700** (2011) 55 [[arXiv:1011.4661](https://arxiv.org/abs/1011.4661)] [[INSPIRE](#)].
- [2] C.-H. Chen, C.-Q. Geng, C.-C. Lih and C.-C. Liu, *Study of $B \rightarrow K^*(0)(1430) \ell \bar{\ell}$ decays*, *Phys. Rev. D* **75** (2007) 074010 [[hep-ph/0703106](https://arxiv.org/abs/hep-ph/0703106)] [[INSPIRE](#)].
- [3] T.M. Aliev, K. Azizi and M. Savci, *Analysis of rare $B \rightarrow K^*(0)(1430) \ell^+ \ell^-$ decay within QCD sum rules*, *Phys. Rev. D* **76** (2007) 074017 [[arXiv:0710.1508](https://arxiv.org/abs/0710.1508)] [[INSPIRE](#)].
- [4] M.J. Aslam, C.-D. Lu and Y.-M. Wang, *$B \rightarrow K^*(0) \ell^+ \ell^-$ decays in supersymmetric theories*, *Phys. Rev. D* **79** (2009) 074007 [[arXiv:0902.0432](https://arxiv.org/abs/0902.0432)] [[INSPIRE](#)].
- [5] V. Bashiry, M. Bayar and K. Azizi, *A comparative study on $B \rightarrow K^* \ell^+ \ell^-$ and $B \rightarrow K_0^*(1430) \ell^+ \ell^-$ decays in the Supersymmetric Models*, *Mod. Phys. Lett. A* **26** (2011) 901 [[arXiv:0902.0773](https://arxiv.org/abs/0902.0773)] [[INSPIRE](#)].
- [6] F. Falahati and R. Khosravi, *Double-lepton polarization asymmetries in $B \rightarrow K^{0*}(1430) \ell^+ \ell^-$ decay in the fourth-generation standard model*, *Phys. Rev. D* **83** (2011) 015010 [[INSPIRE](#)].
- [7] B.B. Sirvanli, K. Azizi and Y. Ipekoglu, *Double-Lepton Polarization Asymmetries and Branching Ratio in $B \rightarrow K_0^*(1430) \ell^+ \ell^-$ transition from Universal Extra Dimension Model*, *JHEP* **01** (2011) 069 [[arXiv:1011.1469](https://arxiv.org/abs/1011.1469)] [[INSPIRE](#)].
- [8] C.-D. Lu and W. Wang, *Analysis of $B \rightarrow K_J^*(\rightarrow K\pi) \mu^+ \mu^-$ in the higher kaon resonance region*, *Phys. Rev. D* **85** (2012) 034014 [[arXiv:1111.1513](https://arxiv.org/abs/1111.1513)] [[INSPIRE](#)].
- [9] F. Falahati and R. Khosravi, *Two-Higgs-doublet model and double-lepton polarization asymmetries in $B \rightarrow K^{0*}(1430) \ell^+ \ell^-$ decay*, *Phys. Rev. D* **85** (2012) 075008 [[INSPIRE](#)].
- [10] S. Rai Choudhury, A.S. Cornell, G.C. Joshi and B.H.J. McKellar, *Analysis of the $B \rightarrow K^*(2)(\rightarrow K\pi) \ell^+ \ell^-$ decay*, *Phys. Rev. D* **74** (2006) 054031 [[hep-ph/0607289](https://arxiv.org/abs/hep-ph/0607289)] [[INSPIRE](#)].
- [11] H. Hatanaka and K.-C. Yang, *Radiative and Semileptonic B Decays Involving the Tensor Meson $K(2)^*(1430)$ in the Standard Model and Beyond*, *Phys. Rev. D* **79** (2009) 114008 [[arXiv:0903.1917](https://arxiv.org/abs/0903.1917)] [[INSPIRE](#)].
- [12] H. Hatanaka and K.-C. Yang, *Radiative and Semileptonic B Decays Involving Higher K-Resonances in the Final States*, *Eur. Phys. J. C* **67** (2010) 149 [[arXiv:0907.1496](https://arxiv.org/abs/0907.1496)] [[INSPIRE](#)].
- [13] S.R. Choudhury, A.S. Cornell and N. Gaur, *Analysis of the $\bar{B} \rightarrow \bar{K}(2)(1430) \ell^+ \ell^-$ decay*, *Phys. Rev. D* **81** (2010) 094018 [[arXiv:0911.4783](https://arxiv.org/abs/0911.4783)] [[INSPIRE](#)].
- [14] W. Wang, *B to tensor meson form factors in the perturbative QCD approach*, *Phys. Rev. D* **83** (2011) 014008 [[arXiv:1008.5326](https://arxiv.org/abs/1008.5326)] [[INSPIRE](#)].
- [15] K.-C. Yang, *B to Light Tensor Meson Form Factors Derived from Light-Cone Sum Rules*, *Phys. Lett. B* **695** (2011) 444 [[arXiv:1010.2944](https://arxiv.org/abs/1010.2944)] [[INSPIRE](#)].

- [16] R.-H. Li, C.-D. Lu and W. Wang, *Branching ratios, forward-backward asymmetries and angular distributions of $B \rightarrow K_2^* l^+ l^-$ in the standard model and new physics scenarios*, *Phys. Rev. D* **83** (2011) 034034 [[arXiv:1012.2129](#)] [[INSPIRE](#)].
- [17] M. Junaid, M.J. Aslam and I. Ahmed, *Complementarity of Semileptonic $B \rightarrow K_2^*(1430)$ and $K^*(892)$ Decays in the Standard Model with Fourth Generation*, *Int. J. Mod. Phys. A* **27** (2012) 1250149 [[arXiv:1103.3934](#)] [[INSPIRE](#)].
- [18] N. Katirci and K. Azizi, *B to strange tensor meson transition in a model with one universal extra dimension*, *JHEP* **07** (2011) 043 [[arXiv:1105.3636](#)] [[INSPIRE](#)].
- [19] S.R. Choudhury, A.S. Cornell and J.D. Roussos, *Analysis of the lepton polarisation asymmetries of $\bar{B} \rightarrow \bar{K}_2(1430) \ell^+ \ell^-$ decay*, *Eur. Phys. J. C* **71** (2011) 1751 [[arXiv:1105.5901](#)] [[INSPIRE](#)].
- [20] T.M. Aliev and M. Savci, *$B \rightarrow K_2 \ell^+ \ell^-$ decay beyond the Standard Model*, *Phys. Rev. D* **85** (2012) 015007 [[arXiv:1109.2738](#)] [[INSPIRE](#)].
- [21] I. Ahmed, M.J. Aslam, M. Junaid and S. Shafaq, *Model independent analysis of $B \rightarrow K^*(2)(1430) \mu^+ \mu^-$ decay*, *JHEP* **02** (2012) 045 [[INSPIRE](#)].
- [22] PARTICLE DATA GROUP collaboration, J. Beringer et al., *Review of Particle Physics (RPP)*, *Phys. Rev. D* **86** (2012) 010001 [[INSPIRE](#)].
- [23] N. Ghahramany, R. Khosravi and Z. Naseri, *Analysis of rare semileptonic $B_c \rightarrow D_s - 0^*(2317) \ell^+ \ell^-$ decays*, *Phys. Rev. D* **81** (2010) 036005 [[INSPIRE](#)].
- [24] T. Wang, D.-X. Zhang, B.-Q. Ma and T. Liu, *B_c Meson Rare Decays in the Light-cone Quark Model*, *Eur. Phys. J. C* **71** (2011) 1758 [[arXiv:1004.4274](#)] [[INSPIRE](#)].
- [25] C.Q. Geng, C.-W. Hwang and C.C. Liu, *Study of rare $B_c^+ \rightarrow D_{d,s} +$ lepton anti-lepton decays*, *Phys. Rev. D* **65** (2002) 094037 [[hep-ph/0110376](#)] [[INSPIRE](#)].
- [26] G. Buchalla, A.J. Buras and M.E. Lautenbacher, *Weak decays beyond leading logarithms*, *Rev. Mod. Phys.* **68** (1996) 1125 [[hep-ph/9512380](#)] [[INSPIRE](#)].
- [27] C.-H. Chang, J.-K. Chen and G.-L. Wang, *Instantaneous formulation for transitions between two instantaneous bound states and its gauge invariance*, *Commun. Theor. Phys.* **46** (2006) 467 [[INSPIRE](#)].
- [28] E.E. Salpeter and H.A. Bethe, *A Relativistic equation for bound state problems*, *Phys. Rev.* **84** (1951) 1232 [[INSPIRE](#)].
- [29] E.E. Salpeter, *Mass corrections to the fine structure of hydrogen-like atoms*, *Phys. Rev.* **87** (1952) 328 [[INSPIRE](#)].
- [30] S. Mandelstam, *Dynamical variables in the Bethe-Salpeter formalism*, *Proc. Roy. Soc. Lond. A* **233** (1955) 248 [[INSPIRE](#)].
- [31] W.-L. Ju, G.-L. Wang, H.-F. Fu, T.-H. Wang and Y. Jiang, *The Study of Rare $B_c \rightarrow D_{s,d}^{(*)} \bar{l} l$ Decays*, *JHEP* **04** (2014) 065 [[arXiv:1307.5492](#)] [[INSPIRE](#)].
- [32] A. Faessler, T. Gutsche, M.A. Ivanov, J.G. Korner and V.E. Lyubovitskij, *The Exclusive rare decays $B \rightarrow K(K^*) \bar{l} l$ and $B_c \rightarrow D(D^*) \bar{l} l$ in a relativistic quark model*, *Eur. Phys. J. direct* **C 4** (2002) 18 [[hep-ph/0205287](#)] [[INSPIRE](#)].
- [33] M. Bauer, B. Stech and M. Wirbel, *Exclusive Nonleptonic Decays of D, D(s) and B Mesons*, *Z. Phys. C* **34** (1987) 103 [[INSPIRE](#)].

- [34] C.-H. Chang and Y.-Q. Chen, *The Decays of $B(c)$ meson*, *Phys. Rev. D* **49** (1994) 3399 [[INSPIRE](#)].
- [35] G.-L. Wang, *Decay constants of P -wave mesons*, *Phys. Lett. B* **650** (2007) 15 [[arXiv:0705.2621](#)] [[INSPIRE](#)].
- [36] G. Cvetič, C.S. Kim, G.-L. Wang and W. Namgung, *Decay constants of heavy meson of 0 -state in relativistic Salpeter method*, *Phys. Lett. B* **596** (2004) 84 [[hep-ph/0405112](#)] [[INSPIRE](#)].
- [37] G.-L. Wang, *Decay constants of heavy vector mesons in relativistic Bethe-Salpeter method*, *Phys. Lett. B* **633** (2006) 492 [[math-ph/0512009](#)] [[INSPIRE](#)].
- [38] G.-L. Wang, *Annihilation Rate of $2++$ Charmonium and Bottomonium*, *Phys. Lett. B* **674** (2009) 172 [[arXiv:0904.1604](#)] [[INSPIRE](#)].
- [39] Z.-H. Wang, G.-L. Wang, H.-F. Fu and Y. Jiang, *B/c decays to heavy-light orbitally excited mesons*, *Int. J. Mod. Phys. A* **27** (2012) 1250049 [[INSPIRE](#)].
- [40] N. Isgur and M.B. Wise, *Excited charm mesons in semileptonic \bar{B} decay and their contributions to a Bjorken sum rule*, *Phys. Rev. D* **43** (1991) 819 [[INSPIRE](#)].
- [41] H.-Y. Cheng and C.-K. Chua, *Production of P -wave Charmed Mesons in Hadronic B Decays*, *Phys. Rev. D* **74** (2006) 034020 [[hep-ph/0605073](#)] [[INSPIRE](#)].
- [42] BELLE collaboration, K. Abe et al., *Study of $B^- \rightarrow D^{*0}\pi^-$ ($D^{*0} \rightarrow D^{(*)+}\pi^-$) decays*, *Phys. Rev. D* **69** (2004) 112002 [[hep-ex/0307021](#)] [[INSPIRE](#)].
- [43] H.-Y. Cheng, *Hadronic B decays involving even parity charmed mesons*, *Phys. Rev. D* **68** (2003) 094005 [[hep-ph/0307168](#)] [[INSPIRE](#)].
- [44] G. Ecker, J. Gasser, A. Pich and E. de Rafael, *The Role of Resonances in Chiral Perturbation Theory*, *Nucl. Phys. B* **321** (1989) 311 [[INSPIRE](#)].
- [45] R.C. Verma, *Decay constants and form factors of s -wave and p -wave mesons in the covariant light-front quark model*, *J. Phys. G* **39** (2012) 025005 [[arXiv:1103.2973](#)] [[INSPIRE](#)] and private communication.
- [46] H.-Y. Cheng, C.-K. Chua and C.-W. Hwang, *Covariant light front approach for s wave and p wave mesons: Its application to decay constants and form-factors*, *Phys. Rev. D* **69** (2004) 074025 [[hep-ph/0310359](#)] [[INSPIRE](#)] and private communication.
- [47] H.-F. Fu, Y. Jiang, C.S. Kim and G.-L. Wang, *Probing Non-leptonic Two-body Decays of B_c meson*, *JHEP* **06** (2011) 015 [[arXiv:1102.5399](#)] [[INSPIRE](#)].
- [48] H.-F. Fu, G.-L. Wang, Z.-H. Wang and X.-J. Chen, *Semi-leptonic and non-leptonic B meson decays to charmed mesons*, *Chin. Phys. Lett.* **28** (2011) 121301 [[arXiv:1202.1221](#)] [[INSPIRE](#)].
- [49] Y. Jiang, G.L. Wang, T. Wang, W.L. Ju and H.F. Fu, *Nonleptonic production of charmed P -wave mesons from \bar{B}_s^0 and \bar{B}^0 decays*, *Int. J. Mod. Phys. A* **28** (2013) 1350110 [[INSPIRE](#)].
- [50] Y. Jiang, G.L. Wang, T.H. Wang and W.L. Ju, *Semileptonic Production of Scalar and Tensor p -Wave Charmed Mesons*, *Chin. Phys. Lett.* **30** (2013) 101101 [[INSPIRE](#)].
- [51] Z.-h. Wang, G.-L. Wang and C.-H. Chang, *The B_c Decays to P -wave Charmonium by Improved Bethe-Salpeter Approach*, *J. Phys. G* **39** (2012) 015009 [[arXiv:1107.0474](#)] [[INSPIRE](#)].

- [52] H. Hatanaka and K.-C. Yang, $K(1)(1270)$ - $K(1)(1400)$ Mixing Angle and New-Physics Effects in $B \rightarrow K(1)\ell^+\ell^-$ Decays, *Phys. Rev. D* **78** (2008) 074007 [[arXiv:0808.3731](#)] [[INSPIRE](#)].
- [53] V. Bashiry, Lepton polarization in $B \rightarrow K_1\ell^+\ell^-$ Decays, *JHEP* **06** (2009) 062 [[arXiv:0902.2578](#)] [[INSPIRE](#)].
- [54] V. Bashiry and K. Azizi, Forward-backward Asymmetry and Branching Ratio of $B \rightarrow K(1)\ell^+\ell^-$ Transition in Supersymmetric Models, *JHEP* **01** (2010) 033 [[arXiv:0903.1505](#)] [[INSPIRE](#)].
- [55] A. Ahmed, I. Ahmed, M. Ali Paracha and A. Rehman, $K_1(1270) - K_1(1400)$ mixing and the fourth generation SM effects in $B \rightarrow K_1\ell^+\ell^-$ decays, *Phys. Rev. D* **84** (2011) 033010 [[arXiv:1105.3887](#)] [[INSPIRE](#)].
- [56] Y. Li, J. Hua and K.-C. Yang, $B \rightarrow K1\ell^+\ell^-$ Decays in a Family Non-universal Z' Model, *Eur. Phys. J. C* **71** (2011) 1775 [[arXiv:1107.0630](#)] [[INSPIRE](#)].
- [57] C. Chang and G. Wang, Spectrum for Heavy Quarkonia and Mixture of the Relevant Wave Functions within the Framework of Bethe-Salpeter Equation, *Sci. China Phys. Mech. Astron.* **53** (2010) 2005 [[arXiv:1003.3827](#)] [[INSPIRE](#)].
- [58] A. Deandrea, N. Di Bartolomeo, R. Gatto, F. Feruglio and G. Nardulli, Penguin contributions to rates and CP asymmetries in nonleptonic B decays: Possible experimental procedures and estimates, *Phys. Lett. B* **320** (1994) 170 [[hep-ph/9310326](#)] [[INSPIRE](#)].
- [59] H.-Y. Cheng and B. Tseng, Nonfactorizable effects in exclusive charmless B decays, [hep-ph/9708211](#) [[INSPIRE](#)].
- [60] N.G. Deshpande, B. Dutta and S. Oh, Branching ratios and CP asymmetries of B decays to a vector and a pseudoscalar meson, *Phys. Lett. B* **473** (2000) 141 [[hep-ph/9712445](#)] [[INSPIRE](#)].
- [61] A. Ali, G. Kramer and C.-D. Lu, Experimental tests of factorization in charmless nonleptonic two-body B decays, *Phys. Rev. D* **58** (1998) 094009 [[hep-ph/9804363](#)] [[INSPIRE](#)].
- [62] Y.-Y. Keum, H.-n. Li and A.I. Sanda, Fat penguins and imaginary penguins in perturbative QCD, *Phys. Lett. B* **504** (2001) 6 [[hep-ph/0004004](#)] [[INSPIRE](#)].
- [63] C.-D. Lu, K. Ukai and M.-Z. Yang, Branching ratio and CP-violation of $B \rightarrow \pi\pi$ decays in perturbative QCD approach, *Phys. Rev. D* **63** (2001) 074009 [[hep-ph/0004213](#)] [[INSPIRE](#)].
- [64] M. Beneke, G. Buchalla, M. Neubert and C.T. Sachrajda, QCD factorization for $B \rightarrow \pi\pi$ decays: Strong phases and CP-violation in the heavy quark limit, *Phys. Rev. Lett.* **83** (1999) 1914 [[hep-ph/9905312](#)] [[INSPIRE](#)].
- [65] D. Ebert, R.N. Faustov and V.O. Galkin, Rare Semileptonic Decays of B and B_c Mesons in the Relativistic Quark Model, *Phys. Rev. D* **82** (2010) 034032 [[arXiv:1006.4231](#)] [[INSPIRE](#)].
- [66] C.Q. Geng, C.-W. Hwang and C.C. Liu, Study of rare $B_c^+ \rightarrow D_{d,s}\bar{l}l$ decays, *Phys. Rev. D* **65** (2002) 094037 [[hep-ph/0110376](#)] [[INSPIRE](#)].
- [67] H.-M. Choi, Light-front quark model analysis of the exclusive rare $B_c \rightarrow D_{(s)}(\ell^+\ell^-, \nu\bar{\nu})$ decays, *Phys. Rev. D* **81** (2010) 054003 [[arXiv:1001.3432](#)] [[INSPIRE](#)].
- [68] T. Wang, D.-X. Zhang, B.-Q. Ma and T. Liu, B_c Meson Rare Decays in the Light-cone Quark Model, *Eur. Phys. J. C* **71** (2011) 1758 [[arXiv:1004.4274](#)] [[INSPIRE](#)].
- [69] K. Azizi and R. Khosravi, Analysis of the rare semileptonic $B_c \rightarrow P(D, D_s)\ell^+\ell^-/\nu\bar{\nu}$ decays within QCD sum rules, *Phys. Rev. D* **78** (2008) 036005 [[arXiv:0806.0590](#)] [[INSPIRE](#)].

- [70] K. Azizi, F. Falahati, V. Bashiry and S.M. Zebarjad, *Analysis of the Rare $B_c \rightarrow D_{s,d}^* \ell^+ \ell^-$ Decays in QCD*, *Phys. Rev. D* **77** (2008) 114024 [[arXiv:0806.0583](#)] [[INSPIRE](#)].
- [71] M.A. Paracha, I. Ahmed and M.J. Aslam, *Semileptonic charmed B meson decays in Universal Extra Dimension Model*, *Phys. Rev. D* **84** (2011) 035003 [[arXiv:1101.2323](#)] [[INSPIRE](#)].
- [72] A. Ahmed, I. Ahmed, M.A. Paracha, M. Junaid, A. Rehman and M.J. Aslam, *Comparative Study of $B_c \rightarrow D_s^* \ell^+ \ell^-$ Decays in Standard Model and Supersymmetric Models*, [arXiv:1108.1058](#) [[INSPIRE](#)].
- [73] I. Ahmed, M.A. Paracha, M. Junaid, A. Ahmed, A. Rehman and M.J. Aslam, *Analysis of $B_c \rightarrow D_s^* \ell^+ \ell^-$ in the Standard Model Beyond Third Generation*, [arXiv:1107.5694](#) [[INSPIRE](#)].
- [74] Y. Jiang, G.L. Wang, T.H. Wang and W.L. Ju, *Study of singlet-triplet mixing via semileptonic decays*, *Chin. Phys. C* **37** (2013) 013101 [[INSPIRE](#)].
- [75] J.-M. Zhang and G.-L. Wang, *B_s Semileptonic Decays to D_s and D_s^* in Bethe-Salpeter Method*, *Chin. Phys. Lett.* **27** (2010) 051301 [[arXiv:1003.5576](#)] [[INSPIRE](#)].
- [76] C.-H. Chang, H.-F. Fu, G.-L. Wang and J.-M. Zhang, *Some of semileptonic and nonleptonic decays of B_c meson in a Bethe-Salpeter relativistic quark model*, [arXiv:1411.3428](#) [[INSPIRE](#)].
- [77] Q.-T. Song, D.-Y. Chen, X. Liu and T. Matsuki, *Charmed-strange mesons revisited: mass spectra and strong decays*, *Phys. Rev. D* **91** (2015) 054031 [[arXiv:1501.03575](#)] [[INSPIRE](#)].